REPORT DOCUMENTATION PAGE

Form Approved
OMB No. 0704-0188

1. REPORT DATE *(DD-MM-YYYY)*	2. REPORT TYPE	3. DATES COVERED *(From - To)*
06/13/2017	Final Report	7/1/2013 to 3/31/2017

4. TITLE AND SUBTITLE
Continuous Solvothermal Synthesis and Surface Treatment for Improved and Scalable Processing of Ultra-High Temperature Ceramic (UHTC) Nanopowders

5a. CONTRACT NUMBER

5b. GRANT NUMBER
N00014-13-0473

5c. PROGRAM ELEMENT NUMBER

6. AUTHOR(S)
Yigal Blum

5d. PROJECT NUMBER
P21835

5e. TASK NUMBER

5f. WORK UNIT NUMBER

7. PERFORMING ORGANIZATION NAME(S) AND ADDRESS(ES)
SRI International
333 Ravenswood Ave.
Menlo Park, CA 94025

8. PERFORMING ORGANIZATION REPORT NUMBER

9. SPONSORING/MONITORING AGENCY NAME(S) AND ADDRESS(ES)
Office of Naval Research
875 North Randolph St.
Arlington, VA 22203-1995

10. SPONSOR/MONITOR'S ACRONYM(S)
ONR

11. SPONSOR/MONITOR'S REPORT NUMBER(S)

12. DISTRIBUTION/AVAILABILITY STATEMENT
Approved for public release; distribution is unlimited.

13. SUPPLEMENTARY NOTES

14. ABSTRACT
The project attempted to develop a wet, environmentally-controlled, continuous synthesis/processing route for high-purity non-agglomerated boride, carbide, and nitride nanoparticles of preferred transition metal elements such as Zr, Hf, and Ta. The proposed generic approach consisted of solvothermal reactions in pressurized vessels. The Approach was abandoned after 2 years due to the presence of large carbon content, derived from the organic solvents. The revised objective was to assess the potential of 2 new polymeric precursors to boron carbonitride and boron nitride as weak interface coatings for SiC/SiC composites. This approach was found to be promising and deserves further evaluation in a systematic mode.

15. SUBJECT TERMS
Ultrahigh Temperature Ceramics (UHTC), Non-Oxide Ceramic Nanoparticles, Solvothermal Synthesis, Preceramic Polymers, Polymeric Precursors to Boron Nitride, Polymer-Derived Ceramics, SiC/SiC Composites, Ceramic Matrix Composites (CMC), Interface Coatings, Boron Carbonitried, Boron Nitride.

16. SECURITY CLASSIFICATION OF:			17. LIMITATION OF ABSTRACT	18. NUMBER OF PAGES	19a. NAME OF RESPONSIBLE PERSON
a. REPORT	b. ABSTRACT	c. THIS PAGE			Yigal Blum
					19b. TELEPHONE NUMBER *(Include area code)*
U	U	U	U	74	650-859-4367

INSTRUCTIONS FOR COMPLETING SF 298

1. REPORT DATE. Full publication date, including day, month, if available. Must cite at least the year and be Year 2000 compliant, e.g. 30-06-1998; xx-06-1998; xx-xx-1998.

2. REPORT TYPE. State the type of report, such as final, technical, interim, memorandum, master's thesis, progress, quarterly, research, special, group study, etc.

3. DATE COVERED. Indicate the time during which the work was performed and the report was written, e.g., Jun 1997 - Jun 1998; 1-10 Jun 1996; May - Nov 1998; Nov 1998.

4. TITLE. Enter title and subtitle with volume number and part number, if applicable. On classified documents, enter the title classification in parentheses.

5a. CONTRACT NUMBER. Enter all contract numbers as they appear in the report, e.g. F33315-86-C-5169.

5b. GRANT NUMBER. Enter all grant numbers as they appear in the report. e.g. AFOSR-82-1234.

5c. PROGRAM ELEMENT NUMBER. Enter all program element numbers as they appear in the report, e.g. 61101A.

5e. TASK NUMBER. Enter all task numbers as they appear in the report, e.g. 05; RF0330201; T4112.

5f. WORK UNIT NUMBER. Enter all work unit numbers as they appear in the report, e.g. 001; AFAPL30480105.

6. AUTHOR(S). Enter name(s) of person(s) responsible for writing the report, performing the research, or credited with the content of the report. The form of entry is the last name, first name, middle initial, and additional qualifiers separated by commas, e.g. Smith, Richard, J, Jr.

7. PERFORMING ORGANIZATION NAME(S) AND ADDRESS(ES). Self-explanatory.

8. PERFORMING ORGANIZATION REPORT NUMBER. Enter all unique alphanumeric report numbers assigned by the performing organization, e.g. BRL-1234; AFWL-TR-85-4017-Vol-21-PT-2.

9. SPONSORING/MONITORING AGENCY NAME(S) AND ADDRESS(ES). Enter the name and address of the organization(s) financially responsible for and monitoring the work.

10. SPONSOR/MONITOR'S ACRONYM(S). Enter, if available, e.g. BRL, ARDEC, NADC.

11. SPONSOR/MONITOR'S REPORT NUMBER(S). Enter report number as assigned by the sponsoring/ monitoring agency, if available, e.g. BRL-TR-829; -215.

12. DISTRIBUTION/AVAILABILITY STATEMENT. Use agency-mandated availability statements to indicate the public availability or distribution limitations of the report. If additional limitations/ restrictions or special markings are indicated, follow agency authorization procedures, e.g. RD/FRD, PROPIN, ITAR, etc. Include copyright information.

13. SUPPLEMENTARY NOTES. Enter information not included elsewhere such as: prepared in cooperation with; translation of; report supersedes; old edition number, etc.

14. ABSTRACT. A brief (approximately 200 words) factual summary of the most significant information.

15. SUBJECT TERMS. Key words or phrases identifying major concepts in the report.

16. SECURITY CLASSIFICATION. Enter security classification in accordance with security classification regulations, e.g. U, C, S, etc. If this form contains classified information, stamp classification level on the top and bottom of this page.

17. LIMITATION OF ABSTRACT. This block must be completed to assign a distribution limitation to the abstract. Enter UU (Unclassified Unlimited) or SAR (Same as Report). An entry in this block is necessary if the abstract is to be limited.

13 June 2017
Final Report

Continuous Solvothermal Synthesis and Surface Treatment for Improved and Scalable Processing of Ultra-High Temperature Ceramic (UHTC) Nanopowders

SRI Project Number P21835
The material is based upon work supported under ONR award number N00014-13-1-0473

Report Period: 01 July, 2013 – 31 March 2017

Prepared by: Dr. Yigal Blum, Associate Director
Chemical Science and Technology Laboratory
Advanced Technology & Systems Division
Tel.: (650) 859-4367; Fax: (650) 859-4321
yigal.blum@sri.com

Performing Organization: SRI International
Menlo Park, CA

Prepared for: Office of Naval Research, Materials Division (Code 332)
One Liberty Center
875 N. Randolph Street, Suite 1425
Arlington, VA 22203-1995

Attention: Dr. Eric Wuchina

CONTENTS

FIGURES

TABLES

AWARD INFORMATION

Award Number:	N00014-13-1-0473
Title of Research:	Continuous Solvothermal Synthesis and Surface Treatment for Improved and Scalable Processing of Ultra-High Temperature Ceramic (UHTC) Nanopowders
Principal Investigator:	Yigal Blum
Organization:	SRI International

TECHNICAL DISCUSSION

1. TECHNICAL GOALS AND OBJECTIVES

1.1 Long-Term Goals

Lightweight materials that function at ultrahigh temperatures (above 1500 °C) are essential for enabling hypersonic vehicle performance for extended periods. Non-oxide particulate composites and fiber-reinforced silicon carbide are the two main families of ceramic materials that are currently considered for the hot sections of hypersonic vehicles.

Composites consisting of borides, carbides, and nitrides of early transition metals, combined with silica-forming phases such as silicon carbide and metal silicides, serve as the current advanced ultra-high-temperature ceramic (UHTC) materials. Such UHTC materials are the main candidates for leading edges and propulsion systems of future hypersonic vehicles. However, UHTC component consolidation is extremely difficult, requiring ultra-high temperatures under high pressure. Their machining is similarly difficult due to their remarkable hardness. UHTC nanoparticles are expected to provide advantageous sintering capabilities with consequently improved performance. Nevertheless, nanoparticle synthesis, handling, and processing impose a new set of technical hurdles and cost constraints.

Silicon-carbide fiber-reinforced silicon-carbide matrix composites (SiC/SiC) are the lightweight materials considered to withstand the highest temperature in an oxidative environment out of all currently produced or studied composites. For achieving and maintaining their critical fracture toughness, fiber-reinforced composites require a weak interface between the fibers and the matrix, and this interface needs to be sustained at the operating conditions.

1.2 Original Objective (Years 1 & 2)

The project objectives were to develop a wet, environmentally-controlled, continuous synthesis/processing route for high-purity non-agglomerated boride, carbide, and nitride nanoparticles of preferred transition metal elements such as Zr, Hf, and Ta. The proposed "all-wet" approach will eventually allow a complete, environmentally inert, continuous process, starting with highly purified chemical reagents and ending with field-assisted sintering techniques (FAST) consolidation without exposing the bare nanopowders to an oxidative environment or forming hard-to-break agglomerations.

1.3 Revised Objective (Year 3)

The use of boron-nitride (BN) and boron-carbo-nitride (BCN) preceramic polymers as the interface coating for silicon carbide (SiC) fiber reinforces SiC matrix composites (SiC/SiC composites). Such composites are of top interest for jet engine and hypersonic vehicles that are operating at temperatures above 1000 °C and 1400 °C, respectively. In order to retain the toughness of the composite, it is imperative to form a weak bond between the fibers and the

matrix. Such interface layers are currently achieved by very expensive chemical vapor deposition (CVD) techniques that place tens-of-nanometer thick layers of carbon and subsequent BN on top of SiC fiber yarns. The cost of these nanometric layers can be the most expensive element in the overall composite.

Simpler techniques to achieve such robust but weak interfaces, which resist chemical reactivity with both the fibers and matrix as well as severe oxidative environments, have been an objective for R&D in the past 40 years. Recently, we have developed new precursors to BN and BCN that consist of nonaromatic structures (in contrast to other BN precursors reported in the literature). In the third year of the project we investigated if thin coatings on top of SiC fibers (Hi-Nicalon) could be easily processed as practical and suitable interface coatings. Since the current practice of the interface coatings is to separately deposit first the C and then the BN layers, we wanted to assess the option of having a single, amorphous BCN coating consisting of a molecular or nanometric hybrid of C and BN structures.

2. BACKGROUND *(for original objective)*

2.1 Relevance of Effort to Naval Needs

Interest in hypersonic vehicles and weapons is on the rise and points to the need for new ultra-high-temperature materials for the leading edges of the wings on hypersonic vehicles and nose tips for missiles flying in atmospheric conditions, as well as for propulsion system components.[1] Sharp leading edges are required for enhancing hypersonic vehicle speed, maneuverability, cross range, and energy efficiency; however, such sharp edges impose significantly higher temperature requirements on the materials constituting the external skin of the hypersonic vehicle. While the leading-edge materials of the former space shuttles were rated to peak temperatures of 1650 °C for durations of minutes only, the sharp leading-edged vehicles will require thermal protective materials performing above 2000 °C for durations of hours. Ultra-high temperature ceramics (UHTCs) are the main candidates for advancing hypersonic vehicle technologies that include such sharp edges.

Ultra-high temperatures and very high-pressure processes are associated with the sintering step of UHTC.[2] Recent attempts to densify UHTC at ambient pressures have required the removal of any native oxide layer from the reacting particles.[3] Use of nonagglomerated and unoxidized nanoparticles to advance sintering processes, such as the electric field-assisted sintering technique (FAST), has resulted in subsequent improvement of UHTC performance.[4]

Hence, ONR has issued Special Notice 13-SN-0001, which included the following topic: (Topic 2) *"Novel Nanomaterial Approaches to Processing of Ultra-High Temperature Materials,"* with the subtopic *"(1) Development of processing routes for the synthesis of high purity nanoparticles of candidate UHTC phases such as ZrB_2, TaC, HfB_2, etc."*

2.2 Proposed Concept for Continuous Synthesis-Surface Treatment of UHTC Nanopowders

We proposed to assess a manufacturing-suitable continuous process that combines two novel elements for improved processing of UHTC, hence improving the overall performance of the densified products at comparable or lower production costs. Our proposed approach combined (a) solvothermal synthesis[5] of high-purity UHTC nanopowders consisting of metal boride, carbide, and nitride phases followed by (b) *in-situ* wet surface treatment to address powder compaction, oxidation resistance, and environmental hazards. The proposed solvent-based solvothermal synthesis approach is expected to be practical and scalable and to allow the formation and use of surface-treated nonagglomerated nanoparticles obtained in a wet environment under pressure/temperature conditions that are significantly lower than those used by typical processes for solid- or gas-phase synthesis of UHTC particles.

2.2.1 Solvothermal Synthesis – Status and Relevant Technical Breakthroughs

Per definition, the "solvothermal process" is a chemical reaction in the presence of a solvent in a closed system at a temperature higher than the boiling point of the solvent. The reaction pressures can be the consequence of the solvent vapors alone or may be further enhanced by externally pressurized gases. The selected temperature and pressure (sub- or supercritical conditions) depend on the required thermodynamic and kinetic conditions for obtaining the target material via the involved process.[6]

In the case of aqueous solutions, the processes are defined as "hydrothermal" and were developed long ago. Hydrothermal processes are usually appropriate for the preparation of hydroxides, oxyhydroxides, or oxides. Consequently, the term "solvothermal" is used primarily to define reactions with non-aqueous solvents to prepare non-oxide materials.

Direct hydrothermal syntheses from aqueous solutions of oxides, crystals, and gems and mass production of zeolites have been practiced industrially for decades. Growing R&D activities have emerged in the past decade for scaling-up oxide nanopowder synthesis by hydrothermal reactions. More recently, the focus of hydrothermal processes has been shifted to scaled-up syntheses of oxide nanoparticles.[7, 8] A large pilot plant with a capacity of 30 tons/year has been built in Korea to form nanoparticles by hydrothermal processes. A continuous process for hydrothermal reactions has also been proposed and demonstrated in the UK.

Over the last 25 years, there has been a growing interest outside the USA in employing solvothermal reactions to prepare micro- or nanoparticles with different morphologies. The selection of the composition of the solvent opens new research areas for stabilizing materials belonging to different classes of materials (alloys, nitrides, sulfides, borides, etc.). Although high temperatures are used in typical reactor operations, the temperature conditions are very mild compared with other synthesis approaches for making the same crystalline phases. The high-pressure conditions in many of these cases shift the thermodynamic equilibrium into domains that are not achieved by thermal conditions alone.

It should be noted that the definition of "solvothermal synthesis" above is different than that recently reported by Graeve et al., which uses the same definition for the formation of TaC but bases the process on a combustion reaction in an unpressurized, open reaction vessel with no solvent added as an aid to the reaction (see discussion above).[9,10]

Solvothermal reactions include different reaction-types. Most reactions fall under the categories of the following five types: (a) oxidation-reduction, (b) metathesis reactions, (c) hydrolysis, (d) thermolysis, and (e) complex-formation. In our effort, we will primarily involve combinations of types (a) and (b). Solvothermal reactions have been developed in different scientific domains including synthesis of novel materials, processing of functional materials, crystal growth at low-temperature, preparation of micro- or nanocrystallites that are well defined in size and morphology, low-temperature sintering; and thin film deposition.

In recent years, growing R&D activities to form nonoxide nanopowders via solvothermal synthesis have been reported, utilizing either organic or other inorganic solvents (e.g., NH_3, CO_2) under elevated pressures but not necessarily supercritical conditions. Initially, the research was geared toward the synthesis of II-V and II-VI semiconductor and magnetic powders (e.g., GaN[11] and ZnS[6]) and, more recently, the formation of high-temperature phases of ceramic nanopowders has been demonstrated, including the synthesis of TiB_2,[12,13] cubic BN,[14] AlN,[15] and SiC.[16,17] Hence, the formation of boride, carbide, and nitride nanopowders via solvothermal reactions has

already been demonstrated. Examples are illustrated in Figure 1. Figure 2 is a collection of published micrographs of various boride, carbide, and nitride nanoparticles synthesized by solvothermal reactions.

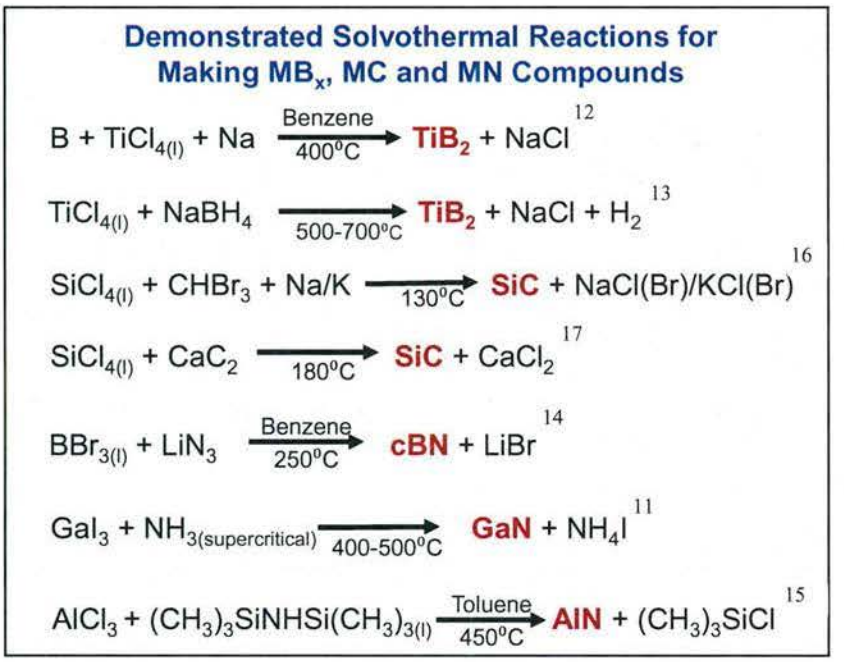

Figure 1. Demonstrated solvothermal reactions for making nonoxide metal borides, carbides, and nitrides that can serve as the basis for similar synthesis of the proposed Zirconium-based UHTC.

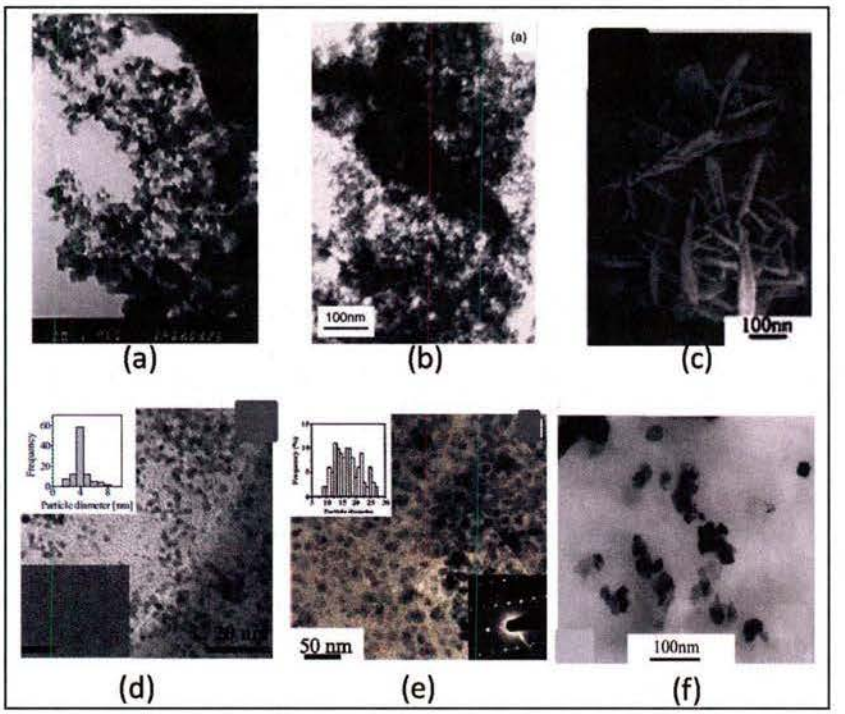

Figure 2. Transmission electron microscopy (TEM) images of nanopowders synthesized by the solvothermal approach: (a) TiB_2,[12] (b) TiB_2,[13] (c) SiC,[17] (d) GaN,[11] (e) AlN,[15] and (f) cBN.[14]

2.2.2 Industrial High-Pressure Synthesis

Many of the reported solvothermal reactions mentioned above were performed in sealed quartz tubes; these limit the quantities that can be produced and therefore are not industrially practical. Furthermore, the pressure conditions developed in such sealed tubes may not be too high considering the low strength of quartz. Large, high-pressure, high-temperature reactor vessels for high-volume production are commonly used in chemical and petrochemical industries. Such reactions are performed under more drastic conditions than anticipated for those proposed here. Hence, we have confidence that the studied reactions are suitable for scale-up. Examples of such high-pressure/temperature mass productions are: NH_3 from H_2 and N_2 (NH_3 is the number-one volume chemical produced worldwide; 150-300 atm, 400-500 °C); MeOH from H_2 and CO (200 atm, 315 °C); hydrocracking (gasoline production; ~ 200 atm, 425 °C); and low-density polyethylene (1000-3600 atm, 150-375 °C).

Several of the solvothermal reactions that were recently reported and are relevant to the planned synthesis of Zr borides, carbides and nitrides were performed in benzene as a solvent. The supercritical conditions for benzene are 47.7 atm at 288.5 °C. Other relevant solvents with their supercritical conditions are ammonia (112 atm, 133 °C), carbon dioxide (72.9 atm, 32 °C), toluene (40 atm, 318.64 °C), and carbon tetrachloride (45 atm, 283°C). These pressure / temperature variables are significantly milder than those used for the large-scale chemical productions mentioned above. Therefore, we have confidence in the viability of scaling up the solvothermal reactions.

2.2.3 Compatibilizing Surface Treatment

Surface modifications by organosilane reagents are common in industrial applications to allow improved adhesion, wettability, electroactivity, and water-repellant qualities, among others. In these cases, the reactive bonding sites are already connected to the characteristic's modifying group.[18]

This approach is not suitable for bonding long or bulky functional groups (e.g., polymers). In most cases, the surface silanization involves functional groups with a carbon chain length of no more than 12 carbon atoms. In order to achieve longer functional groups, techniques have been developed to first apply a coupling agent that has an alkoxysilane group to bond to the particle surface and another reactive group that can initiate polymerization of an organic polymer.[19]

Our group at SRI has considerable expertise in modifying surfaces that include nanoparticles with functional monolayers of bulky organic and biological groups. SRI's approach separates the process into two simple steps.

(a) Bonding a coupling reagent with two dissimilar reactive sites: one that reacts with the substrate exclusively to form a monolayer and a second that is available for selective reactions with the polymer or other organic-containing species.

(b) Bonding the free reactive site of the coupling agent to a large species (polymeric or biological) as illustrated in Figure 3.

These techniques were used to establish polymer nanocomposites with homogeneous nonagglomerated nanoparticles,[20] smudge- and stain-resistant coatings, antibody bonding to phosphor particles, and more. A series of patents has been granted based on this platform, and several patent applications are under evaluation.[21,22]

A major advantage of this platform approach for surface modification is that we can exclusively form a single monolayer or less; thus, no excessive unnecessary layer is formed. The process is performed without removing nanoparticles from a solvent; therefore, the intermediates do not agglomerate or oxidize. This technique will be complementary to the overall formation of nonagglomerated particles.

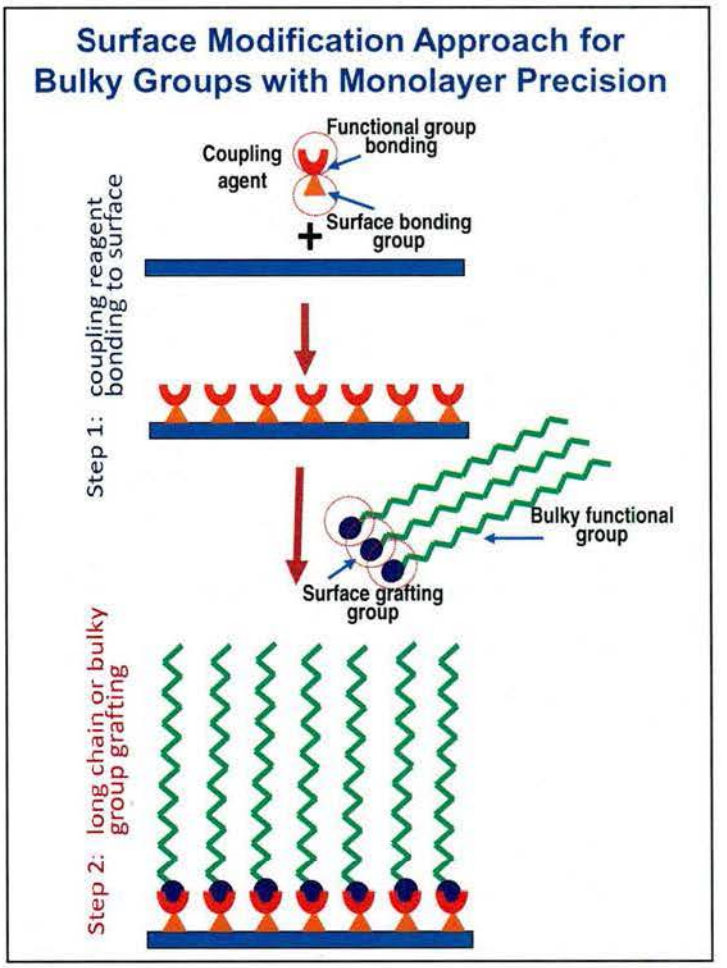

Figure 3. SRI's strategy for covalently bonding bulky surface modifiers at monolayer precision.

A very important advantage in previous work was the strong covalent bonding of the modifier to the substrate's surface. However, strong bonding of a silanol to the UHTC nanoparticles may lead to Si and O inclusion and consequently result in a negative effect. Assuming the formation of spherical ZrB_2 nanoparticles of 50 nm diameter, the surface area of the particles will be roughly 20 m^2/g. If a complete monolayer of a silanol is deposited at the surface, it will introduce about 2 mol% of Si and O to the surface of the particles, which may remain there permanently. During the high-temperature processing of the treated nanoparticles, this may cause the formation of phases of minor ZrO_2 and $ZrSi_2$ or their mixed interstitial phases with the base boride, carbide, or nitride phases. The oxide phase is expected to negatively affect the sinterability.[3] The silicide phase may contribute to the oxidation protection in a manner similar to that of the anticipated performance of SiC in UHTC composites. The Si and O contamination may be removed at ~ 1000 °C in the form of gaseous SiO species. Thus, the fate of Si and O as a function of processing steps must be studied carefully so that we may develop alternative surface treatments as needed.

There is less concern about the linear hydrocarbon groups bonded to the silanization reagents, since they are anticipated to be eliminated by low-temperature decomposition into volatile molecules. In fact, if residual carbon is deposited by pyrolytic reactivity, it may aid in the removal of native oxygen via the formation of CO at ~ 1000-1500 °C.

If necessary, alternative surface modifiers can be employed that do not introduce Si or O. The use of long-chain organic acids, such as stearic acid or acetylacetonate compounds with a long organic group, are expected to form strong complexation with Zr atoms at the nanoparticle surface.[23] Such organic complexes are expected to be vaporized via decomposition at 200-300 °C.

The potential of using organohydroboranes (RBH_2 and R_2BH) is envisioned such that it would interact with Zr-OH groups at the surface and form Zr-O-BR_2 species. These reagents can be easily formed by hydroboration (or purchased commercially). They can be later eliminated via pyrolysis or controlled hydrolysis. "Contamination" of boron is not an issue. We are not aware of any attempt to use this approach elsewhere.

Organoamines are also potential modifiers by forming Zr←:NR_3 adducts at the surface, especially in the case of ZrN, since residual nitrogen will not constitute contamination. However, they may not form a stable enough complexation to the surface, particularly in the presence of moisture.

The above-discussed types of surface modifiers are illustrated in Figure 4.

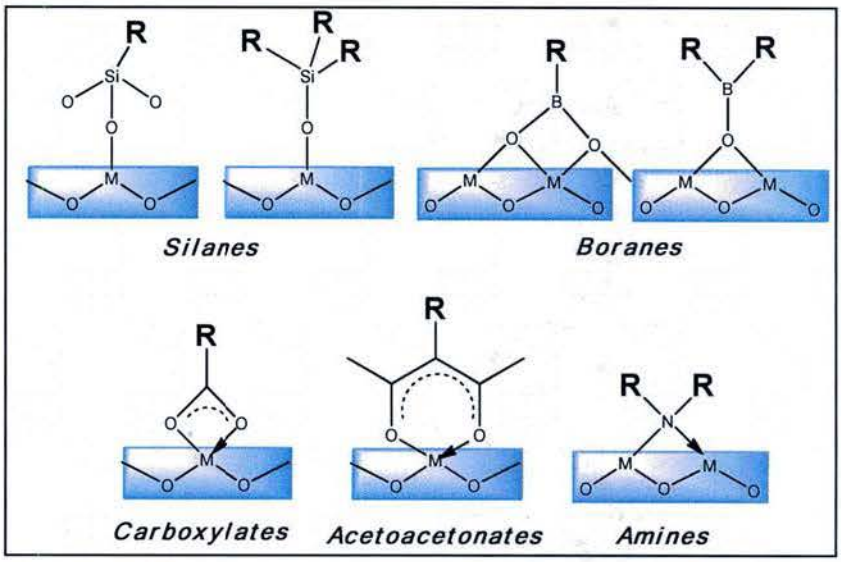

Figure 4. Modifiers with various chemical bonding to the surface's elements. The bonding is either directly to the metallic element or to oxygen of the native oxide/hydroxide layer covering the surface of nonoxide ceramics.

3. TECHNICAL APPROACH

3.1 Introduction

The originally proposed wet approach targeted the elimination of a range of hurdles associated with the formation and processing of UHTC nanoparticles. We will combine the formation of pure nanoparticles by wet chemistry at industrially scalable volumes under relatively mild pressure and temperature. The synthesized and crystallized nanoparticles will be purified from byproducts and transferred for further processing as slurries (without their removal from the solvents) to eliminate agglomerations and oxidative exposure, ease densification, and reduce voids at the green state. In addition, health and safety concerns associated with airborne nanoparticulates will be eliminated.

3.3.1 Solvothermal Synthesis

The original thrust of the proposed work was to synthesize non-agglomerated nanoparticles of UHTC phases that can be transferred without removal from a solvent to a surface-treatment step followed by slurry processing of green-body shapes. We will explore new reactions for making selected borides, nitrides, and boride nanopowders via solvothermal synthesis in the presence of nonaqueous solvents at a temperature range of 200 to 600 °C and pressures of up to 100 atm. Literature reports indicate that some of these reactions can form crystalline nanoparticles even below 200 °C, as shown earlier in Figure 1. Other intriguing reactions that can form borides, carbides, and nitrides are displayed in Figure 5.

We focused on Zr-based UHTC phases, but other elements can be considered per the expressed interest of the Navy. Aside from the fact that nonoxide Zr ceramics are attractive for UHTC applications, the selection of Zr as the focus element is due to the practical availability of reagents containing Zr and literature regarding synthesis of such compounds.

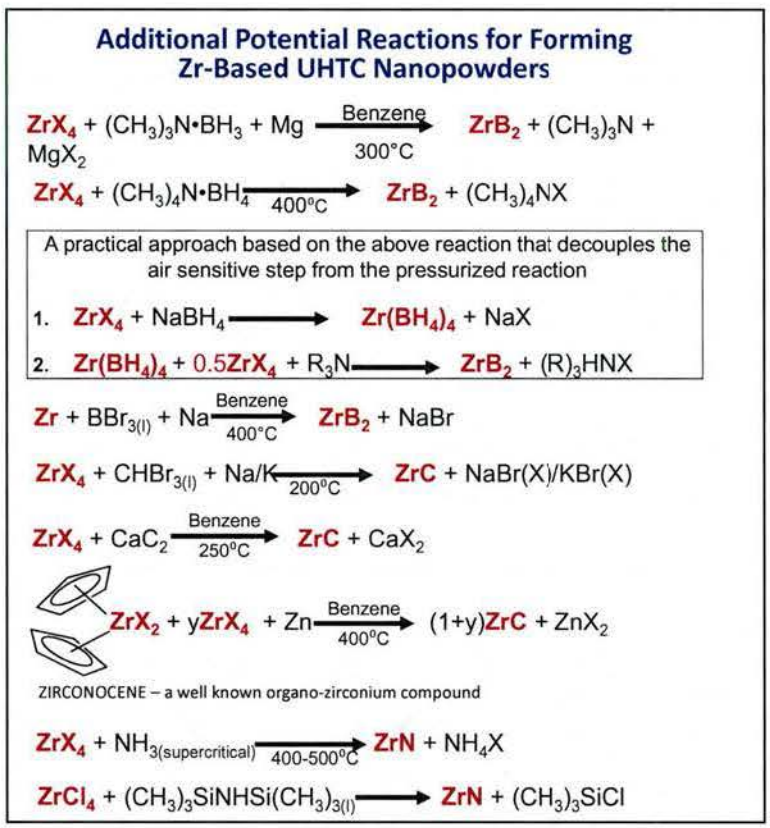

Figure 5. Potential solvothermal reactions for making boride, carbide, and nitride ceramics. Compounds in red are examples of the borides, carbides, and nitrides that will be attempted in the project with zirconium as the focal element.

It is possible that the formation of off-stoichiometry compositions (MB_x and MC_x) may later aid in the densification via reactive sintering. For example, synthesis of substoichiometric borides can support sintering if boron or carbon powder is added to the sintering blend. These additional powders may not be required, as we have demonstrated in previous studies that Zr and Hf can react with a SiC phase to form a mixture of metal boride and metal carbide phases.[24,25] Similarly, the formation of mixed phases, MB_xC_y or MB_xN_y, may be useful in advancing subsequent sintering.

Reaction Variables

Criteria for selecting the potential reactions were initially related to safety issues associated withpracticing the solvothermal reactions and using highly oxidizable reagents (air and moisture sensitive). As the project progressed, we gave preference to reactions that use lower-cost reagents and seem to be scalable. During the study, we considered a variety of variables as discussed below.

Transition metal (Zr) reagents. We assumed that all the reactions in Figure 1 that form boride, carbide, and nitride phases can be performed with other elements such as Zr, Hf, Ta, and W with similar UHTC performance if they are introduced in the form of metal chlorides (MCl_x) or bromides (MBr_x). Possibly, metal nitrates will perform similarly, but the nitrate group may serve as an oxidation element.

Boron and carbon reagents. Carbon and boron sources can be introduced as powders of the elements themselves. This has been demonstrated in forming TiB_2, in which metallic boron powder was used as a reactant. Alternatively, B and C reagents can be added as chloride or bromide compounds, e.g., BBr_3, CCl_4, or CBr_4. The advantages to using the liquid or soluble compounds are that they can be homogeneously mixed at the molecular level, are easily removed after the reactions, and can serve as the solvents themselves.

Hydroboranes ($X{\cdot}BH_3$ adducts, where X can be trialkylamines, ethers, or organosulfides) and ammonium-hydroborate compounds (R_4NBH_4) may be also suitable reagents as shown by the successful reaction of $TiCl_4$ with $NaBH_4$ in Figure 1. In this case, the generated salt byproducts (R_4NCl or R_4NBr) can be removed by dissolving them in polar organic solvents to avoid the need for water as a solvent.

Nitrogen reagents. Suitable nitrogen precursors are most likely be ammonia or ammonia salts. Ammonia is the best choice because it can also serve as the solvent, is very low cost, and its chemical engineering is well established to address safety considerations. Other reagents, such as hydrazine[26] and triazene that were used in previous solvothermal production of nitrides, are inferior selections due to their health-hazard and explosive potential as well as their significantly higher cost.

Other approaches using Li_3N as the source of nitrogen also present safety hazards and are expensive.[27] One alternative may be to use a high-boiling-point solvent like acetamide, CH_3CONH_2, that can potentially serve as an ammonia donor and oxygen scavenger at elevated temperatures. Finally, a benign source of nitrogen can be disilazane, $(CH_3)_3SiNH(CH_3)_3$, which is a liquid that can serve also as solvent and its byproduct, $(CH_3)_3SiCl$, is volatile and can elegantly remove the Cl after the reaction.

Reducing and coupling agents. The use of the reducing agents Na and K has been described in the literature.[12,16] We will attempt to replace these with less air-sensitive elements such as Ca,

CaH_2, and Mg. The reactions of halometallic and halocarbon compounds in the presence of reducing agents are defined as "coupling reactions" and are similar to well-known C-C, C-Si, and Si-Si coupling reactions such as the Wurtz reaction[28] (in the presence of Na and Na/K) or Grignard reaction[29] (Mg) as illustrated in Figure 6. The latter coupling reagent, Mg, is less sensitive to oxygen and moisture than Na and Na/K and may be more practical for scale-up if found to be reactive. Also, $NaBH_4$ can be used either as a reducing agent or as both the boron source and reducing agent.

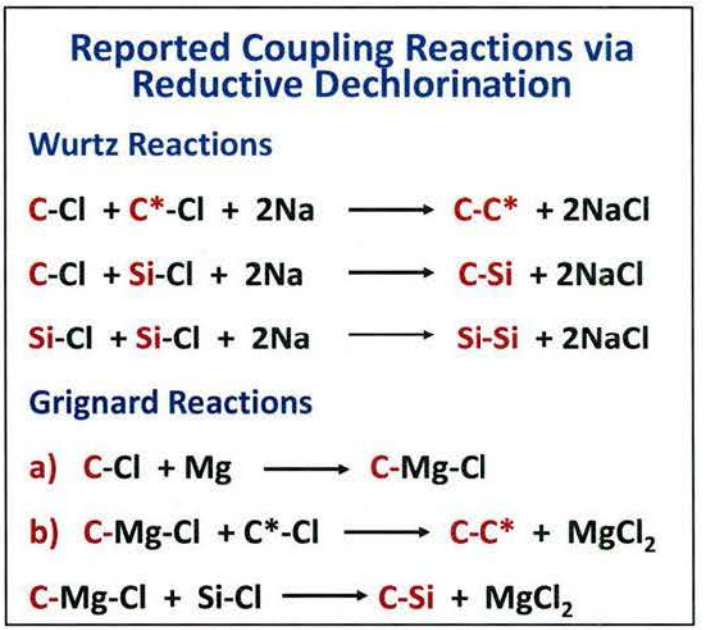

Figure 6. Reductive coupling reactions of halocarbon and halosilanes in which efficient formation of coupled C-C, C-Si, and Si-Si bonds has been scaled-up to commercial levels.

Solvents. Literature reports indicate that some of these reactions can form nanoparticles even below 200 °C. Such conditions are convenient for using simple organic solvents as the reaction media. Benzene is a good candidate for solvothermal reactions;[12,14] however, we considered selecting other hydrocarbon or aromatic solvents since benzene is considered carcinogenic. If we must use benzene, appropriate health and safety procedures for handling it already exist because benzene is used heavily by the chemical industry as a starting reagent.

The boiling point of such organic solvents may play a major role in regulating the excess pressure in the pressurized reactors. However, if significantly higher pressures are needed for boosting the selected reactions, the reactors can be pressurized with N or Ar as is common in industrial organic fuel, petrochemical, and polyhydrocarbon mass-scale reactors.

Some of the reagents are liquids under the applied pressure conditions and can also serve as the solvent medium for the reactions (e.g., NH_3, BBr_3, CCl_4, and CBr_4). This option may be useful for forming supercritical conditions similar to the powerful hydrothermal reactions practiced in the formation of oxide nanoparticles.

The use of other common halocarbon solvents, such as $CHCl_3$ (chloroform) and CH_2Cl_2, can be considered as both solvents and sources for C. These may be of interest since halide (chloride) byproducts (and consequently the reducing agents) need to be removed from the product mixture after the reaction is completed; however, these may lead to the formation of corrosive HCl, which will make them inconvenient for industrial scale-up.

Nanoparticle purification. The generated nanoparticles can be purified at industrial scale via wet techniques without drying the nanoparticles or exposing them to oxidation. Therefore, the purified nanoparticles can be surface treated in a continuous mode and further prepared for the sintering of a molded structure—all under environmentally controlled conditions.

3.1.2 Surface-Treated Nanoparticles for Advancing UHTC Processing

The second thrust of our work is *in-situ* surface treatment of the formed nanoparticles by wet techniques. Typically, nanoparticles agglomerate strongly due to their very high surface area and electrostatic forces. While most current synthesis techniques for UHTC nanoparticles lead to hard agglomerations due to fusion between particles that cannot be broken down into individual nanoparticles, agglomerations yield high-viscosity processing slurries, limiting inhomogeneity and the formation of void defects during sintering.

Surface treatment by means of bonding monolayers of long organic polymeric chains to the individual nanoparticle surfaces will improve the dispersion of the nanoparticles in solvents and reduce or eliminate the need for molding binders. Simultaneously, the monolayers will aid oxidation resistance by preventing hydrolytic processing and oxygen diffusion at ambient temperatures.

SRI's surface-modification platform. We planned to first explore the surface-modification platform that has evolved in our lab over the past 10 years. This platform has been described in a series of patents and patent applications involving the formation of nanoparticle-polymer homogeneous composites and the alteration of physical surface characteristics. This SRI surface-modification platform (see Figure 3) allows the chemical bonding of polymers and oligomers to inorganic surfaces including nanoparticles. The techniques allow forming "monolayers" of bonded polymers at various surfaces including inorganic nanoparticles without excessive deposition of the polymeric films. We have demonstrated formation of films that enhance the dispersion of nanoparticles and dramatically reduce slurry viscosities and do not exhibit the typical agglomerations associated with the incorporation of nanopowders. No drying time is required for the nanoparticles between the synthesis, purification, surface-treatment, and UHTC formulation steps. Potentially, the surface modification can be performed before any byproducts (such as inorganic salts) are removed from the synthesis mixture to prevent oxidation.

We planned to use low-molecular weight hydrocarbons as the functional groups to be bonded to the surface. The organically modified surface can provide better compatibility with the slurry solvents, add lubricity (hence lowering the viscosity) during the green-body processing, and reduce the surface oxidation capability. Such long linear and nonaromatic organic functional groups can be cleanly eliminated by decomposition to hydrocarbon gases at around 200-300 °C during the firing of the processed structure, leaving a negligible excess of carbon. However, carbon residue at the level of 1% may be beneficial to: (a) "etch" native oxide layer around the UHTC particles and ease the sintering or (b) form a minor carbide phase if in contact with borides or nitrides.

In previous activities, we used reactive organo-alkoxysilane reagents to bond to the surface of nanoparticles by forming M-O-Si-organic species at the surface. In this case, traces of Si (up to 2 mol%) can accumulate, leading to the formation of a minute silicide phase, which can serve as a part of the overall silica forming phase. Such efficient use of silicide $MoSi_2$ has been studied by UHTC research groups.[30,31]

3.2 Original Approach (Years 1&2)

We employed an emerging solvothermal synthesis approach performed in industrially scalable closed reactors at temperatures ranging between 200 and 700 °C. The synthesis incorporates wet filtration and purification under a controlled atmosphere when necessary.

We expect the purified nanoparticle slurries to be surface-treated without being removed from the solvent or exposed to an oxidative environment. The resultant monolayer film is designed to

- Enhance dispersion
- Prevent agglomeration
- Ease the formulation and compaction steps
- Be removable via volatilization at the green-body processing stage

Solvothermal synthesis is similar to hydrothermal reactions performed at subcritical and supercritical conditions, where non-aqueous solutions are employed instead of water. It allows reactions under reducing and oxygen-free environments and further processing of the evolved non-agglomerated nanoparticles in slurries without solvent removal (which leads to agglomeration) or exposure to oxidizing environments before nanoparticles are processed to become structural components.

The surface modification of particles and nanoparticles for easing their processing has been studied to a limited extent with more conventional ceramic particulates; however, such studies were not reported for UHTC elements. We planned to develop surface modifiers that will not contaminate the final processed composites.

3.2 Revised Approach (Year 3)

Due to difficulties in achieving the original objective, the objective in the third year has been revised, per ONR's program manager request. The newly selected process was to use newly developed polymeric precursors to boron nitride (BN) and boron-carbonitride (BCN) as weak interfacial coatings for silicon carbide (SiC) in SiC/SiC composites. This revision was based on discussions with the project Program Manager, using the advantage of the development of polymeric precursors to BN and BCN in another project, performed in parallel, for a completely different application/

4. RESULTS – RESEARCH ACTIVITIES (YEARS 1&2)

4.1 Summary of Activities (Years 1 & 2)

The research in Year 1 included the following activities.

- Reactor system and procedure handling modifications (*significant effort in Year 1*)
- Two rounds of synthesis experiments and evaluation geared to the synthesis of ZrB_2 with reference to the literature reporting of similar TiB_2 synthesis (*before and after overhauling the reactor system*)
- Powder product analysis and heat treatment
- Surface modification reactions for ZrB_2 nanoparticles
- Study of the suspension of ZrB_2 nanoparticles in a broad range of solvents

The research in Year 2 included the following activities.

- Additional reactor system and procedure-handling modifications (*minor effort in Year 2*)
- Synthesis efforts to produce Zr-based nanopowders that contain B, N, and C
- Most of the initial effort focused on ZrB_2
- Enhanced activities related to ZrN (*not completed by the end of Year 2*)
- The effort to form ZrC started at the end Year 2 (*not completed*)
- Activities aimed at solving the problem of carbon phase, derived from the organic solvents in the reaction under extreme conditions
- A minor activity to assess the reactions between metallic Zr powder and polymer-derived ceramics consisting of BN and BN-C amorphous networks

Below, we discuss our progress in each of these areas.

4.2 Synthesis Activities (Years 1&2)

4.2.1 Reaction Assembly Setup

We assembled the reactor system to be used in a mode where the reactor itself can be disconnected and moved in and out of a dry box for loading the sensitive reagents and unloading the reaction products. This effort also involved significant health and safety activities that are mandatory at SRI at the beginning of new projects. For this specific project, the safety assessment was a critical issue, prompted by the need to perform high-pressure reactions (up to 5000 psi) at high temperatures (up to 500 °C) with fire and chemical hazardous reagents such as metallic sodium, hydrochloride-releasing salts, and flammable organic solvents. For this project, we had to rearrange the enclosed lab space so the reactor can be operated and monitored remotely. We also purchased new reactor accessories to ensure that we are not using deteriorated ones.

Our initial design used a 300 ml stirred Hastalloy C high-pressure reactor (Autoclave Engineers, Inc.) equipped with a quartz liner and an internal thermocouple. This reactor was rated to 5,000 psi at 500 °C, which is the anticipated maximum temperature at which the reactor would be used, based on the moles of reactants and the reactor volume.

The seals in the stirred reactor design became problematic, so this reactor was replaced with a non-stirred reactor until a better solution is found for the sealing at the most demanding temperature/pressure conditions. The heated reactor setup was placed in an explosion containment room, and the reactor was controlled and monitored electronically for pressure and temperature and visually through a thick plate of shutter-proof polycarbonate.

Since our project deals with handling both reactive reagents and unclear post-reaction products, which may be air and moisture sensitive, health and safety issues are critical. We retrofitted a designated dry box to allow loading and unloading of the reagents and consequent reaction products inside an inert environment.

4.2.2 Synthesis and Analysis Effort

Synthesis of ZrB_2 Nanoparticles

The initial attempts to synthesize ZrB_2 nanoparticles were based on a protocol for the solvothermal synthesis of TiB_2 reported by Gu et al.[12] Our protocol employed benzene as a solvent for performing the various reactions, as it was used in other reported solvothermal reactions.

The anticipated reaction was:

$$ZrCl_4 + 2\,B + 4.4\,Na\ (\text{in benzene}) \longrightarrow ZrB_2 + 4\,NaCl \qquad (1)$$

We also evaluated another reaction:

$$ZrCl_4 + 2\,BBr_3 + 11.0\,Na\ (\text{in benzene}) \longrightarrow ZrB_2 + 4\,NaCl + 6\,NaBr \qquad (2)$$

In a typical experiment, the reactor is charged with 5 grams of anhydrous $ZrCl_4$ (21.5 mmol), 0.471 grams of boron (43.5 mmol), 2.35 grams of sodium metal (102.3 mmol) and 100 ml of anhydrous benzene in a controlled atmosphere chamber containing dry nitrogen. Typical oxygen and moisture levels are in the single ppm range. The reactor top is then bolted into place and the reactor is removed from the controlled atmosphere box and connected to a purge, vent line, and pressure transducer line via quick-connect connectors. The temperature is then increased at a controlled rate, typically 2 °C/min, to the desired temperature and held for the appropriate length of time. The pressure of the reactor is monitored to inspect leakage and avoid overpressure of the reactor. After the desired soak time at temperature, the reactor is allowed to cool naturally. The reactor is then transferred back into the controlled atmosphere box and opened; the quartz liner is removed, and the contents of the reaction are collected and washed to isolate the ceramic nanopowders from the large amount of salt byproduct.

A portion of the crude reaction mixture is removed from the controlled atmosphere box and the solids are collected by centrifugation for further processing/analysis. The solids are washed with acetone and dried. X-ray diffraction (XRD) analysis is dominated, as expected, by the presence of NaCl. The samples are then washed with water followed by acetone and dried. The water also completes the decomposition of any residual metallic sodium.

Based on the initial analyses, we realized that the products contained excessive amounts of oxygen. Simultaneously, we realized that the self-generated pressure was not as high as expected based on reported literature about benzene vapor pressure as a function of temperature—an indicator for leaks in the reactor system. In addition, we had several incidents of a major drop in pressure, and we noticed deterioration of the seals. Consequently, we decided to upgrade components of the reactor system, and then systematically test it for pressure/temperature stability prior to further synthesis activities.

4.2.3 Upgrading the Reactor System

At this stage, we assigned a chemical engineer from our lab to inspect the high-pressure reactor system and upgrade it in a stepwise fashion (to save allocated budget for this effort). The chemical engineer has previous experience in setting up high temperature/pressure reactor systems. The work involved step-by-step checking and fixing all potential leaking spots during the handling and the operation of the high pressure/temperature reactor. It required more iterations and time than anticipated, but we succeeded in minimizing the expenses associated with this upgrade. For the time being, we have removed the stirring system to eliminate potential leaking with this type of reactor head. The system is now expected to withstand a pressure of over 4000 psi at 400 °C and go to 500 °C at a lower pressure. The critical point for benzene is 710 psi at 289 °C. The pressure profile of benzene heated in the reactor (with no additional reagents) is shown in Figure 7.

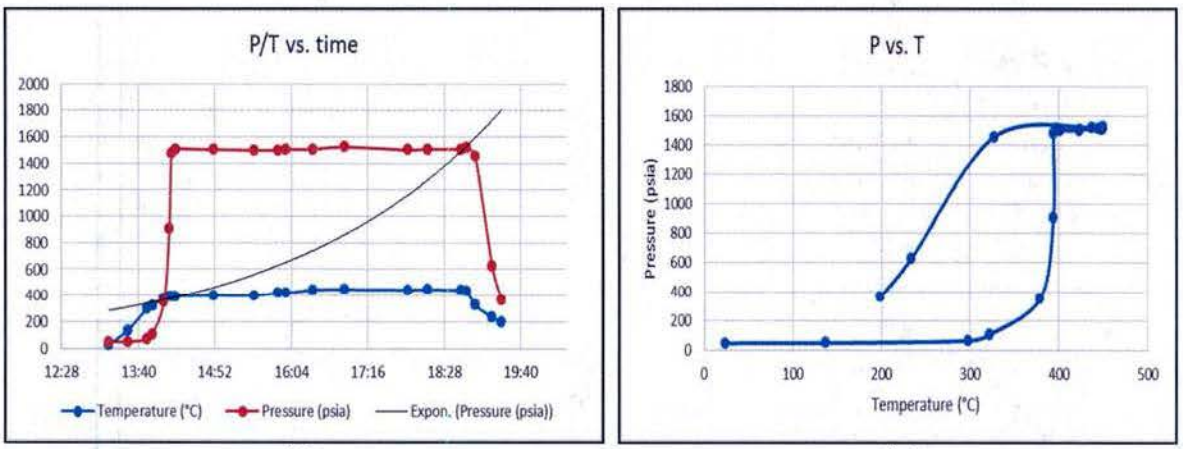

(a) (b)

Figure 7. The pressure-temperature relationship of Benzene in the high pressure reactor

4.2.4 Beginning a Second Round of High-Pressure Reactions

A second round of reaction experiments were performed after the system modifications and upgrades. The reactor performed well, and the reliability concerning oxidation during the reaction itself has been achieved. Since we still identified a high level of oxygen, we assessed other aspects of the synthesis that could introduce oxygen. Water washing of the reaction product to quench the excess sodium and remove sodium chloride was suspected as an oxygen donor and was further assessed as described later in the report.

Since our early tests for forming ZrB_2 were based on literature regarding the formation of TiB_2, and our results did not match our anticipated observations, we decided to run a similar reaction to the reported literature for comparative purposes:

$$TiCl_4 + 2\,B + 4.4\,Na\ (\text{in benzene}) \longrightarrow TiB_2 + 4\,NaCl \quad (3)$$

We also added another reaction for forming ZrB_2 where we use Zr as a reagent:

$$Zr + 2\,BBr_3 + 6.6\,Na\ (\text{in benzene}) \longrightarrow ZrB_2 + 4\,NaCl + 6\,NaBr \quad (4)$$

In all of these reactions, we observed the disappearance of sodium and formation of (a) Zr- (or Ti-) based black nanopowders (agglomerated, thus far) and (b) sodium salts. However, in contrast to the reported literature, we did not detect any crystalline phases in the as-synthesized powders. Instead, we observed excess oxygen and carbon content in the solid products. We still noticed excessive oxygen while operating the improved reactor system and therefore suspected that it was generated during the post-reaction washing of the sodium salts with water. We developed a revised processing procedure in which we used dry formamide and glycerol (glycerin). As solvents, these exhibit significant dissolution capability for sodium chloride. From this, we assessed that the oxygen level had, indeed, been reduced, while NaCl removal was sufficient.

The carbon formation from the organic solvents was not reported by the previous literature reporting similar solvothermal reactions. Potentially, the internal temperature in the reported literature and our reactions are different. In our case, we measured the internal temperature; in the literature reports, the reactants were hermetically sealed in a quartz vessel and the temperature inside was not actually monitored. Also, catalytic effects imposed by the stainless steel walls of our reactor may play a role in the carbon incorporation. However, when we heated benzene alone under the same reaction conditions, we did not observe its decomposition at all. Thus, it is clear that the reactive reactants and their by-product may have a very active role in the benzene (or even hydrocarbon) condensation. Indeed, $TiCl_4$ and its variations are known catalysts for olefin polymerization and aromatic compound alkylation (Friedel-Craft reaction).

4.2.5 Additional Information about Nanopowder Synthesis

The initial assumption was that we should obtain similar reactions and reactivities when switching from $TiCl_4$ to $ZrCl_4$ with one caveat—$TiCl_4$ is a liquid soluble in benzene, while $ZrCl_4$ is a non-soluble solid. In an attempt to assess whether the formation of carbon and excess oxygen are associated with the shift from using $TiCl_4$ to $ZrCl_4$, we repeated the reported procedures for

making TiB_2 that had been mostly performed in small quartz tubes that were sealed by fusing the quartz with a torch.

The observations revealed that:

- The reactivity is high, and the reactions include the disappearance of the reactive sodium metal and the mass formation of NaCl (and NaBr in one case).
- Nanoparticles are indeed formed in all the different solvothermal reactions we have performed.
- The benzene solution does not show any soluble organic products (intermediates) that could be formed by decomposing or condensing the benzene itself under the very harsh conditions (high temperature and pressure, reductive and oxidative agents). Thus, if a carbon phase is formed, its intermediates are very unstable and further react to form the solid material.

Our observations also revealed two major differences from the reported literature:

- The powder products (black in all cases) do not possess any crystalline phases at the end of the reactions. The phases are formed only by further heating the powders to 1000 and 1500 °C.
- There is an excessive level of oxygen present, which we initially attributed to leaks in the reactor under high pressure.
- We discovered that, at least in Reaction (2), we ended with very high carbon content, which is then responsible for the formation of a significant phase of zirconium carbide (ZrC) via carbothermal reduction at temperatures above 1200 °C. This means that benzene has indeed reacted with either the zirconium reagent, metallic sodium, or itself to form a solid species containing carbon.
- Reaction of $TiCl_4$ with B (Reaction 3), which repeats the reported literature (except the reactor system), also indicates the absence of crystalline phases before being heated at higher temperature and the presence of a significant level of oxygen and some free carbon.

Based on the above observations, we suspected that either the reaction reagents were contaminated with oxygen, or washing the NaCl away by water leads to excessive oxidation. We therefore assessed the use of formamide and glycerol as potential solvents for removing the NaCl without exposure to excessive amounts of water. Coincidentally, these two solvents have excellent suspension capabilities that may be suitable for preventing agglomeration of the nanoparticles, as discussed earlier.

We also assessed the option of oxygen impurities in the reaction reagents. Analysis of the commercial boron powder indicated it contains about 1.5 wt% of oxygen, which is very difficult to eliminate; however, it did not explain the presence of over 10 wt% oxygen in the final quantitatively made product.

4.3 Suspensions of ZrB_2 Nanoparticles in Organic Solutions

A second objective in the project planning is to generate suspensions of the developed nanoparticles in solvents for preventing non-reversible agglomerations prior to the powder processing. Due to the high surface area and oxidation sensitivity of the nanoparticles, their processing in organic solvents is considered to be advantageous with final evaporation of the solvent after all the powders and additives are homogeneously mixed.

The work in this effort was performed with commercially available ZrB_2 nanopowder with average particle size of 50 nm (Purchased from a Chinese source). The powder did not contain significant hard agglomerations.

4.3.1 Attempts to Bond Surface Modifiers

In our initial attempts, we have assessed the covalent binding of organosilane surface modifiers used for compatibilization and functionalization purposes. We also tested a few complexation reagents that cannot covalently bond to the surface. Instead they can form strong chelation bonding at the surface. The reagents that were tested are

- octyltrichlorosilane
- dodecyltrichlorosilane
- dodecyltrialkoxysilane
- diphenyldichlorosilane
- allyltriethoxysilane
- aminopropyltriethoxysilane
- aminoethyl-aminopropytrialkoxysilane

The amino-organosilanes that were deposited are used as coupling agents for further reactivity of their amino functional groups with compounds containing carboxylic acid, epoxy, isocyanate and other active organic groups.

All the above tested reagents generated no or very slight bonding to the surface after we washed the treated particles with additional toluene. Dodecyltrichlorosilane and diphenylchlorosilane treatments seemed to slightly improve the suspension. These reagents are characterized by both Si-Cl highly reactive groups and a large organophilic functional groups. However, we could not detect their presence at the nanoparticle surfaces with Fourier transform infrared spectroscopy (FTIR) analysis, suggesting that their presence at the surface is very low.

We planned to assess a series of organic chelating reagents, which were mostly consisted of carboxylic acid, amines, ketones and combinations thereof (for example, natural amino acids, amino caproic acid, hexandinitrile, dicyanobenzene, phthalic acid, acetylacetone). However, we did not execute these plans after revealing that some organic solvents are excellent medium for suspending the Zr containing nanoparticles.

Examples for Surface Modifying Treatment

This evaluation was performed by following surface treatment approaches of nanoparticles that were previously developed at SRI, using alkoxysilane and chlorosilane reagents with long organic groups such as dodecyl (12 C) and octyl (8 C). The analysis was performed by FTIR, primarily to look for the appearance of any signals due to the presence of C-H of the organic chain of the silane agent. As an example, the C-H region for dodecyl trichlorosilane (DTClS) is shown in Figure 8. If the surface modification rendered to be successful, we expected to see signal intensity in the same spectral region as the C-H observed in the unbound silane. In the case of the alkoxysilane reagent, we have not seen any evidence of the anticipated absorption above the noise level, indicating that this reaction was not successful. In the case of the chlorosilane, there was an indication for surface modification by the appearance of very low intensity signals in the appropriate spectral region (2800-3100 wavenumbers). This is a very low level of modifier bonding to nanoparticles based on previous experience. The reaction time for this experiment was 3 hours.

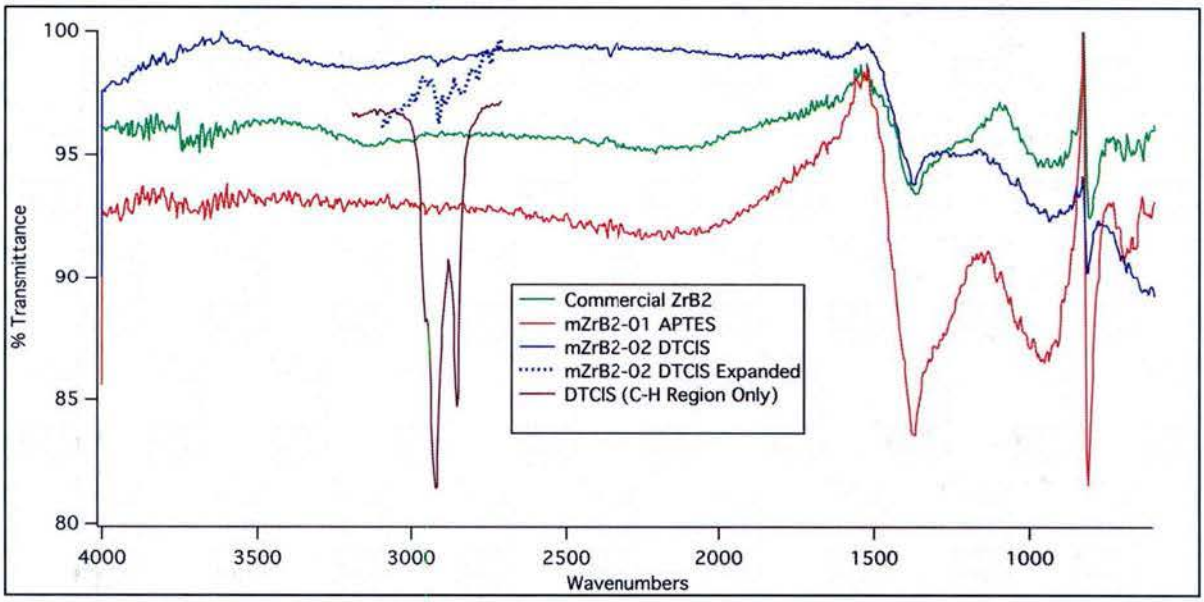

Figure 8. FTIR of commercial ZrB_2 nanopowders and results from alkoxysilane and chlorosilane surface treatment

4.3.2 Suspension in Various Solvents

In parallel, we evaluated the suspension of ZrB_2 nanoparticles in various solvents. Good suspensions of nanoparticles indicate that the particles are not significantly agglomerated. We actually had very promising results, finding several solvents that are superiorly suspending the nanoparticles over other typical solvents. All the solvents are polar ones as a few attempts to use cyclohexane or toluene demonstrated very poor suspension capabilities.

Table 1 ranks the various solvents with lower numbers indicating better suspension. The best solvents as of now are acetonitrile, formamide, glycerin (a very viscous solvent), acetone and tetrahydrofuran (THF). There is no direct correlation between the suspension capability and the polarity or the type of the functional group, although all the best solvents are polar in their characteristics. Thus, the affinity is not just a function of the particle surface polarity or acidity.

Table 1: Solvent ranking for suspending ZrB_2 nanoparticles

Good Suspending Solvents	Relative Ranking	Medium Suspending Solvents	Relative Ranking	Bad Suspending Solvents	Relative Ranking
Glycerin (glycerol)	1	Acetylacetone	6	Isopropanol	11
Acetonitrile	2	Water	7	Ethanol	12
Formamide	3	Ethoxyethanol	8	Methoxyethanol	13
Acetone	4	Methyl etheyl ketone (MEK)	9	Dimethylformamide (DMF)	14
Tetrahydrofurane (THF)	5	N-methyl pyrrolidone (NMP)	10	Toluene	15

These observations are encouraging and can aid in the processing of ZrB_2 nanoparticles, once synthesized and processed without a drying step. Furthermore, we consider formamide and glycerol as solvents capable of dissolving sodium salts in non-aqueous conditions. This capability may be critical, as we currently suspect that washing the sodium salts with water introduce high level of oxygen into the nanoparticulate product. This problem and its potential solution are further discussed later.

To further validate the suspension capability as a measure of non-agglomeration of the nanoparticles, we run a series of particle size analyses of the commercial ZrB_2 nanoparticles in various solvents. We have used a Horiba Particle Size Analyzer that assesses the particle size based on a static light scattering technique that uses centrifugation. The results shown in Figure 9 indicate a strong correlation between the suspension observation and agglomeration of the particles in various solvents. Inadequate solvents show significant fraction of particles in the range of a few to tens of microns, indicating the formation of large agglomerates. In contrast, good suspending solvents, show very little agglomerations above 1 micron.

4.4 Powder Product Analysis

4.4.1 Analysis of Reaction Products before Upgrading the Reactor System

We used the following techniques for evaluating the synthesized powders: X-Ray Powder Diffraction (XRD), Thermal Gravimetric Analysis (TGA), elemental analysis, Fourier Transform Infra Red (FTIR), Scanning Electron Microscopy (SEM) with Energy Dispersive Spectroscopy (EDS) and particle size analysis.

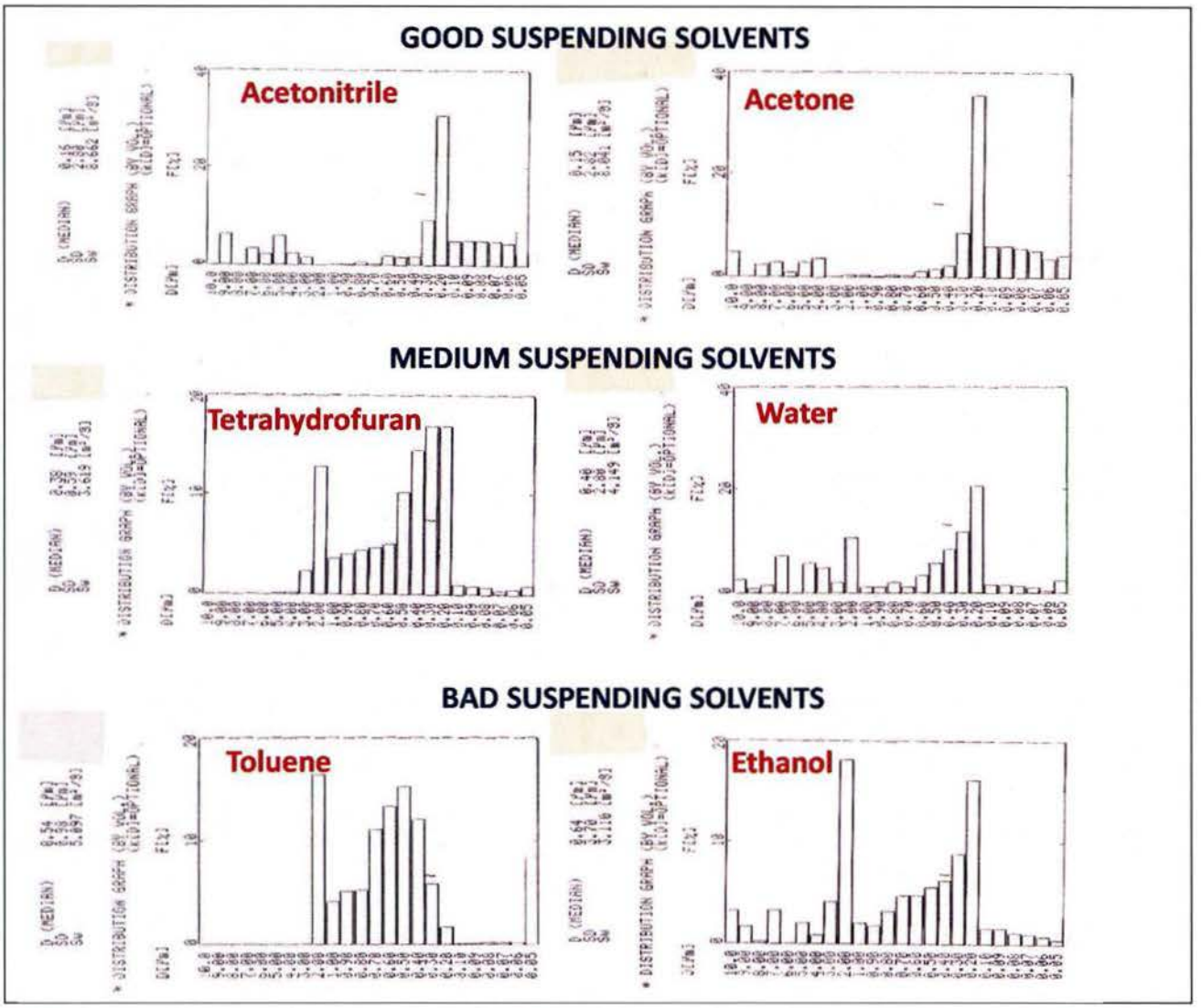

Figure 9. Particle size analysis using a centrifugation technique can be used to estimate the potential of solvents to suspend nanoparticles. While good solvents reveal high population of particles in the submicron regime, the bad solvents show significant agglomerate in the 1 to 10 microns and low fraction of submicron particles.

Note that large peaks at 2.0 and 0.2 microns are exaggerated due to non-linear acceleration of the centrifuge at these points.

At the early stage of the research (before upgrading the reactor system), we focused on Reaction (1), following the reported literature for TiB_2 synthesis under solvothermal reaction conditions.[12] A black powder product consisting of slightly agglomerated nanoparticles was obtained. There was no metallic sodium visible in the reaction mixture although a slight bubbling reactivity was observed when water was added for removing the NaCl byproduct. We could not detect free boron powder since it is amorphous and does not give an XRD signature.

The product mixture did not contain crystallized ZrB_2 according to XRD analysis (see Figure 10a). This is in contrast to the literature reported for similar TiB_2 synthesis. A washed product that was further heated to 1000°C revealed XRD signature of ZrO_2 (Figure 10b). A strong crystalline ZrB_2 pattern was detected only when the sample was further heated to 1500°C as

shown in Figure 10c. The crystalline phase of ZrB_2 was the sole phase in one case, while in others, it appeared with low levels of zirconium oxides (including Na_2ZrO_3).

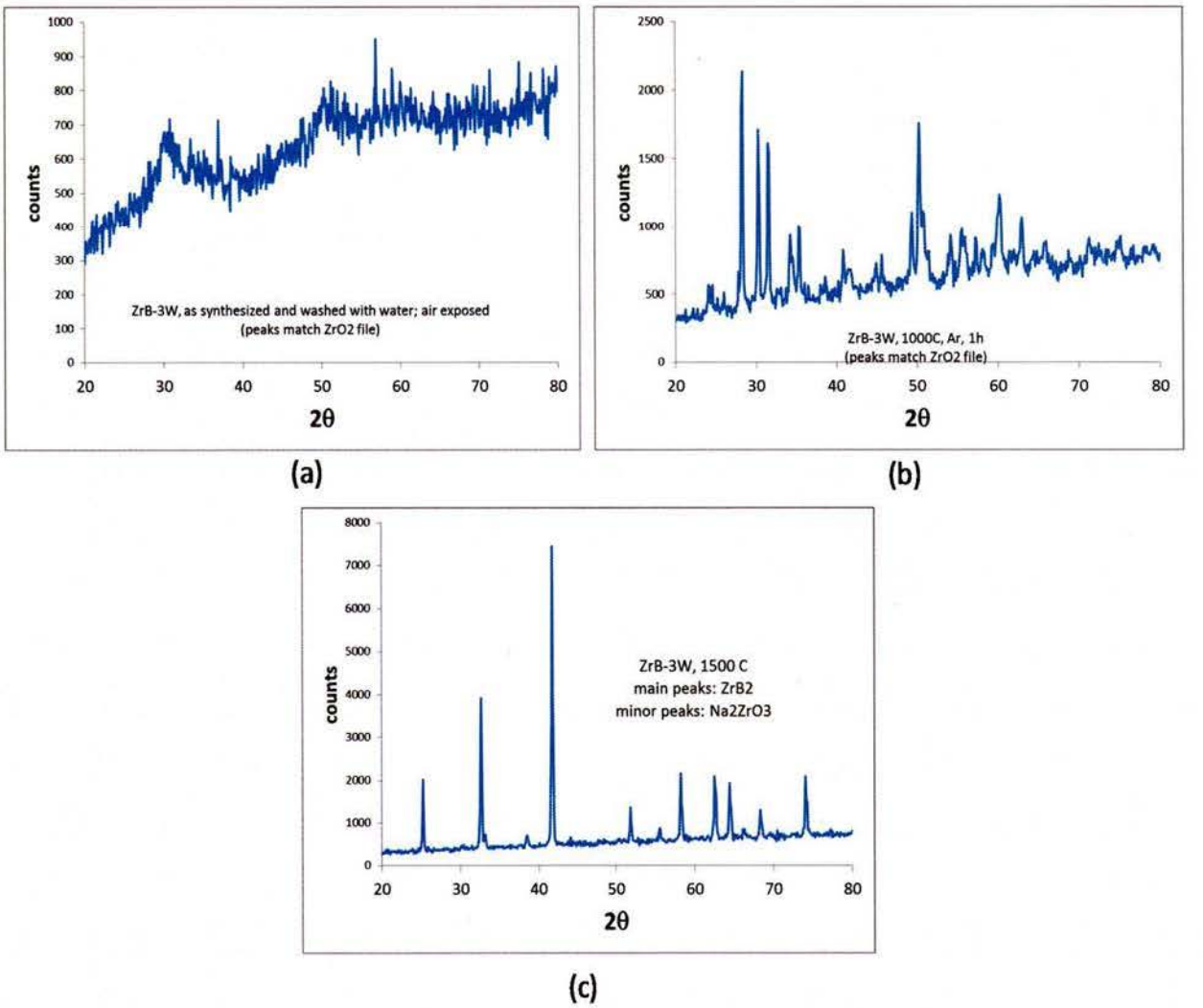

Figure 10. The XRD spectra of a typical reaction after (a) synthesis and washing off NaCl, (b) heating to 1000 ºC, and (c) heating to 1500 ºC.

Although the oxide phases at low temperatures can be minor phases due to oxygen contamination or represent surface contamination while the rest of the boride material is still amorphous, we have indicated by EDS the presence of significant level of oxygen. Therefore, we assumed that the ZrB_2 phase formation at high temperature was the result of borothermal reaction of ZrO_2 with residual metallic boron as shown in Reactions (5) and (6), where BO_x vapors are the byproducts:

$$ZrO_2 + 4B \longrightarrow ZrB_2 + 2BO_{(g)} \quad \text{(yield of 68wt\% calculated)} \qquad (5)$$

$$ZrO_2 + 3B \longrightarrow ZrB_2 + 2BO_{x(g)} \text{ (yield of 73wt\% calculated)} \quad (6)$$

Later in our research, we revealed that significant levels of carbon are also present in the powdery product, and currently, we also postulate Reaction (7):

$$ZrB_{(2-x)}O_{(x)} + xC \longrightarrow ZrB_2 + ZrC \ (+ ZrB_xC_y?) + xCO(g) \quad (7)$$

We observed weight loss in the range of 10-15 wt%, when the washed product powders were heated to 1000 °C, and 35-37 wt% when heated from 1000 °C to 1500 °C. The later range is within the expectation for borothermal or carbothermal reductions.

The early stage FTIR analyses supported the conclusions from the XRD analysis, indicating that ZrB_2 was not formed in the initial solvothermal reaction but formed during carbothermal or borothermal reduction at 1500 °C. The FTIR analysis consisted of casting thin films of powder solutions over pieces of intrinsic silicon wafer substrates and evaluating the IR spectra in the transmission mode. It was not obvious if any Zr-based oxides were generated from the FTIR of the as-made products. For example, ZrB2-03W shown in Figure 11 was rather featureless and may have indicated the formation of mixed Zr-B-O-C phases. The solvothermal reaction product heated to 1000 °C (sample ZrB_2-03W 1000 °C) had features very similar to a sample of commercial ZrO_2 obtained from Alfa Chemical as well as that of an oxidized nanoparticulate ZrB_2 that was commercially obtained (see Figure 11). The FTIR of the solvothermal product heated to 1500 °C clearly indicated that the ZrO_2 generated at lower temperatures is no longer present.

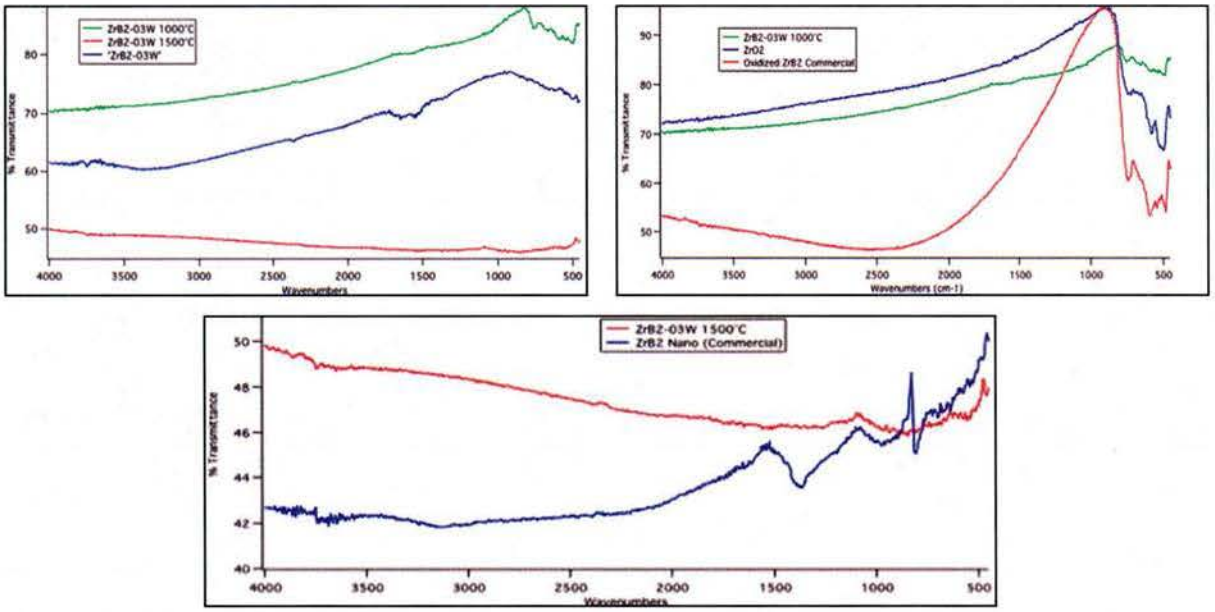

Figure 11. FTIR of solvothermal product and subsequent thermal products

Microstructure analysis revealed the formation of spherical nanoparticles in the range below 100 nm. They were quite uniform in their size and currently still agglomerated, as anticipated after complete drying or if an oxide phase binds them together (see Figure 12). They remained nanosized after heating to 1500 °C, but their morphology turned into orthorhombic crystalline structures (Figure 13).

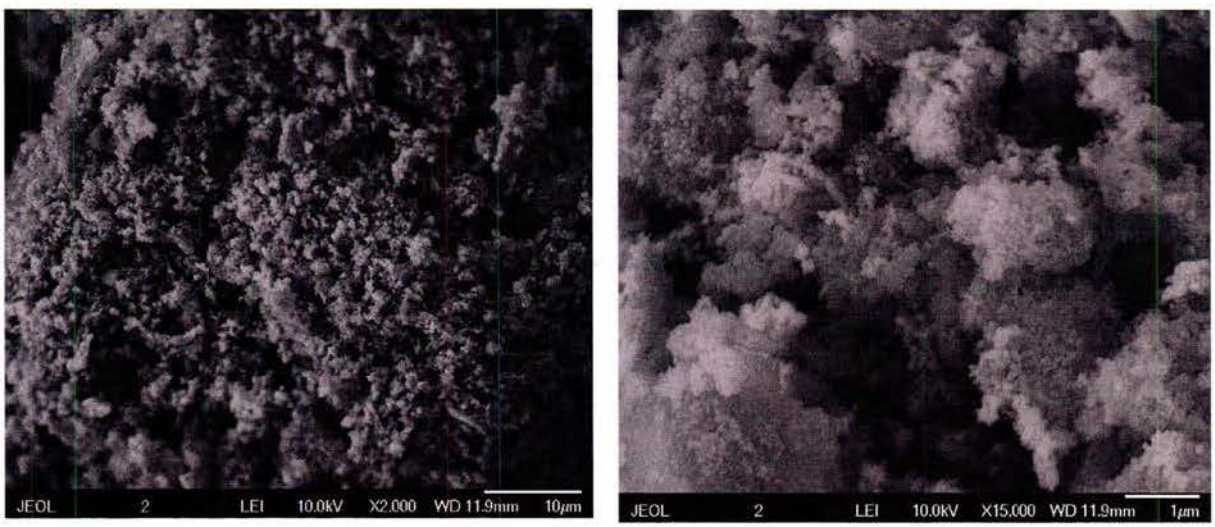

Figure 12. Nanopowder from Reaction (1) after heating at 1000 °C

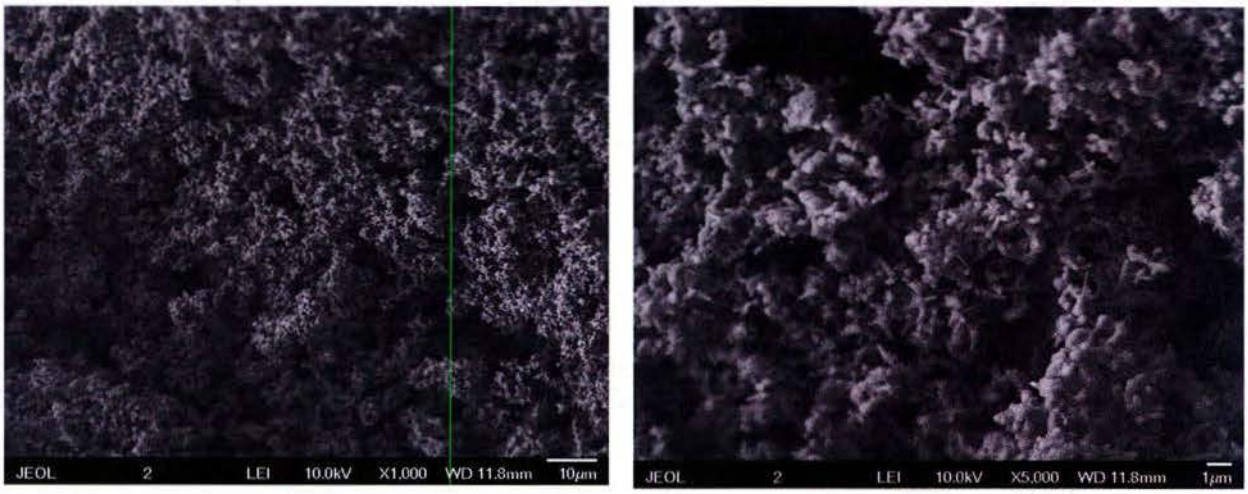

Figure 13. Nanopowder from Reaction (1) after heating at 1500 °C

The benzene solvent remained very clear and clean, and H-NMR of the solvent revealed no new organic compounds in spite of the high temperatures and highly reducing reagents that are associated with the reaction.

4.4.2 Analysis of Powders after Upgrading the Reactor System

Due to various leak incidents, lack of maintaining high pressure, and oxygen contamination, we paused the reaction experiments and ran through a series of upgrading and deteriorating part replacement for the reactor and its surrounding system. A chemical engineer was assigned to perform the upgrading and testing. The experimental research was resumed after the system was tested several times with benzene only, heated to 450 °C. The pressure developed in the reactor reached 1600 psi (~110 atm), and it was successfully retained over the course of the experiment.

Reaction (3) – TiB_2 Nanopowder Synthesis ("Control Reaction"). Another control evaluation was introduced by attempting to follow the same procedure described in the literature for making TiB_2 nanoparticles. We ran the reaction in parallel to the reaction of forming ZrB_2. We obtained black powder that consisted of agglomerated nanoparticles as shown in Figure 14 alongside the EDS analysis. The EDS analysis reveals a significant level of oxygen and carbon. Initially, the carbon was attributed to the adhesive tape used to bond the powder to the mounting stem. However, we now have more evidence for the presence of significant level of carbon in the powder itself. The carbon phase seems to be "free carbon."

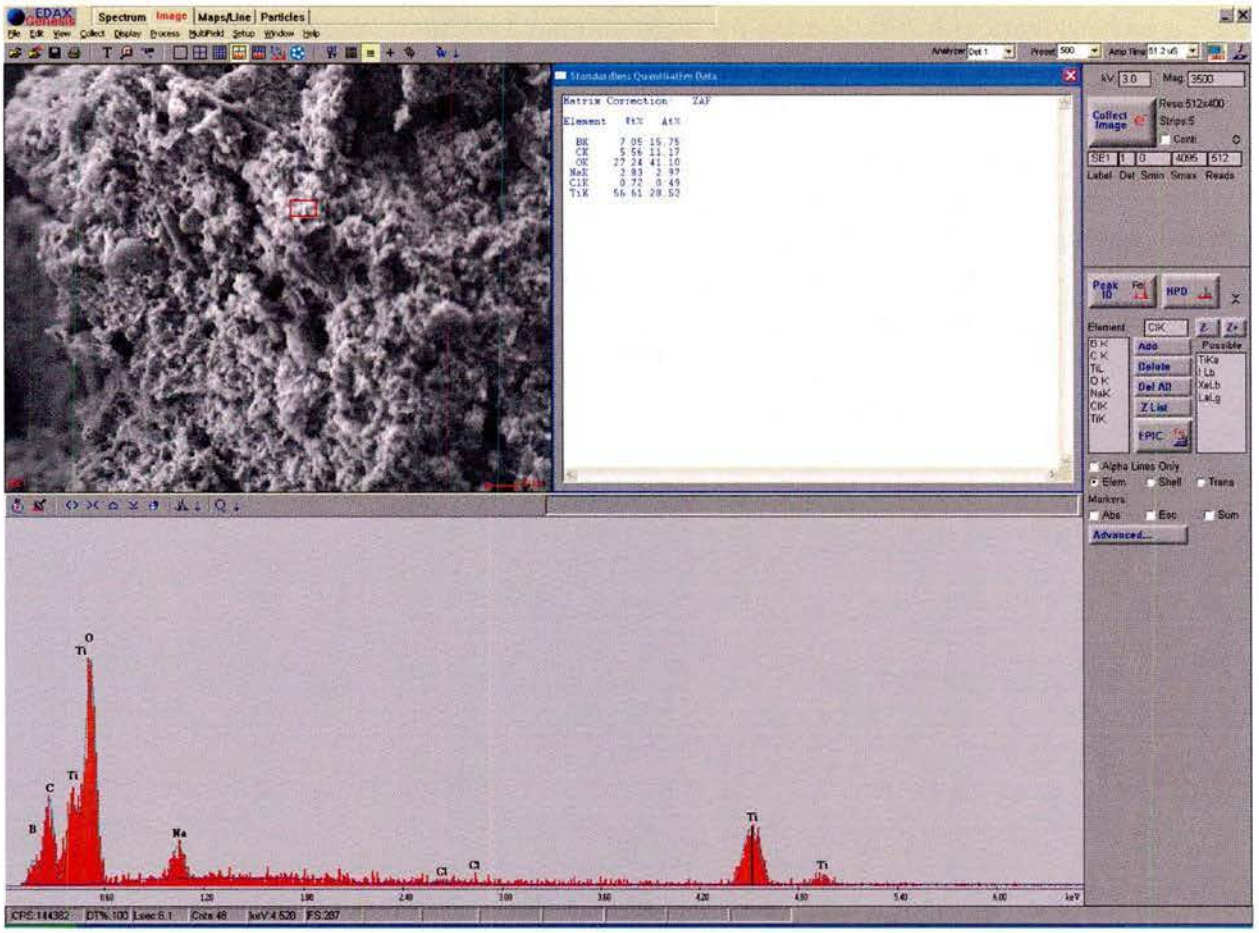

Figure 14. SEM and EDS analyses of TiB_2 product after its synthesis. The analysis reveals the formation of nanodomains and the presence of significant fractions of oxygen and carbon. Some residual NaCl is also observed.

When the powder is tested by TGA in air, there is a significant drop of weight starting at about 350 °C, while oxidation of TiB_2 resulted in a large weight gain. Figure 15 shows the TGA of the TiB_2 product that was either washed to remove the NaCl or not. The samples were heated in both argon and air. The TGA revealed the following observations:

a) Washed powder loses weight at low temperature, indicating water desorption and metal hydroxyl bond condensation (release of water).

b) No additional weight loss is observed up to 1000 °C for washed powder pyrolyzed in argon beyond the low temperature loss. This indicates that the carbon content in the sample is completely inorganic, by the end of the solvothermal reaction!

c) Heating above 1000 °C is out of range of our TGA instrument. Nevertheless, we recorded significant weight loss, when the samples heated first at 1000 °C were further heated to 1500 °C. This weight loss is associated with carbothermal and/or borothermal reactivity, since oxygen reduction is observed by EDS of the 1500 °C samples.

d) A significant weight loss is associated with the sublimation of NaCl above 800 °C in the case of unwashed samples. This sublimation may be considered in the future as an

optional method for eliminating the NaCl without washing. It should be considered only if removal of the salts will be unsuccessful with the selected dry solvents recommended in this report. Dry formamide and glycerol were selected to replace water in washing away the salts. It should be noted that both solvents are also excellent solvents for suspending the nanoparticles.

e) Samples pyrolyzed in air lose weight between 350 °C and 500 °C. This weight loss is attributed to oxidation of carbon. Then, a weight gain is observed, associated with the oxidation of TiBx and TiCx species. The relatively low gain in weight suggests that a large fraction of the nanoparticles is already oxidized.

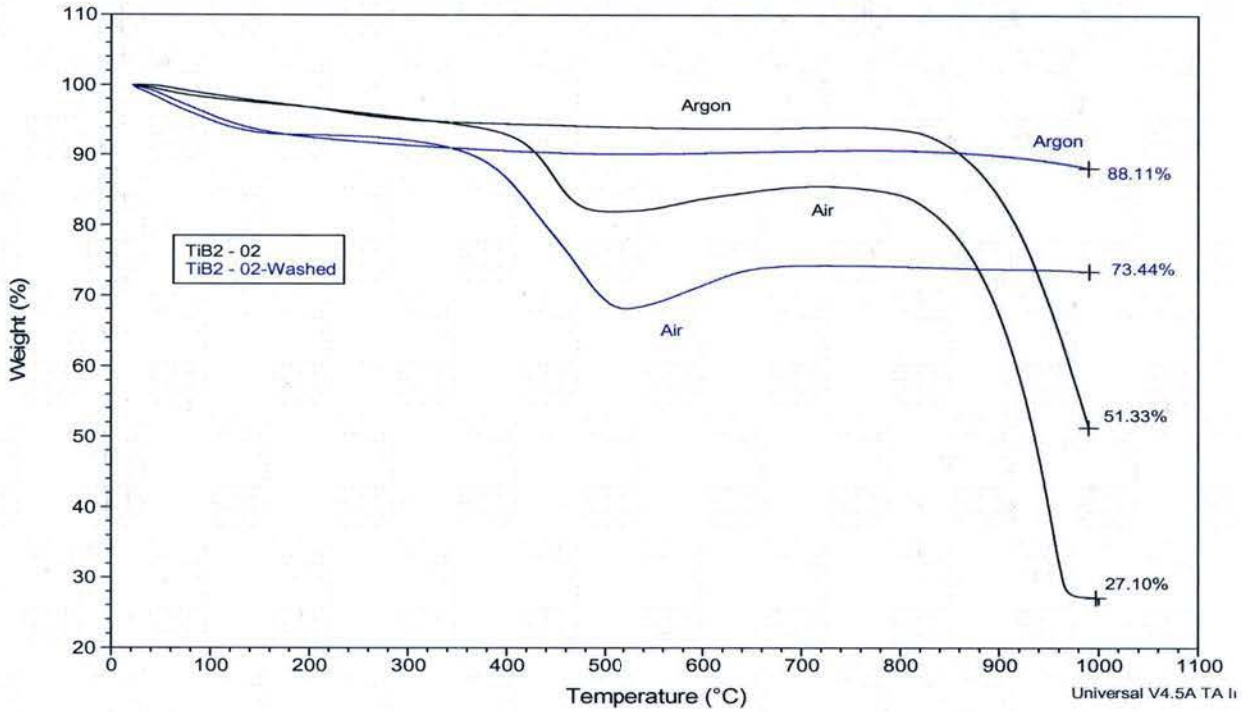

Figure 15. TGA of nanoparticles from a reaction to form TiB_2 with and without washing out the NaCl, performed in Ar and Air.

The XRD analysis of the as synthesized TiB_2 is amorphous and crystalline phases are generated once the material is heated to 1000 °C. The crystalline phases at 1000 °C consist of titanium suboxides and TiC.

Reaction (2) is another example of a reaction that was run before and after upgrading the reactor system. In this reaction, we started with both the Zr and B reagents in the form of halide compounds ($ZrCl_4$ and BBr_3). Thus, there is no concern that the powder product contains any residual metallic boron, which is difficult to identify if not reacted due to its amorphous stage and low EDS signature.

The information in Table 2 is from a reaction run after the reactor upgrading. The elemental analysis, EDS, XRD at intermediate stages and TGA patterns all revealed that there was still a significant oxidation. Thus, we suspected that the post-reaction processing reported in the

literature, which included a water wash to eliminate the sodium salts, is a major source for oxygen contamination. We then switched to the use of dry formamide and glycerin as washing solvents, due to the relatively high solubility of NaCl in these solvents (far better than alcohols). Conveniently, these solvents are also among the best for suspending ZrB_2 nanoparticles!

Table 2: Elemental analyses of Reaction (2) performed after the upgrading of the reactor system

Sample	Elemental Analysis (wt%)								Mol Ratios Relative to Zr						
	Zr	B	C	O	Na	Cl	H	Total	Zr	B	C	O	Na	Cl	H
As synthesized	28	2.6	37.4	18	2	0.2	1.8	90.0	1	0.78	10.1	3.66	0.28	0.02	5.9
After heating 1500C (3h)	43	2.4	53	2.2	0	0	0	100.6	1	0.47	9.37	0.29	0	0	0

We still observed the presence of high excess of carbon. This was not anticipated based on the fact that the benzene solvent remained very clean, i.e., no formation of other soluble benzene byproducts was detected by the sensitive H-NMR analysis.

Clearly, this aspect need to be investigated in future studies. Potentially, the internal temperature and/or pressure inside the reactor were higher than obtained in the literature procedure. We therefore planned to investigate the potential to eliminate the excess carbon by reducing the temperature and pressure.

The level of boron is already lower than introduced at the beginning of the synthesis stage. It is roughly 40% of the boron introduced as a reactant. It means that much of the BBr_3 was not reacted. This can be another reason for the presence of excess oxygen in the as synthesized products due to the high activity of the unsaturated Zr containing product(s).

The high carbon content is responsible for the carbothermal reduction occurring at 1500 °C, leading to the formation of mainly ZrC in this specific reaction as indicated by the XRD analysis shown in Figure 16. Most of the oxygen disappeared. A more complete carbothermal reduction was achieved, when the heating at 1500 °C was extended beyond 3h. Some of the boron disappeared, indicating a secondary well known reaction of borothermal reduction.

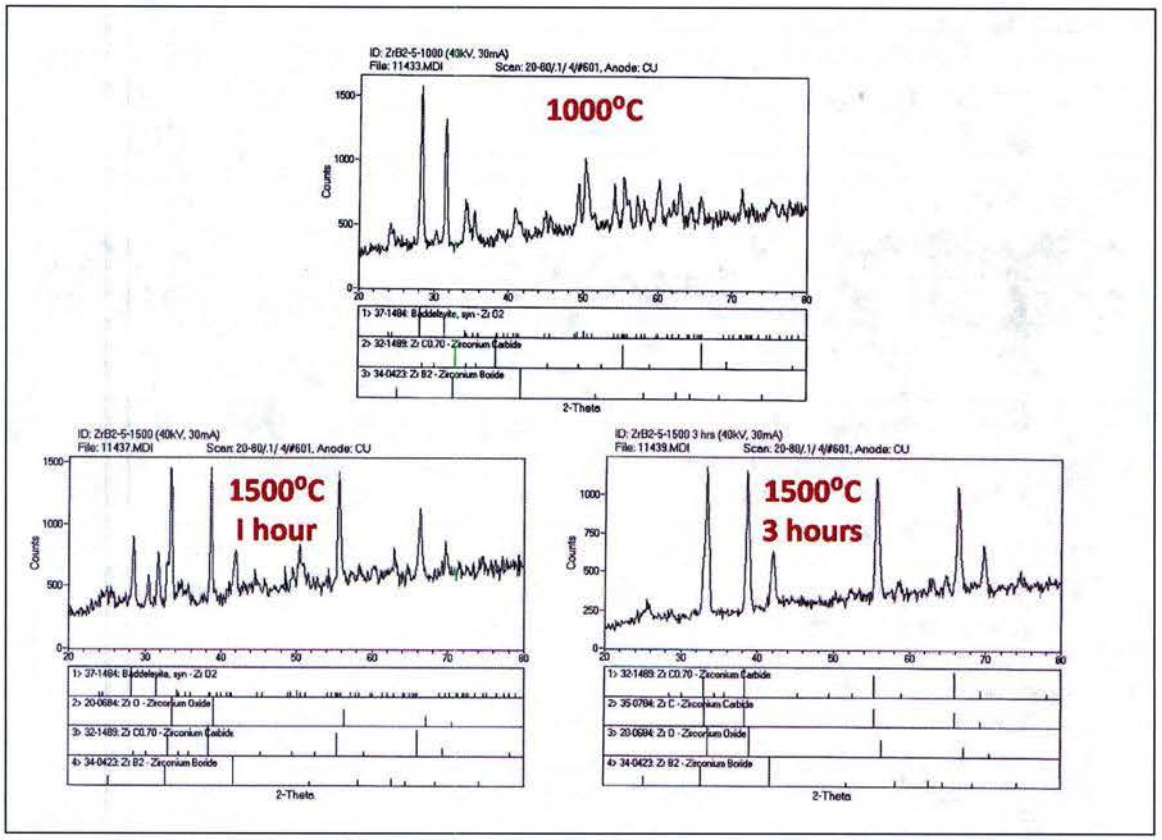

Figure 16. XRD of powder formed by the reaction between $ZrCl_4$ and BBr_3. Although the oxide phase is still dominant at 1000 °C, some ZrC and traces of ZrB_2 are observed. At 1500 °C, ZrC and ZrB_2 are enhanced and the oxide phases disappear.

4.5 Second Iteration Synthesis (Year 2)

4.5.1 Solvothermal Synthesis Activities

The first year of the project the research focused on developing the reactor system and then assessing the synthesis of ZrB_2 nanoparticles based on a protocol for the solvothermal synthesis of TiB_2 reported by Gu et al. Our protocol employed benzene as a solvent for performing the various reactions, as it is used in other reported solvothermal reactions.

The following reactions were initially assessed aside reactions (1) to (4) discussed above:

Reactions to form ZrN nanoparticles

$$ZrCl_4 + 5NH_3 \longrightarrow ZrN + 4NH_4Cl + 1.5H_2 \quad (8)$$

$$ZrCl_4 + Li_3N \longrightarrow ZrN + LiCl \quad (9)$$

(benzene, 350 °C, 3000 psi)

Reactions to generate ZrC directly

$ZrCl_4 + CCl_4 + 8\ Na \longrightarrow ZrC + 8NaCl$ (10)
(benzene, 350 °C, 3-4 Ksi)

Reactions to assess the reactivity of Zr powder with polymeric precursor to borocarbonitride that can be a donating source for N, B, and C to form ZrN, ZrC, and ZrB_2 phases.

Zr powder+ BN-C (& BN) polymer $\longrightarrow$ ZrN *(nano crystallized)* (11)
(nanocrystalline ZrN but no crystalline ZrC or ZrB_2 by XRD even at 1500 °C!)

Synthesis of Zirconium Boride

The main effort to synthesize ZrB_2 consisted of Reactions (1) and (2) under various temperature and pressure conditions as well as attempts to replace benzene with heptane as a potential solvent that is not carbonized during the reaction. During the loading of the reagents into the reactor inside a designated and modified dry box, the oxygen and moisture levels were in the single-ppm range but full sealing (final tightening of the reactor bolts) could be done only outside the box.

Also, the reactor was transferred back into the dry box at the end of the reaction after slightly loosening the bolts outside the box.

The next step was the decomposition of unreacted reagents (Na, $ZrCl_4$ and BBr_3). This step was performed with dry alcohols in order to form soluble metal alkoxy groups. In the case of Na, we observed the release of H_2 gas.

The generated salts were then removed by washing the product from the generated salts. According to the literature, the wash is performed with water, which makes the products vulnerable to oxidation. We developed a washing process in dry formamide so as not to incorporate water. After the formamide wash, we completed the process with an additional wash in acetone.

Reaction (1) was also performed with heptane as a replacement for the "conventional" benzene, which formed a carbon phase. However, even in this case, we observed the formation of carbonaceous material (as in the case of benzene). With heptane as the solvent, the dispersion of the reactants became an issue. Overall, the reaction in heptane did not generate as much pressure as benzene (due to H_2 release) as shown in Figure 17. This is an indication for a lower level of the carbonization reaction.

We considered to assess various ways to eliminate the carbonization problem. One of them is the addition thiophene (or other inhibitors), which have been reported to suppress carbonization of organics. Early observations revealed that the pressure developed in the presence of thiophene is lower than in the case of benzene by itself as shown in Figure 18.

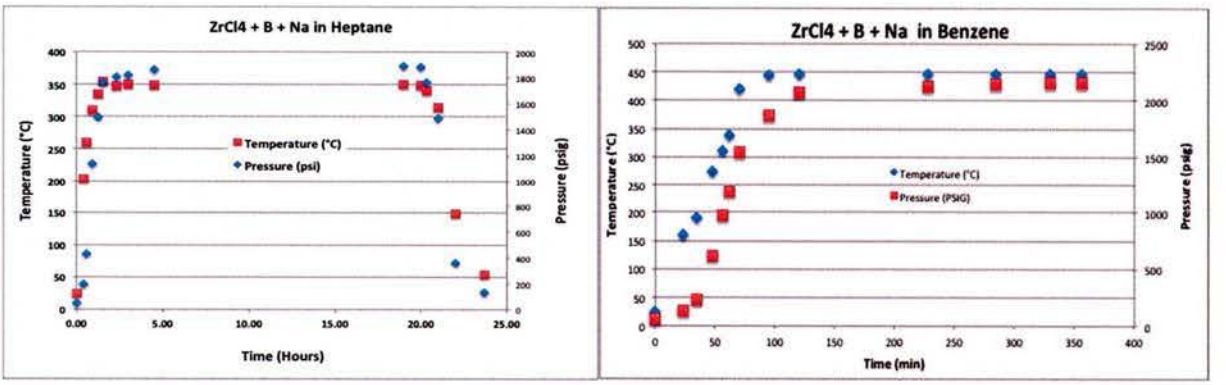

Figure 17. Lower pressure is generated in the presence of heptane vs. benzene; the reaction is associated with less carbonization and consequent generation of hydrogen.

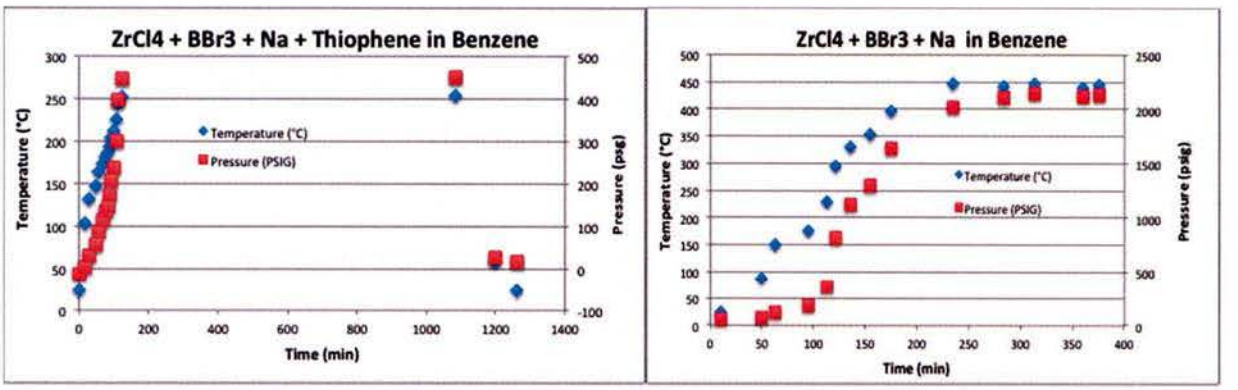

Figure 18. Lower pressure is observed in the presence of thiophene, potentially indicating less release of hydrogen due to carbonization.

We also noticed that the quartz liner inside the reactor was leached by the reactive reagents (or derived salt products, indicated by the presence of Si in the product mix according to X-ray fluorescence (XRF) and energy-dispersive X-ray spectroscopy (EDS) analyses. We have removed the liner, and the reactions were then performed without it. In most reactions, we did not observe significant contamination of metallic elements (Fe, Ni, Cr) associated with the stainless steel reactor walls.

Reaction (4) was new, and we could not find any equivalent reaction described in the literature. In this case, we switched the halide and metal reactants and reacted Zr with BBr_3 in the presence of sodium. The main reason to assess this reaction was the presence of residual boron in Reaction 1. The boron cannot be detected by XRD as it is amorphous in its nature; it is difficult be detect by SEM/EDS. Nevertheless, EDS analyses have revealed the presence of large particles that primarily contain boron. In the reaction with Zr, we did not observe any remaining Zr in the XRD spectrum of the product. Yet, we saw the formation of NaBr, as illustrated in Figure 19. Thus, this reaction deserves a second look in future studies because $ZrCl_4$ is not a very soluble compound in organic solvents, while BBr_3 is a liquid reagent by itself.

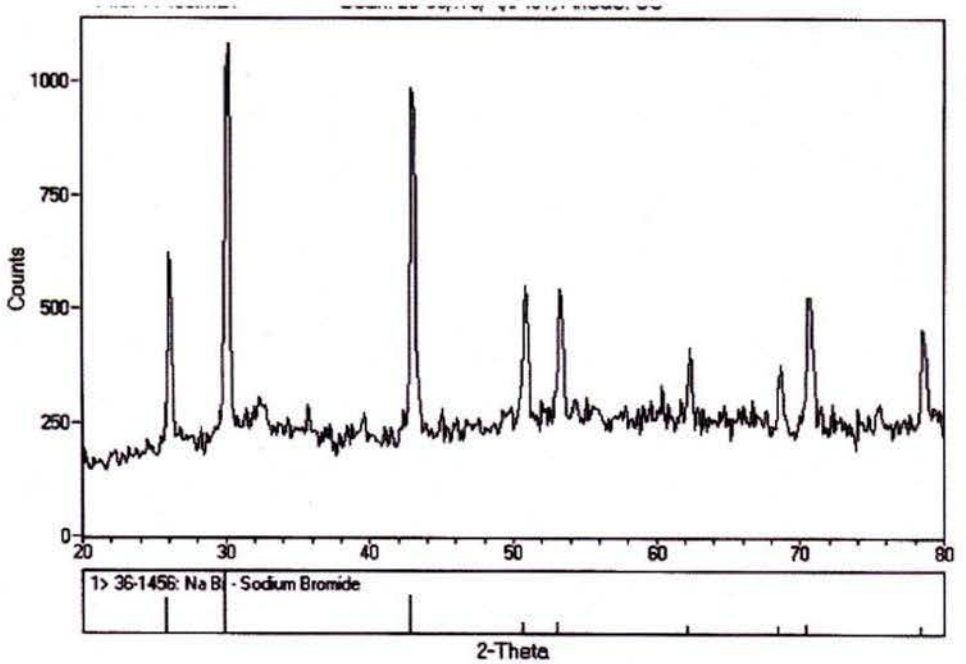

Figure 19. The XRD pattern of the reaction Zr/BBr_3/Na. The Zr disappears and the BBr_3 reacts with the sodium.

General Observations and Conclusions

Overall, high reactivity of the reagents has been detected in all of the reactions tried, thus far, involving the disappearance of all or most of the reagents not added in excess (e.g., Na and Li_3N). Most importantly, the bulk sodium pieces disappeared. Since it was added in excess amount, the residual Na was removed by its reaction with alcohol (isopropanol).

Nanoparticles were formed in all the different solvothermal reactions we have performed. However, it was embedded or deposited on amorphous carbon in all cases when organic solvents were used. In spite of the carbonization reaction, the benzene solution did not show any soluble organic products that could be formed by decomposing or condensing the benzene itself under the very harsh conditions (high temperature, pressure, and reductive and oxidative agents). This means that once the benzene start decomposing, the reaction rapidly led to complete carbonization rather than a stepwise conversion. It is therefore suggested that the reaction is catalyzed by one or more of the reactants or the derived products at the reaction temperature. This claim is supported by the fact that in the absence of reagents, benzene did not show any decomposition patterns or self-condensation products under the same reaction conditions.

Contrary to the reports in the literature, the powder products (black in all cases) did not possess any crystalline phases at the end of the reactions (except in reactions for forming ZrN). The phases were formed only by further heating the powders to 1000 and 1500 °C. There was an excessive level of oxygen presence forming various zirconium oxides (mostly the baddeleyite phase). Throughout the project, we have struggled with the incorporation of oxide, but some improvement has been made by using formamide instead of water as a solvent to remove the by-product salts.

The oxide phases could be removed by further heating to 1500 °C. It occurs due to carbothermal reduction with the residual carbon. Hence, a zirconium carbide (ZrC) phase was generated.

The carbon formation from the organic solvents has not been verified in the literature, although analysis of FTIR and some anecdotal statements reveal that it is indeed formed in solvothermal reactions reported in the literature. Absorbencies in the ranges of 1500-1700 and 2700-3000 cm^{-1} indicate the presence of high levels of C-C and C-H bonds (see Figure 20). Also, when samples are heated in air, there is a significant weight loss associated with the oxidation of the carbon. Then at high temperature, there is evidence of carbothermal reactivity. The high carbon content can also be detected by elemental analysis (as shown in Table 3) and qualitative observation following EDS.

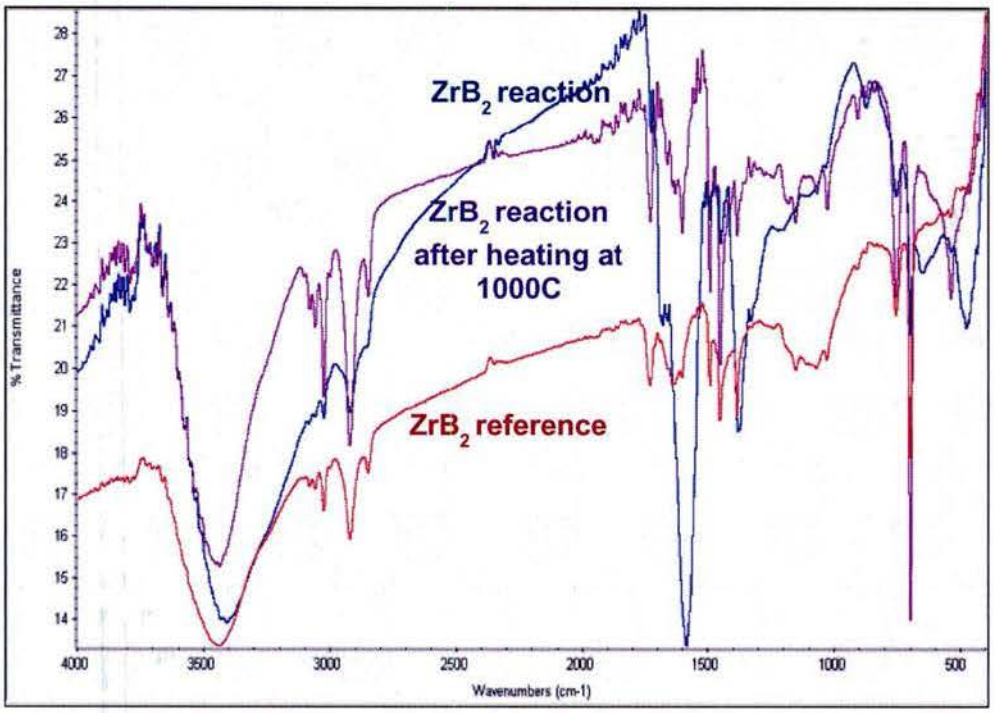

Figure 20. FTIR of the ZrB_2 product as synthesized and after heating to 1000ºC.

Table 3: Elemental analysis of as-synthesized ZrB_2 product before and after heating to 1500 ºC (passed carbothermal reaction).

Sample	Elemental Analysis (wt%)								Mol Ratios Relative to Zr						
	Zr	B	C	O	Na	Cl	H	Total	Zr	B	C	O	Na	Cl	H
As synthesized	28	2.6	37.4	18	2	0.2	1.8	90.0	1	0.78	10.1	3.66	0.28	0.02	5.9
After heating 1500C (3h)	43	2.4	53	2.2	0	0	0	100.6	1	0.47	9.37	0.29	0	0	0

Powder Product Analysis

The following techniques were used for evaluating the synthesized powders: XRD, TGA, elemental analysis, FTIR, SEM with EDS, and particle size analysis.

Overall, the formation of nanoparticles was consistently observed in all the attempted reactions. Some are agglomerated with the residual carbon. The deposited carbon was found in larger-scale features and looked more like polymer-derived products. Some of the large boron particles were still detected after the reaction as a micron-size pulverized material. Figure 21 illustrates some of these observations. Figure 12a reveals a product in which some domains are very high in carbon content, hence indicating the presence of free carbon material adjacent to free boron particles. Figure 21b shows a region with relatively low carbon but evidence for significant oxidation, detected by the EDS, after being heated to 1000 °C. It should be noted that nanoparticles containing Zr are shown as well, indicating that the reacted Zr reagents do form nanoparticles during the solvothermal reactions.

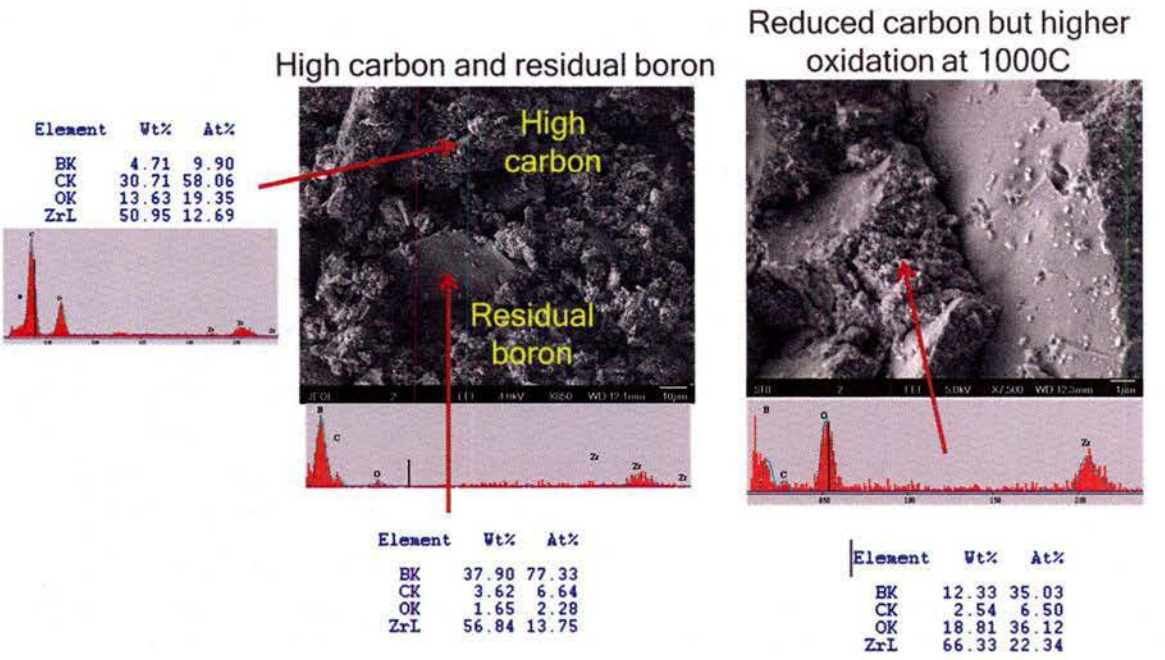

Figure 21. Nanoparticles containing Zr are always produced in the reactions. Varied residual C, B, and O can be detected.

Although the oxide phases at low temperatures can be minor phases due to oxygen contamination or may represent surface contamination while the rest of the boride material is still amorphous, EDS testing showed the presence of significant levels of oxygen. Therefore, we do not rule out the option that much of the ZrB_2 phase formation at high temperature is the result of both carbothermal and borothermal reaction of ZrO_2 with residual metallic boron as shown earlier in reactions (5) and (6).

Figure 22 represents the ZrB_2 particles formed by the borothermal or carbothermal reduction at 1500 °C. In some cases, the particles remained nanometric or grew to micrometer size with platelet or acicular structures as shown in Figure 22. In this case, the ZrB_2 phase was the only crystalline phase in the mixture, and its sharpness revealed the relatively large crystalline size. However, the material still contains a significant amount of carbon in spite of the drastic reduction of the oxygen content relative to the material after heating to 1000 °C.

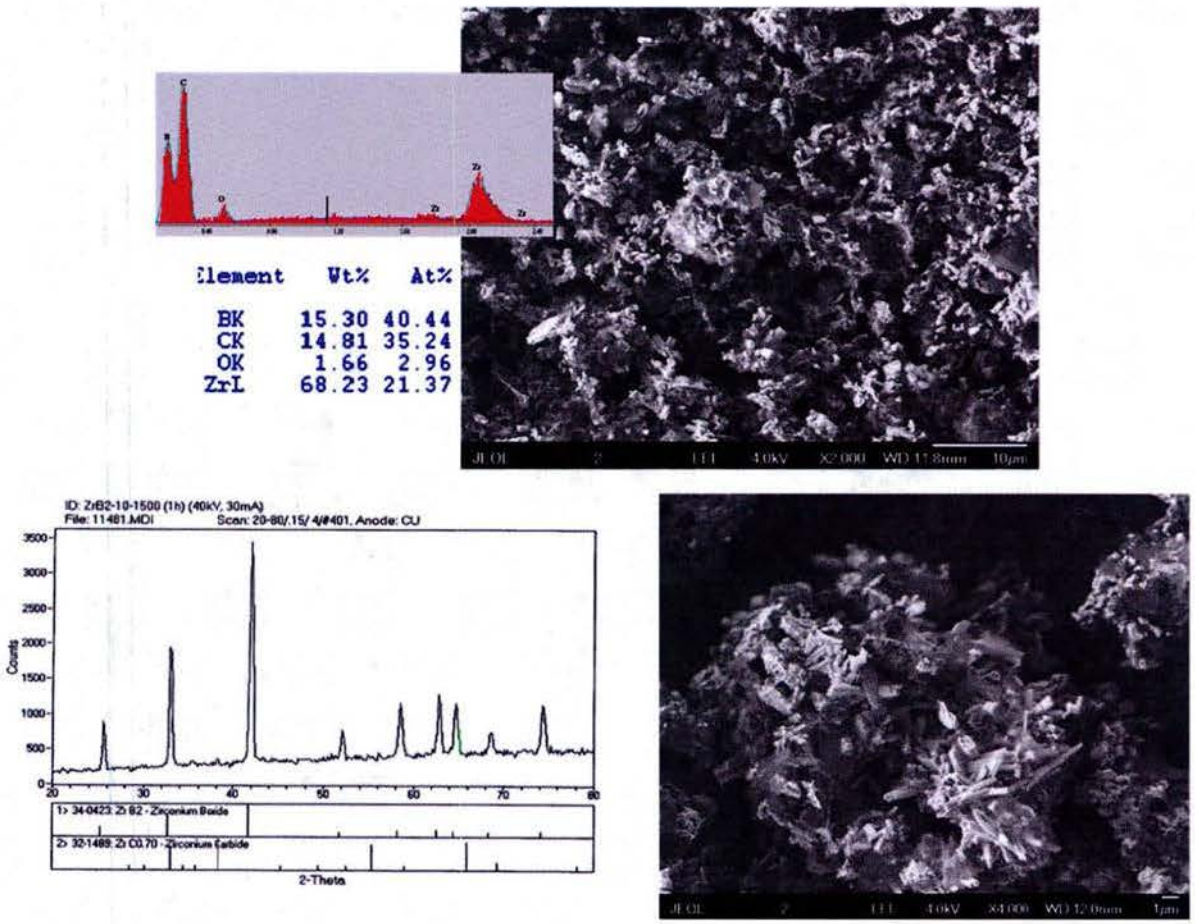

Figure 22. The formation of a nanometric but clear ZrB_2 phase and crystals was observed after carbothermal/borothermal reactivity at 1500 °C, associated with weight loss and the reduction of oxygen content. A high carbon level is still apparent.

Synthesis of Zirconium Nitride

In parallel to the synthesis of ZrB_2, we initiated an effort to synthesize ZrN. This effort was added to the original concept for assessing reactions in which massive amounts of carbon cannot be generated and the reactions do not rely on sodium as reducing agent. As reference, we used a series of synthesis efforts for generating cubic boron nitride by solvothermal reactions in the presence of various nitrogen sources.[32,33,34,35,36,37,38,39,40,41,42,43]

The base reaction was between $ZrCl_4$ and ammonia as both reactant and solvent. The reaction is also associated with the release of hydrogen at a certain temperature during the solvothermal or as a part of the pyrolysis as shown in reaction 12.

$$ZrCl_4 + NH_3 \longrightarrow ZrNx(NH)y + NH_4Cl + H_2 \quad (12)$$

Since NH_3 serves also as the solvent, this reaction can be carried on without organic solvent and it can be similar to a hydro-thermal reaction. Nevertheless, it is expected that, at the reaction temperature, there would be significant level of bridging in (NH) groups due to the incomplete condensation reaction derived from steric hindrance. The presence of Zr-Cl is also feasible. Such an intermediate stage product can be very sensitive to the presence of water and alcohol, and hence may enhance the incorporation of oxygen into the final product as shown in Figure 23. Even at 1500 °C, the presence of ZrN was negligible. There was a significant level of ZrO_2 at this stage due to the lack of carbothermal reduction. Furthermore, the reaction led to leaching of small levels of metal contaminants from the reactor walls (Fe, Cr, Ni).

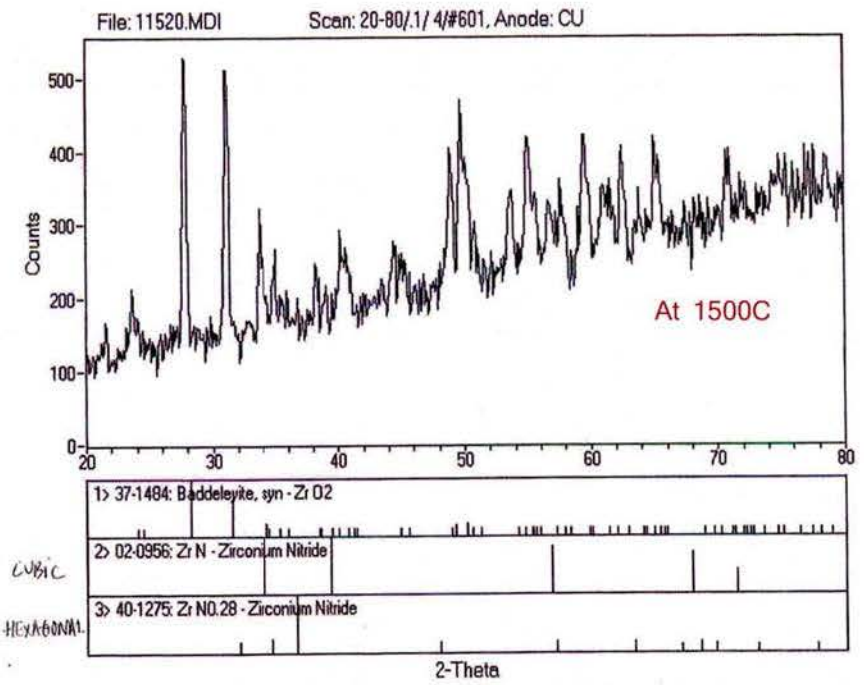

Figure 23. Reaction between $ZrCl_4$ and NH_3 does not show formation of ZrN until heated at 1500 °C. The larger phase of zirconium oxide is due to the hydrolytic instability of the intermediate product.

Due to the inferior results, we have selected another reaction to continue the effort. This is the reaction between $ZrCl_4$ and Li_3N as defined in Reaction (9). This reaction is currently the most promising one as we have obtained crystalline phases already at the reaction stage. The reagents are mild enough not to attack the reactor walls (no traces of stainless steel). Additionally, $ZrCl_4$ by itself is not the aggressive element in corroding the reactor. However, carbon material is still quantitatively formed. Hence, we assumed that the reagents could still catalyze the condensation of benzene. Attempts to replace benzene with heptane have thus far been unsuccessful due to the lack of good dispersion of the Li_3N. The reactivity with organic solvents may be associated with the "super" basicity of Li_3N, although at the same time it is considered to be a strong reducing agent, therefore, it can potentially reduce the $ZrCl_4$ as it is known to reduce copper oxide and silicon tetrafluoride.

During the reaction, nanocrystalline particles were formed as detected by XRD (Figure 23) and observed in SEM images (Figure 24). The wide pattern follows that of cubic ZrN, ZrC or ZrO; all have XRD lines at about the same locations and intensities. Thus, we cannot rule out the presence of any of these phases. Once heated to 1000 °C, there was also formation of oxide phases associated with oxygen incorporation during the processing (Figure 24b). The SEM analysis revealed the presence of Zr-containing nanoparticles but also a significant fraction of amorphous carbon, having a globular "bubble-like" morphology. The Zr-based nanoparticles were agglomerated or glued to the carbon phase. The carbon phase in this reaction seems be at higher level than obtained in other reactions studied in this project. Thus, even in this case, there is a need to evaluate the capability of using carbon-forming inhibitors, solvents that do not form carbon, or inorganic salts.

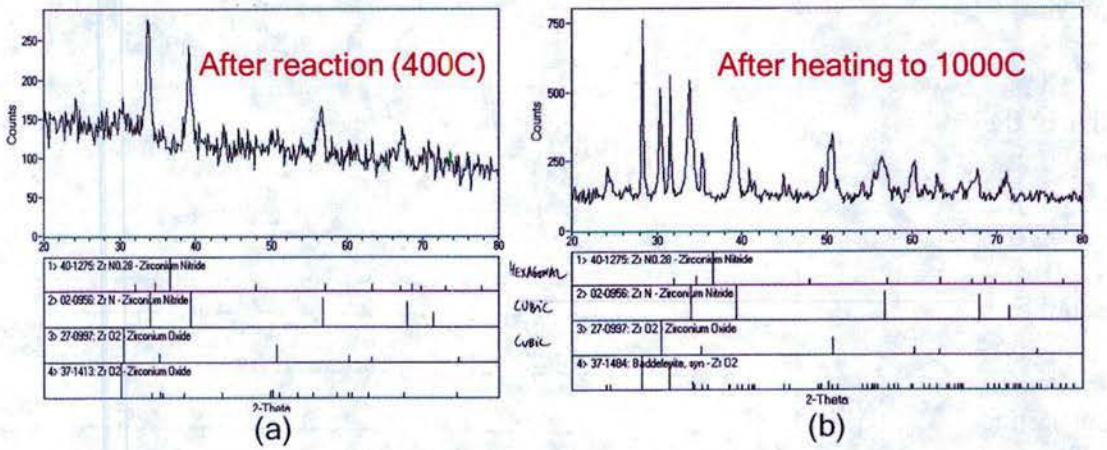

Figure 24. The reaction products of $ZrCl_4/Li_3N$ indicate a nanocrystalline ZrN (cubic) phase after the completion of the reaction. Heating to 1000 °C assists the development of oxide phase, too.

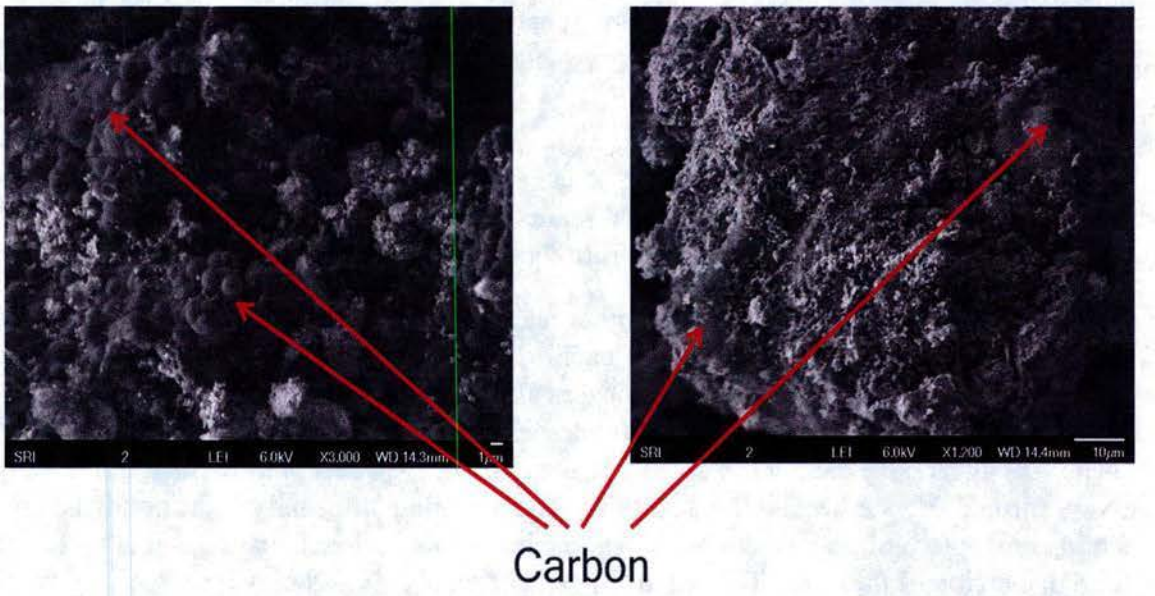

Figure 25. The reaction products of $ZrCl_4/Li_3N$ include nanometric powder of ZrN but also large quantity of amorphous carbon. The carbon features look like polymer derived carbon glass.

Zirconium Carbide Synthesis

We also started looking at the reaction for forming ZrC via Wurtz reaction of $ZrCl_4$ with CCl_4 in the presence of sodium (reaction 7). Also, CCl_4 can serve as a solvent by itself, and we added benzene to avoid its self-conversion to carbon without incorporating the $ZrCl_4$. We still observed high levels of carbon formation in this case, as shown in the FTIR after the reaction and in the SEM/EDS analysis. In future studies, we could evaluate the capability of carrying out this reaction in the absence of an external solvent. The evolution of the carbon phase at the reaction stage was evidenced in the FTIR analysis. There was still presence of C-H bonds suggesting the incorporation of benzene (Figure 26).

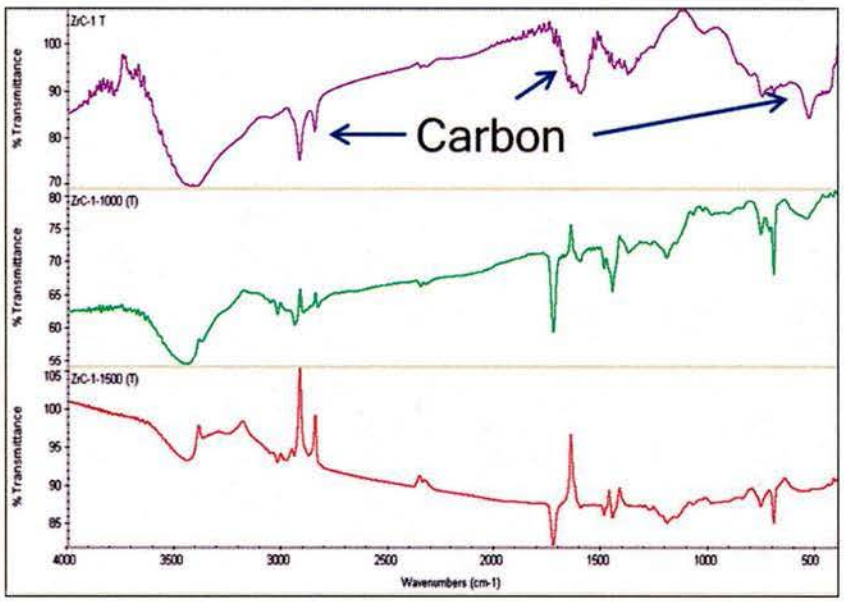

Figure 26. Evidence for carbon formation in the synthesis of ZrC via $ZrCl_4/CCl_4$/Na. The identity of sharp absorbance at 1720 and 690 after heating the product to 1000 and 1500 °C is not clear.

The XRD analysis shown in Figure 27 indicates trace formation of an oxide phase after the reaction, which grew as the material was heated to 700 °C. Then at 1500 °C, there were sharp peaks of ZrC, suggesting carbothermal reactivity and crystalline size growth.

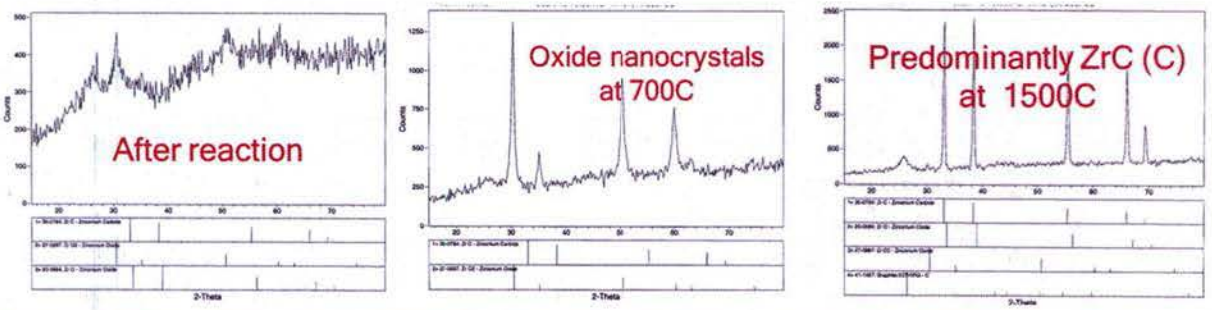

Figure 27. The XRD analysis of ZrC synthesis after reaction (left), 700 °C, and 1500 °C treatment (left).

Indeed, SEM analysis revealed that the particle size was growing between 1000 °C to 1500 °C. Also, the EDS analysis revealed a large excess of carbon, which seemed to be the core material covered by the Zr-containing particles (Figure 28).

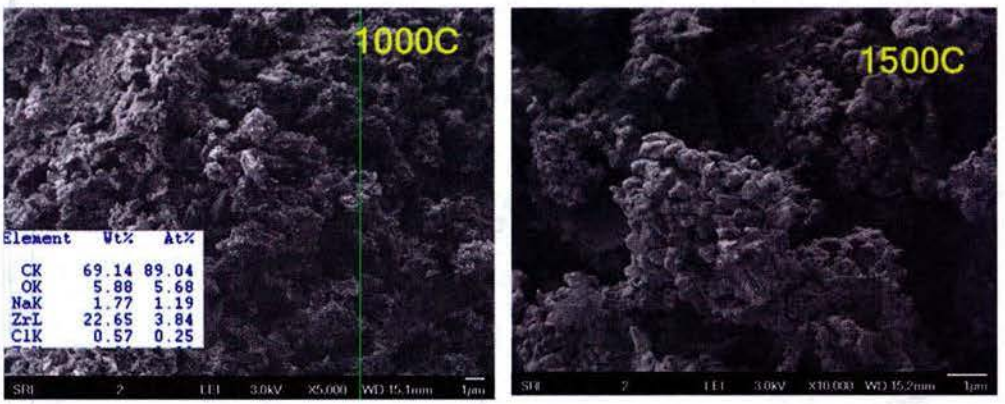

Figure 28. Nanopowder produced by the reaction of $ZrCl_4/CCl_4$/Na after annealing at 1000 and 1500 °C. There is a large excess of carbon on top of which the particles grow. Significant grain growth is observed at 1500 °C.

Polymer-Derived BN and BN-C in the Presence of Reactive Fillers (Zr metal powder)

At the end of Year 2, we initiated a new activity in the project for assessing UHTC composite materials or protective coating via a simple processing technique. This idea was outside the original scope of synthesizing nanoparticles or the use of solvothermal reactions. The concept combines polymeric precursors to BN and BN-C with reactive fillers in which it is anticipated that an in-situ reaction between the reactive metal particles and the polymers will occur. The concept is a derivative of previous activities at SRI to "develop" structures and thick ceramic coatings and matrices for oxide-oxide composites, UHTC thick coatings, and UHTC matrices for fiber-reinforced composites. The newly introduce activity took advantage of the synthesis of new polymeric precursors to BN and BN-C that were developed during different SRI project. The following reactions are anticipated (BN and BN-C are "polymer derived ceramics", PDCs):

$$Zr + BN \longrightarrow ZrB_2 + ZrN \qquad (13)$$

$$Zr + BN\text{-}C \longrightarrow ZrC + BN \text{ (for weak interfaces)} \quad (14)$$

$$Zr + Si + BN \longrightarrow ZrB_2 + Si_3N_4 \quad (15)$$

$$Zr + Si + BN\text{-}C \longrightarrow ZrB_2 + ZrN + SiC \quad (16)$$

$$Zr + Si + BN\text{-}C + N_2 \longrightarrow ZrN + SiC + BN \quad (17)$$

The new BN preceramic polymers are illustrated in Figure 29. They were developed in an attempt to generate an intermediate BN material that is high in its sp^3 content and can transform at relatively low pressure to cubic boron nitride. By adding Zr powder as reactive filler, we anticipated the formation of UHTC phases such as ZrB_2, ZrN, ZrC, and even ZrO_2 (from the oxygen incorporated in the polymer-derived material) wherein the source of the B, N, C and O is the polymer-derived ceramic (PDC). Such composition with in situ phase formation can be used for making UHTC matrices and coatings for fiber-reinforced UHTC composites. Specifically, we thought that the excess of carbon in one of the PDCs would react, allowing the BN network an easy way to form crystalline BN.

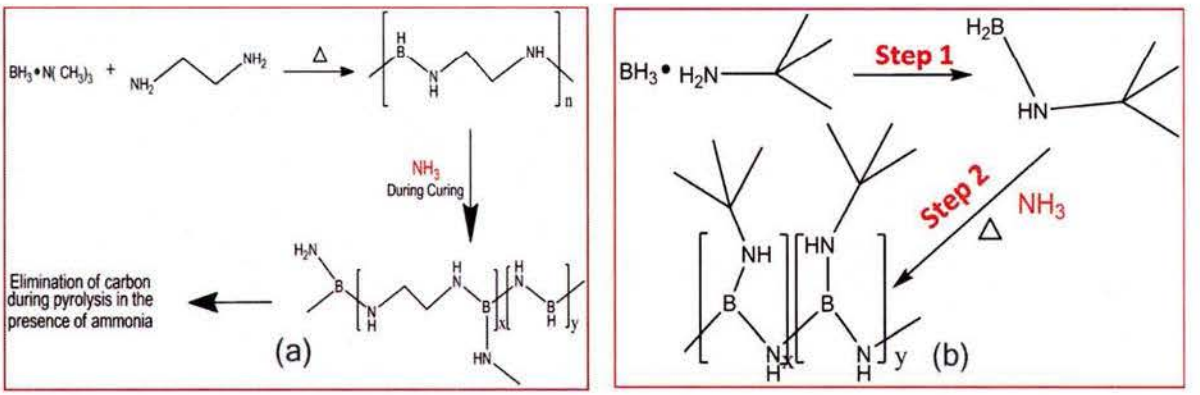

Figure 29. Linear precursors to BN with steric hindrance to prevent aromatization and subsequent formation of hexagonal BN (hBN).

The two assessed preceramic polymers are illustrated in Figure 29. One is made by reacting borane complex with ethylene diamine as an integral part of the polymer backbone. Use of this polymer leads to high retention of carbon in the PDC product. In many cases, pyrolysis in the presence of ammonia leads to the elimination of the carbon content of BN precursors. However, the thermal stability of the polymer leads to the formation of a molten or soft phase of the polymer at elevated temperature, which does not allow the ammonia to remove the organics efficiently during the pyrolysis.

The second polymer incorporates bulky t-butylamine groups into the polymer backbone. This polymer is converted to an amorphous BN with only traces or very low carbon content, even when pyrolyzed in an inert environment. This "clean" pyrolysis is due to the stability of the t-butyl group and its capability to be cleaved by β elimination.

Interestingly, cubic ZrN is the predominant crystalline phase developed in both cases at 1000 °C and further at 1500 °C (see Figure 30). It should be noted that cubic ZrC and ZrO have similar XRD patterns but a bit shifted and the XRD pattern fits better the ZrN phase. However, we have not ruled out that it is a mixed phase of ZrCN, ZrON, or ZrOC.

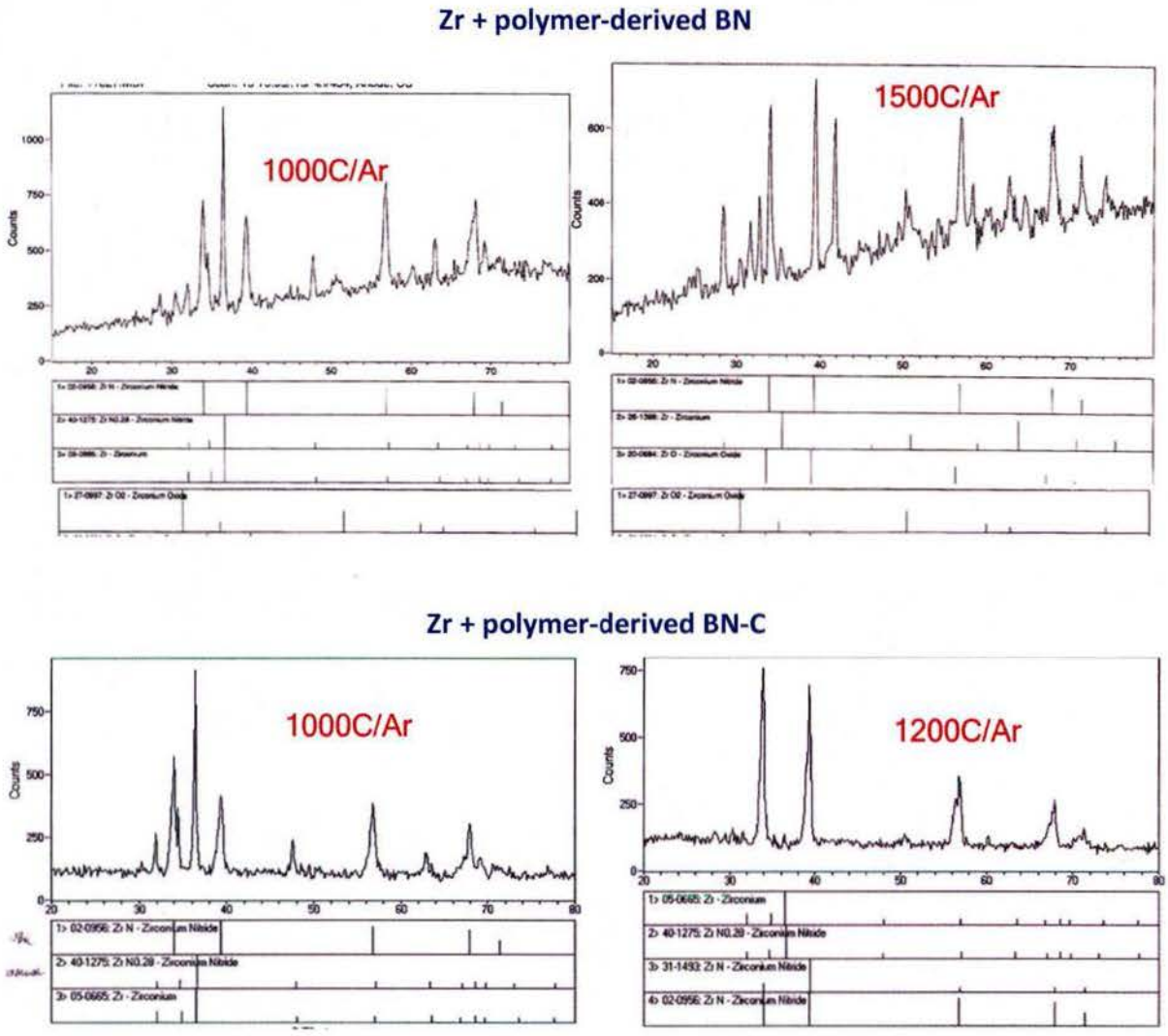

Figure 30. XRD of the products derived from the reaction of Zr powder with: (a) a precursor to BN that does not leave excess carbon and (b) a precursor that converts to BN with homogeneously mixed free carbon material.

There is still some Zr at 1000 °C in both cases, but it disappears at 1200 °C in the presence of high carbon content; for BN it may be still observed at 1500 °C. Oxide phases are also observed.

Surprisingly, no ZrB_2 phases are observed even at 1500 °C! This may be an indication that the boron network is chemically stable and does not easily interact with the reactive filler.

The SEM images of the products with the BN-C precursor at 1000 °C and 1500 °C are given in Figure 31. In both cases, large product particles are a composite, containing the inclusion of Zr-based compounds (Zr itself). The footprints of the Zr particles are easily observed in the amorphous PDC phase. The larger particles look leached. There is no significant difference in the morphology between the 1000 and the 1500 °C powders.

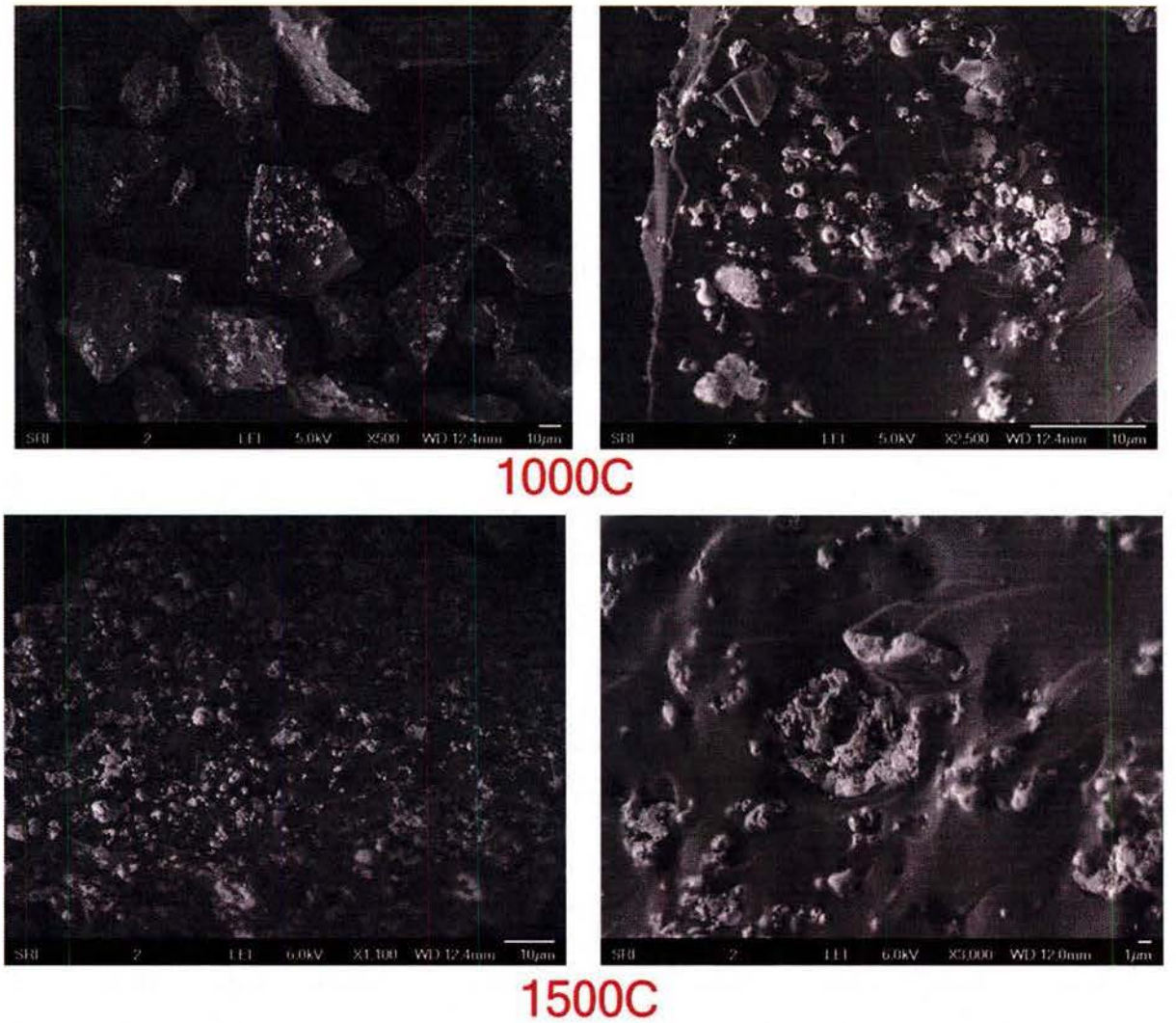

Figure 31. Microstructure of polymer derived BN and BN-C after interactions with Zr powder. It seems that very limited reactivity has happened.

4.6 Recommendations for Further Studies

Although we shifted toward a new topic in Year 3, there are still several approaches that should be assessed for overcoming the synthesis problems discussed above. We recommend to shift the focus toward the replacement of the organic solvents with inorganic ones and the assessment of inhibitors to prevent the polymerization/carbonization of the organic solvents. The following solutions for the problem can be evaluated:

a) Eutectic inorganic salts with low melting points (e.g., LiCl/KCl)

b) Ammonia as a solvent in the formation of ZrN

c) Organoamines and amino salts that cannot interact with the reagents

d) Silanzes, e.g. $(CH_3)_3SiNHSi(CH_3)_3$, that cannot convert to carbon and at the same time serve as donors of NH while forming gaseous species of $(CH_3)_3Si$-Cl as by products, hence removing the excess of chlorine.

e) Inhibitors that can prevent carbonization, e.g. thiophene.

4.7 Use of BN Preceramic Polymers as Interface Coatings for SiC/SiC Composites (Year 3)

4.7.1 Introduction to Revised Scope of Work (Year 3)

Based on the assumption that the remaining funding for Year 3, would not be sufficient and the introduction of the BN preceramic polymers at the end of Year 2, there was a decision per request of ONR's Program Manager to redirect the remained funds for assessing the potential of new polyaminoboranes synthesized at SRI in another government project as precursors for cubic boron nitride (c-BN) as interface coatings between SiC fibers and SiC matrix. These polymeric precursors were linear in their structure and did not contain the typical aromatic (sp^2) chemical structures of other reported precursors to BN. However, as we cured and pyrolyzed these polymers, the polymer derived ceramic gradually converted itself to the more conventional amorphous sp^2-based structures associated with hexagonal BN (h-BN). Nevertheless, these relatively simple and stable polymers can serve as practical precursors to h-BN.

Interface coatings are utmost critical to achieve ceramic composite toughness required for high performance at temperatures reaching and beyond 1500 °C. The typical approach today consists of a double coating of the fiber's yarns. Currently, a first layer of tens of nm of carbon are deposited followed by deposition of BN. Both layers have stacks of hexagonally structured graphite or BN. The lamellar sp^2 structure of h-BN and graphite allows slippage of the layers when shear forces are applied and that is a major reason why the weak interface is accomplished. The other reason is the inertness of carbon and BN materials toward SiC.

Both the C and BN coatings are currently deposited via gas phase (CVD). This approach requires expensive equipment and are slow. Furthermore, the fibers tend to adhere to each other, if the process is not well controlled.

The proposed polyaminoboranes can be converted to either BN or BN/C films deposited over yarns of SiC fibers. Thus, they can be deposited by via dilute solutions.

4.7.2. Employed Polyaminoboranes

The description in this section (pages 51 to 61), characterizing the preceramic polymer is a summary from a report where these polymers have been developed (DARPA Project, Army Contract Number W31P4Q-13-C-0023). This description is important to understand the work performed during the composite formulations and analyses, and is not found in any open publication, thus far.

The information and characteristics described in this section are important for understanding the chemical and pyrolytic nature of the polyaminoboranes used for the fabrication of BN and BN/C interface coatings in Year 3 of the project.) Two new types of sp^3-based preceramic polyaminoboranes (non-aromatic) were used. These were developed in a non-related project that was performed prior to the effort discussed below. The two polymers are (a) polyethylenediaminoborane (PEDAB) and (b) poly-t-butylaminoborane (PBAB). The first polymer incorporates organic moiety (ethylenediamine, EDA) into the linear polymer backbone, thereby inhibiting the tendency to form aromatic rings. The second polymer consists of bulky organic side group (t-butyl) that can sterically hinder cyclization followed by aromatization via dehydrogenation. The t-butyl group is simultaneously expected to cleave and evaporate as hydrocarbon without the formation of a carbon phase.

The synthesis of the two polymeric systems involved the reactions of borane (BH_3) adducts with amines, counting on a dehydrocoupling reaction of B-H with N-H groups to form a new B-N bond. In contrast to other synthetic routes consisting of B-Cl and B-Br chemistry, the hydroborane chemistry does not leave halide contamination and does not require purification of the polymers from the bulk production of halide salts. Figure 32 illustrates the generic reactions for synthesizing the two types of polymers.

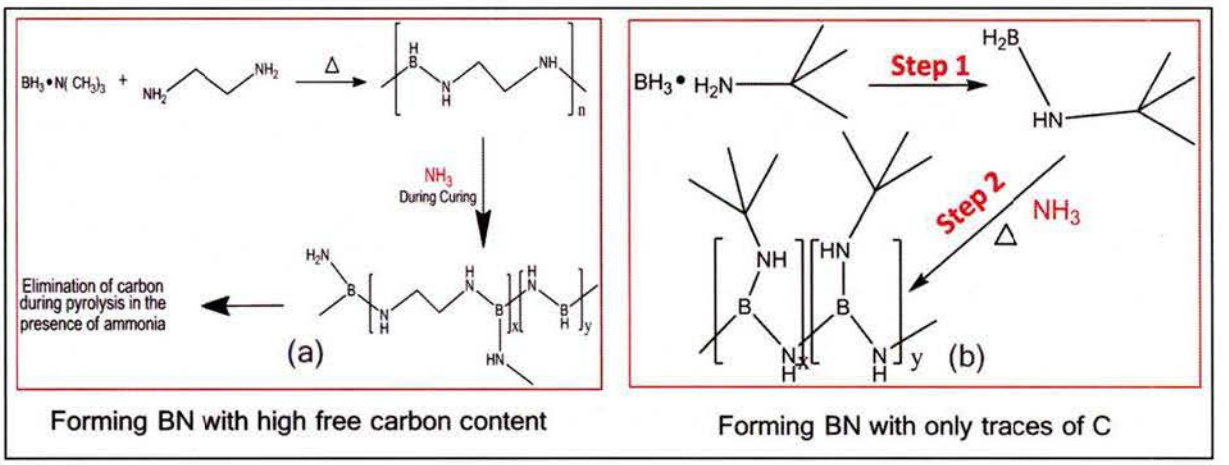

Figure 32. The two preceramic polymer systems SRI developed during the Base Program.

Both polymer systems are much more thermally stable than expected, forming molten phases that are not easily thermoset by crosslinking reactions. In both systems, we noticed the generation of sp^2 structures during the pressurized curing step in the required presence of ammonia, and the increase of sp^2/sp^3 ratio as the temperature increases during the pyrolysis and further annealing steps at higher temperatures and ambient pressure. Therefore, it seems that the network structure of the evolved material still rearranges itself toward the formation of a predominantly hexagonal structure. However, the amorphous phase of the material is more stable at high temperature, as manifested by lack of major crystallization even at 1500 °C

The curing of both polymers requires their reactions with ammonia. The ammonia can extend and crosslink the polymers via additional dehydrocoupling reactions of N-H with B-H groups. The curing is important for achieving stable shapes of products based on preceramic polymers. It is even more important for obtaining high conversion yields from the polymer to the ceramic stage and eliminating the cleavage of volatile B-N containing oligomers. However, the ammonia reactivity during the curing stage leads to the removal of organic groups that inhibit the formation of sp^2 structures. This reactivity, identified as transamination, was found to compete with the crosslinking reactions of the ammonia.

The curing of PEDAB in the presence of ammonia can be carried out during the pyrolysis step, which is also performed in the presence of ammonia as a preferred environmental condition for reducing the carbon content of the final ceramic material. However, in the case of PBAB, we had to develop a curing step with ammonia under pressure. Otherwise, the polymeric material is volatilized and also decomposes easily to volatile fragments due to the excessive stability of the t-butyl group introduced through the t-butyl amine. This phenomenon makes this approach to be a bit more problematic for making coatings over large volume of fibers, but in this case we should try and get in future studies some other types of crosslinking e.g., radiation or radical curing.

The pyrolysis of PEDAB in inert environment (nitrogen) leads to the retention of high carbon content. This is a typical situation for all preceramic polymers that contain organic groups. However, this specific system leads to even higher retention of carbon relative to other polymers with the same level of organic fraction that do not possess aromatic structures.

A technique to eliminate the carbon from PEDAB during the formation of nitride ceramics was developed over 20 years ago in our lab and consists of pyrolyzing the precursors in the presence of gaseous ammonia. This approach is efficient for films or relatively fine particles, as the diffusivity of ammonia in preceramic polymers is limited to less than 4 μm. Nevertheless, we found it difficult to count on this pyrolysis approach due to the stability of the polymer and the melting/softening it goes through. In fact, even the semi-cured polymer powders fused or melted in the temperature range of 300 to 400 °C, forming materials with bulk thicknesses larger than 4 μm. However, the efficiency of the ammonia diffusivity and consequent reactivity can be still very efficient for the coating thickness of interface films.

To circumvent this situation, the focus of the preceramic polymer study has shifted toward the synthesis and processing of PBAB. In this system, once the t-butyl groups cleave during pyrolysis, they have a lower tendency to thermally condense into a carbonaceous material due to steric hindrance and would therefore evaporate as stable isobutene or isobutene gas.

However, the bulkiness of the t-butyl group leads initially to the formation of too-stable intermediates that are either volatile (i.e., not polymeric) or hard to cure. We had to incorporate ammonia into the synthesis to circumvent this stability, hence forming [-BH-NH-] comonomeric units in the overall structure. Due to the high stability, the reaction with the ammonia required high temperature and high concentrations of ammonia. Thus, the reaction had to be performed in a pressure reactor at ~200°C and 1500 psi. The synthesis-curing reactivity includes also transamination in which a t-butylamino group is replaced by ammonia, forming additional [-BH-NH-] units while releasing t-butyl groups in the form of t-butylamine. Therefore, this step requires optimization, an effort that has not been performed yet.

More about the PEDAB system and its characteristics. We attempted to increase the crosslinking reactivity by replacing the borane reagent to the adduct with trimethylamine versus the previously used dimethylamine. The trimethylamine cannot react with the borane and therefore bonds only weakly to the polymer product, if at all. Its potential bonding to the polymer is illustrated in Figure 33.

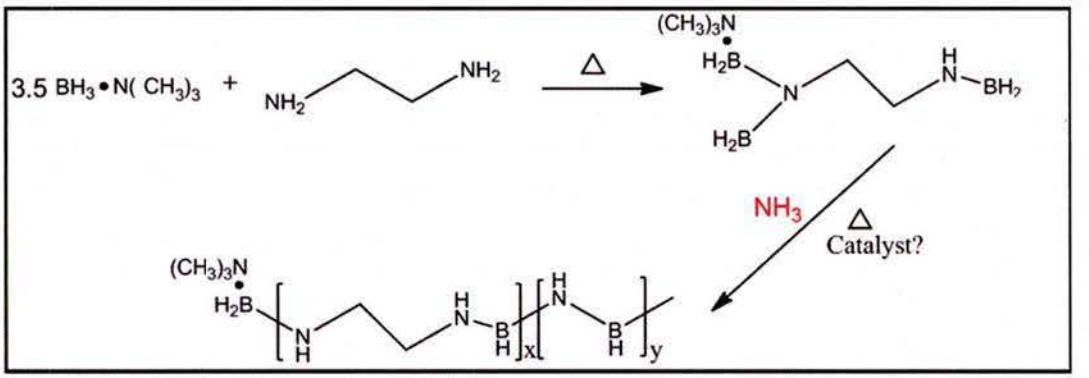

Figure 33. Replacing the dimethylamine with a trimethylamine complexing unit to avoid the formation of irreversible Me_2N-BH- bonds.

Pyrolysis in Nitrogen Atmosphere. The pyrolysis of PEDAB 1:1 in nitrogen atmosphere and in the absence of a curing step involves the melting of the polymer powder during the initial heating causing severe foaming as a consequence once gases are evolved (hydrogen, amines, monomeric and oligomeric volatiles). As shown in Figure 34, curing at 200°C (green line compared to red line) does not improve the overall ceramic yield. This is due to the significant presence of residual carbon after the pyrolysis. The ceramic yield is too high compared to the theoretical yield calculated for forming "pure" BN.

The TGA analysis represents the pyrolytic activity in inert environment. However, in an attempt to reduce the residual carbon content, we switched to pyrolysis in a mixture of about 10 vol% ammonia in nitrogen.

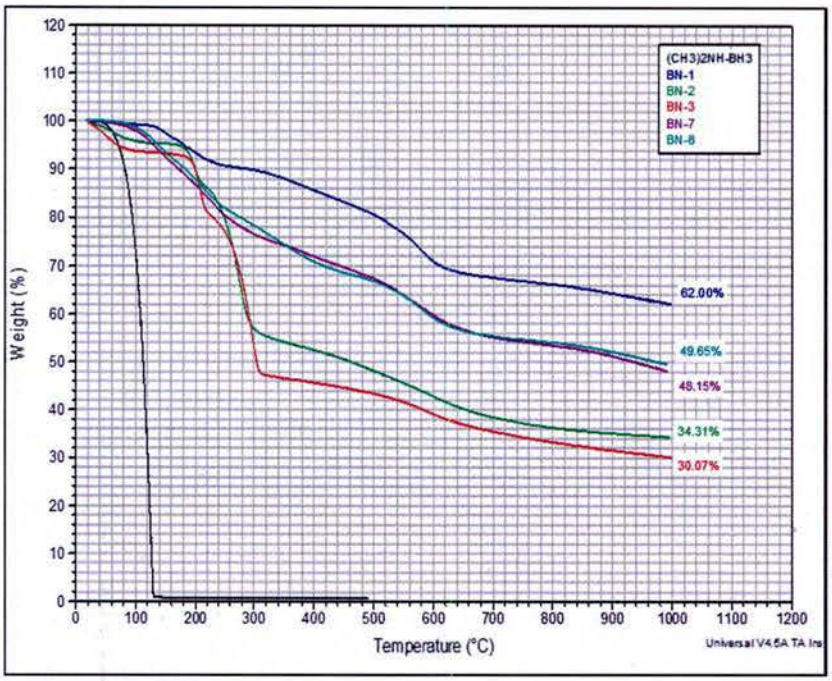

Figure 34. TGA analysis of various reactions between borane and EDA; BN1= 1:1 mol ratio of BH_3:EDA; BN2 = 1:1 with cat., BN3 = 1:1 with cat., where the dimethylamino adduct was reacted first; BN7 = 1:2; BN8 = 1:2 with cat.

The TGA analysis represents the pyrolytic activity in inert environment. However, in an attempt to reduce the residual carbon content, we switched to pyrolysis in a mixture of about 10 vol% ammonia in nitrogen.

Pyrolysis in the Presence of Ammonia. Based on previous experience with polysilazanes as precursors to silicon nitride, we know that ammonia assists very efficiently with the removal of hydrocarbons above 400 °C to eliminate most of the carbon content from the final product. Under these conditions, the organics are removed at temperatures below where they begin to condense into graphene domains. The mechanism of the carbon elimination is not so clear in the field of polymer-derived ceramics. If the organics are bonded to the nitrogen element, a transamination mechanism can be postulated. However, it cannot explain the elimination of carbon when the organic groups (e.g., methyl) are bonded to the metallic element (i.e., Si in our previous studies). Radical mechanisms involving cleavage of the Si-C and N-C bonds was suggested but never proven as the real elimination mechanism.

Pyrolyzed Polymer Analysis. Typical FTIR analyses of pyrolyzed materials are shown in Figure 35, with comparison to commercial hBN and cBN. Sample BN4-2 was pyrolyzed in Ar and BN4-3 was pyrolyzed in NH_3/Ar. Both show a significant presence of sp^3 bands in the absorbance region of cBN apart from the presence of significant sp^2. However, the sp^3 region of cBN is also the region where tetragonal bonds of B-C, N-C and C-C absorb while C=C (graphene), C=N and B-O absorb in the range of the hBN's sp^2.

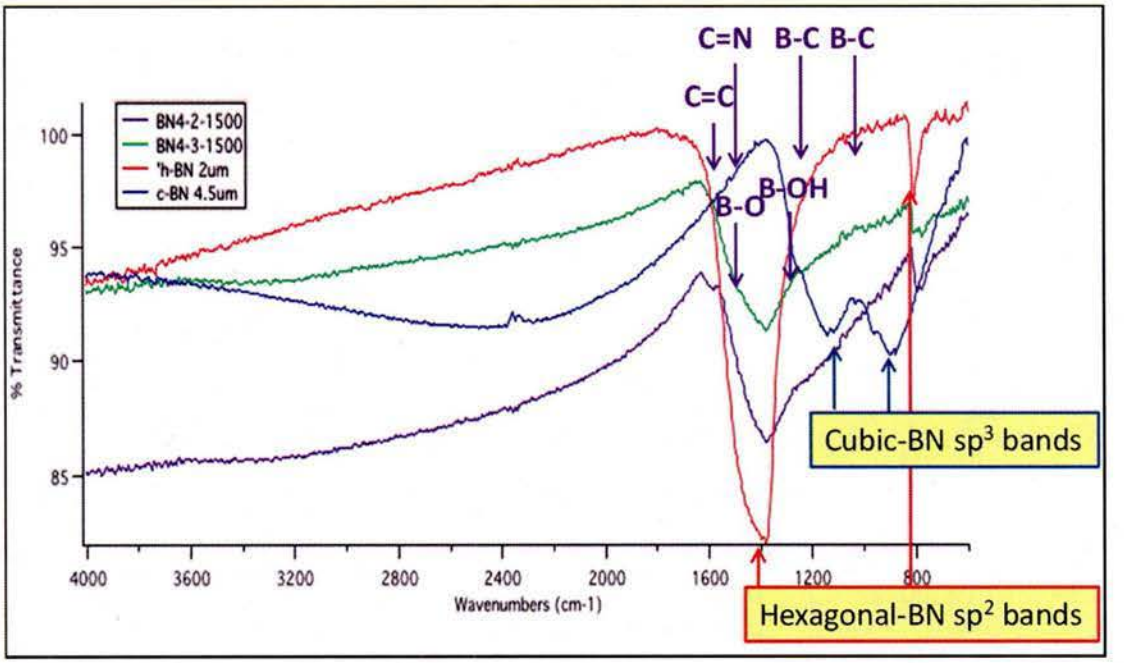

Figure 35. FTIR of polymer pyrolyzed in Ar (BN4-2) and NH_3/Ar (BN4-3) to 1500°C; compared with hBN and cBN samples.

The overall structures of the PDC products seem to be still highly amorphous. In contrast, a conventional precursor to BN (polyborazine, polyborazylene) provides a significant characteristic of organized hBN structures at 1500°C according to XRD, SEM, and TEM analyses.

The PBAB System. Two types of poly-t-butylaminoborane (PBAB) were assessed, as illustrated in Figure 36. Of them, Synthesis 1 (left side) was found to be much more adequate for obtaining a practical preceramic polymers, and it was used for the composite processing. The main difference between the two potential polymeric products is that in Synthesis 2 the nitrogen of the t-butylamine is a part of the main polymeric chain, and in Synthesis 1 it is integrated as a side group. Therefore, the steric hindrance and cleaving reactivity of the t-butyl group at elevated temperatures are expected to be different.

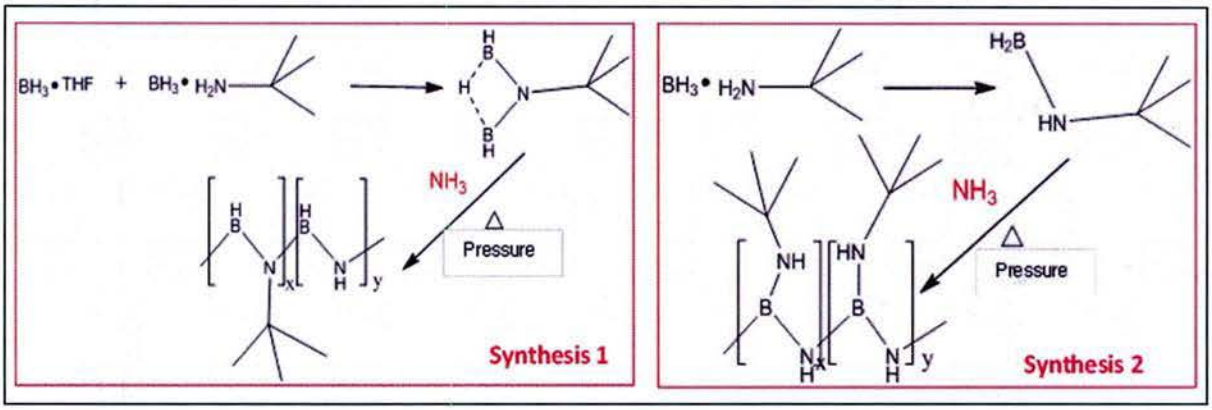

Figure 36. The two synthesis routes selected to achieve PBAP using t-butylamine-borane adduct.

Pyrolytic characteristics. Pyrolysis of the Step 1 product of Synthesis 1 resulted in very low conversion to ceramics, as the product was still highly volatile at around 120°C, as shown in Figure 37. The TGA of the Step 2 product compared with that of the starting material shows a high ceramic yield of over 70 wt%. The fact that the cleavage of organic fragments in the temperature range of 450-600°C indicates that much of the t-butyl amine was replaced by the ammonia via a transamination reaction during the curing stage. Otherwise, the ceramic yield should be in the range of 30 wt%, if all the carbon has remained on the cured polymer backbone before pyrolysis and then mostly cleaved during pyrolysis. The pyrolysis product in nitrogen was white, indicating very low free carbon content.

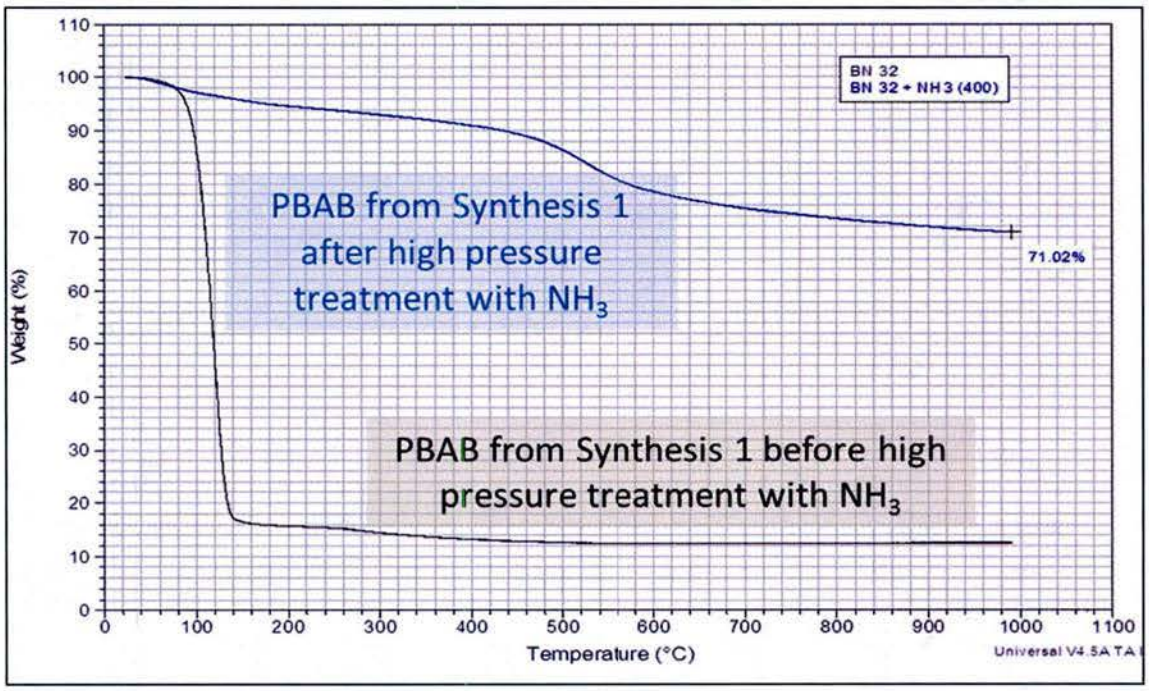

Figure 37. Pyrolysis of PBAB derived from Synthesis 1 before and after ammonia treatment under pressure.

Spectroscopic Analysis. Figure 38 represents the FTIR of polymer synthesized using the Synthesis 1 approach. There are only slight differences in the FTIR signature during the low-temperature reaction of the polymer evolved in Synthesis 1 even after ammonia treatment at low pressure. The B-H peaks (2200-2400 cm^{-1}) are still very strong and organic C-H peaks (2900-3000 cm^{-1}) are present as well, as shown in Figure 38. In contrast, the –N(-H)- bonds (broad band at 3400 cm^{-1}) are weak, while sharp peaks of B–NH_2 are detected in 3200, 3100 and 1570 cm^{-1}. This observation is consistent with the slight dehydrocoupling obtained during the atmospheric reaction with ammonia, yet the condensation of the amino sites via deamination, transamination, or dehydrocoupling is inhibited under these conditions. At this stage there is no significant signature, if at all, that represents sp^2 B-N bonds. In contrast, the sp^3 region of B-N has several strong and sharp absorbance bands.

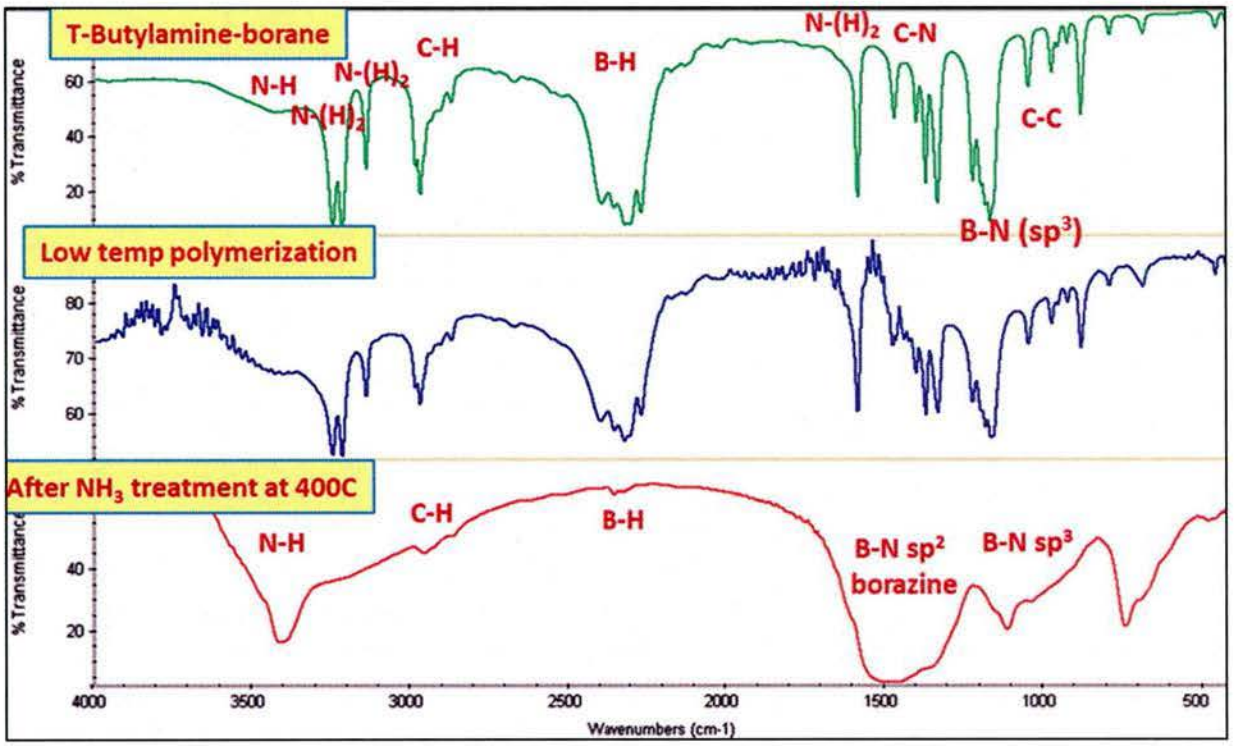

Figure 38. FTIR spectra of PBAB prepared via Synthesis 1 compared with t-butylamine borane adducts and the polymer after pressurized reaction with ammonia at 400 °C.

Once the precursor is cured in ammonia at 400 °C under varied pressure but not exceeding 1600 psi (generated mostly by hydrogen evolution due to the dehydrocoupling reaction between B-H and N-H), the B-H disappears and the C-H is significantly reduced, while the broad –(N-H)- stretches at 3400 cm^{-1} are now significant. At this stage, significant sp^2 B-N structures are established and become more pronounced as the temperature increases (see Figure 39). We can conclude that the reactivity at 400°C goes too far and forms a cured intermediate that is primarily bases of B-NH-B skeleton with sp^2 structure, while most of the t-butyl groups have been removed. Once such an intermediate is pyrolyzed, it shows the predominant formation of and sp^2 material (Figure 39), although it remains mostly amorphous.

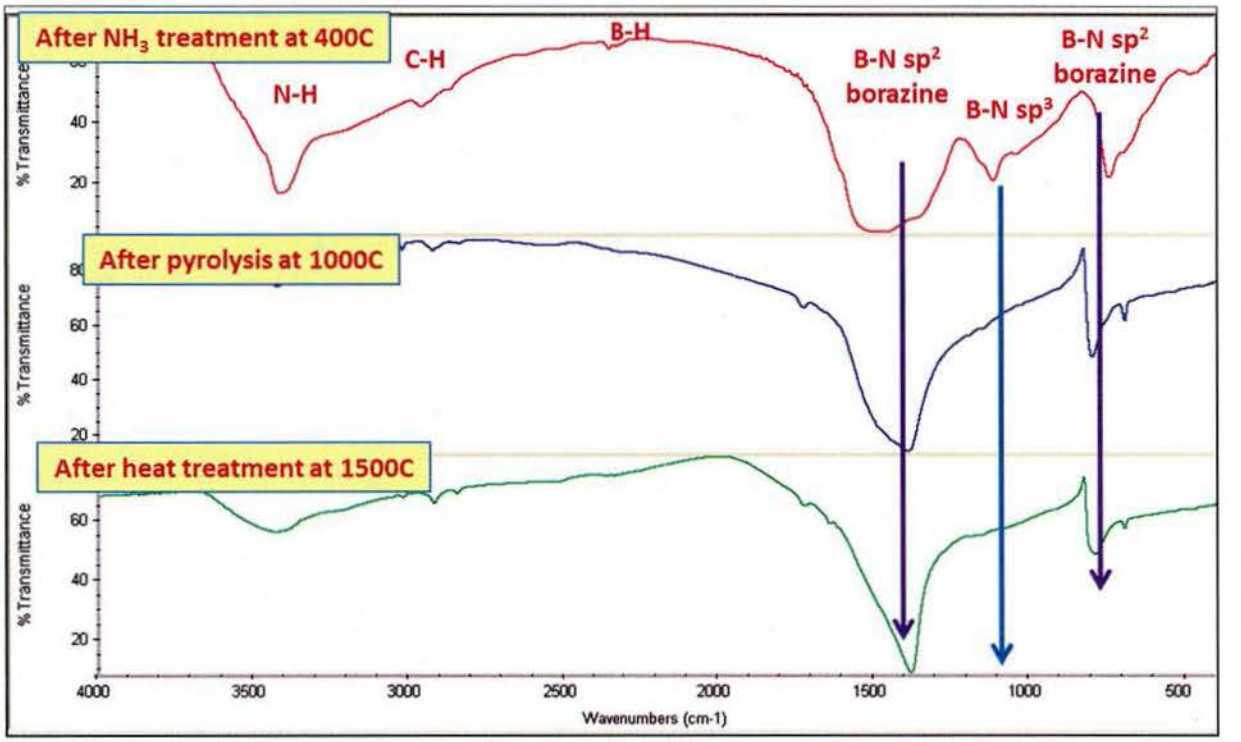

Figure 39. Evolution of sp^2 structure of PBAB treated with ammonia at 400°C under pressure.

Curing. Curing study in the presence of pressurized ammonia confirmed that there is a competition between the crosslinking via dehydrocoupling reaction and transamination, as revealed in the TGA plots in Figure 40. While the pre-pressurized material provides very low ceramic yield, the material cured at or above 200°C do not show significant depletion of material below 400°C. The weight loss above it is associated mostly with the cleavage of the t-butyl groups. Yet, it is much less than expected if each monomeric unit contains a t-butyl group. Therefore, it is clear that much of it has disappeared already during the curing stage. In contrast, curing at 180°C in pressurized ammonia still does not show much greater depletion below 400°C, but there is significantly more removal of t-butyl groups during the next weight-loss step above 400°C.

Also, the FTIR indicates that lowering the temperature and ammonia level in the reaction lead to the retention of more sp^3 type bonding at the cured stage as shown in Figure 41. The red line in the right picture and the green line in the left picture represent Synthesis 1, Step 2, which involved heating at 180°C with 1/5 of the ammonia originally added to Step 2. It still contains sp^2 structures but at significantly lower ratio relative to the sp^3 bands. We are currently studying the pyrolysis of the low-temperature cured material in nitrogen.

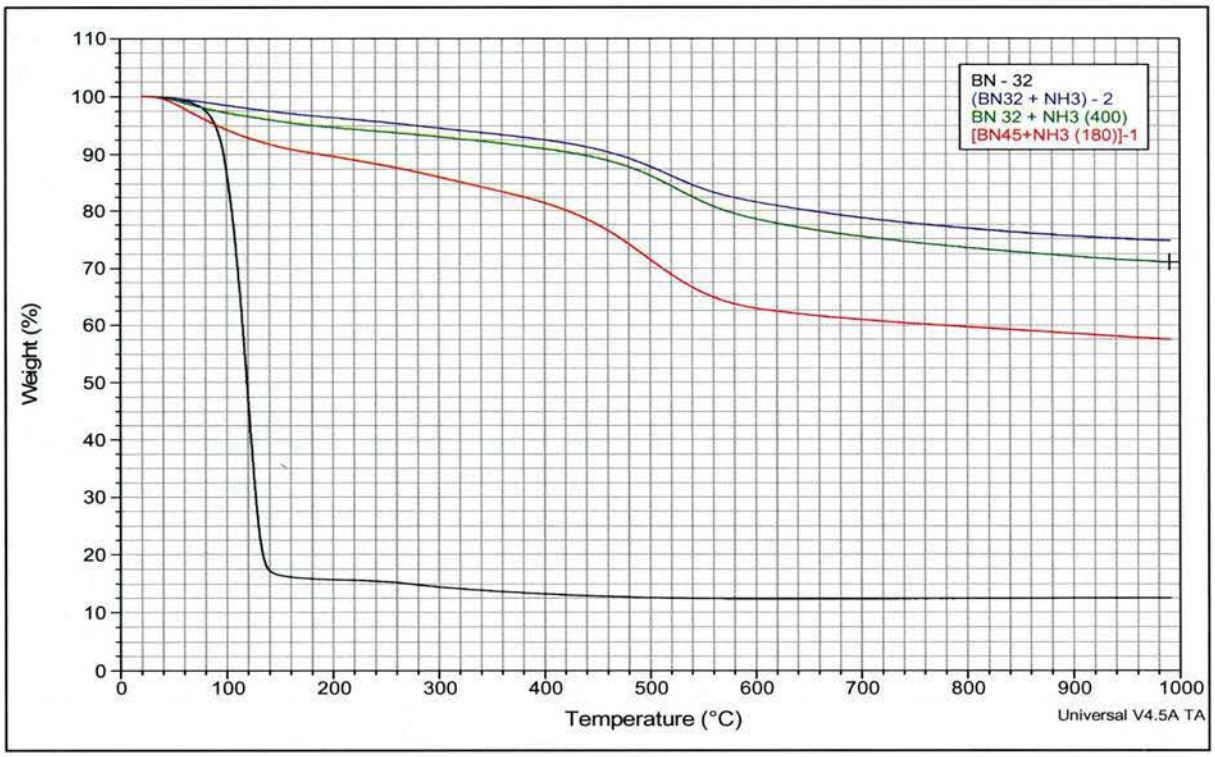

Figure 40. Pyrolysis profiles of PBAB as a function of curing conditions.

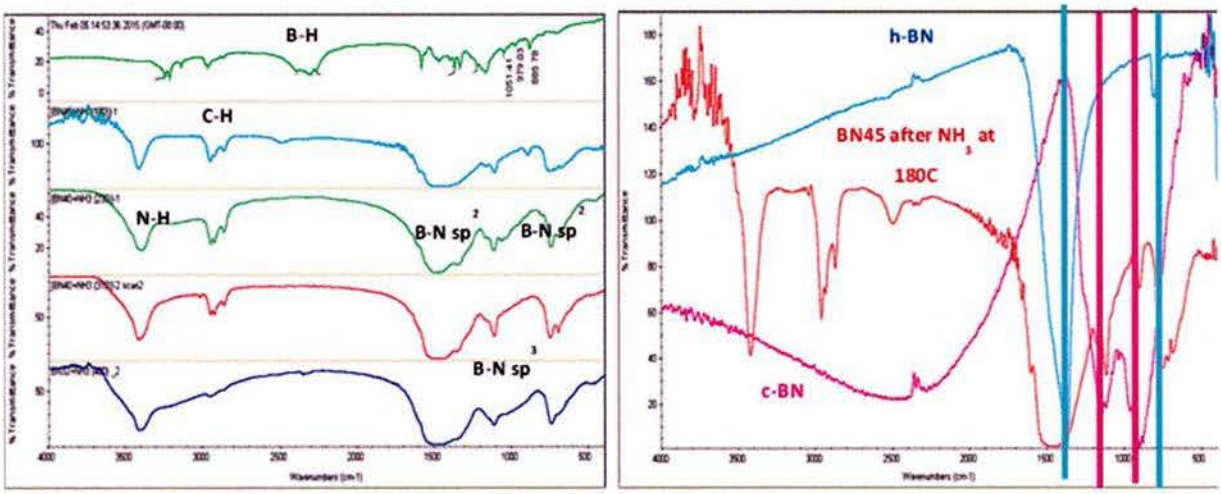

Figure 41. FTIR analysis of PBAB, cured at various conditions with pressurized ammonia.

Pyrolyzed Product. This is the first time we have been able to obtain an off-white pyrolyzed product from any preceramic polymer that contains organic carbon in this study. This remarkable phenomenon is observed for pyrolysis processes in both NH_3/N_2 and, more significant, in the inert N_2 alone. The color by itself is a strong indication of the efficient elimination of carbon content. In general, polymer-derived ceramics are completely black even at the levels of 0.5 wt% carbon. Indeed, the t-butylamine polymers that were pyrolyzed either in NH_3/N_2 mixture or in

pure nitrogen possess less than 0.5% of carbon according to elemental analyses. Thus, the presence of t-butyl groups is an elegant solution for removing carbon from polymeric precursors to boron nitride as well as generically from any other precursors, such as silicon- or aluminum-based ones. Table 4 shows elemental analyses of nitrogen and ammonia pyrolyzed materials. Note that the total wt% does not sum to 100%, indicating that the material is hard to combust or dissolve in acids during the analysis. Oxygen is still present, associated with contamination of the synthesis reagents and the handling of the reactions and processes. The elimination of the carbon when t-butyl groups are grafted to the preceramic polymer is the most significant observation found in this project for enhancing the overall field of preceramic polymers.

Table 4: Elemental analysis of poly t-butylamine-ammonia-borane

Polymer	B (wt%)	N (wt%)	C (wt%)	O (wt%)	Total (wt%)
Synthesis 1 pyrolyzed to 1000°C in the presence of NH_3/N_2	41	35	0.06	11	88
Synthesis 1 pyrolyzed to 1000°C in the presence of N_2 only	35	37	0.16	19	91

The XRD shows some very broad peaks already at 1000 °C in the case of pyrolysis in NH_3/N_2 (see Figure 42). The XRD becomes sharper as the temperature increases. In contrast, we observed a similar pattern only when the temperature reached 1500°C. The formation of nanocrystalline domains at lower temperature is attributed to the extremely low carbon content. The peak at ~43 °C is attributed to hBN for a case in which there is no preferred orientation of the domains. (See calculated XRD of random hBN vs the typical orientated pattern in Figure 43, bottom right corner.) This pattern is very similar to reported patterns of other polymer-derived hBN, e.g., from polyborazylene.

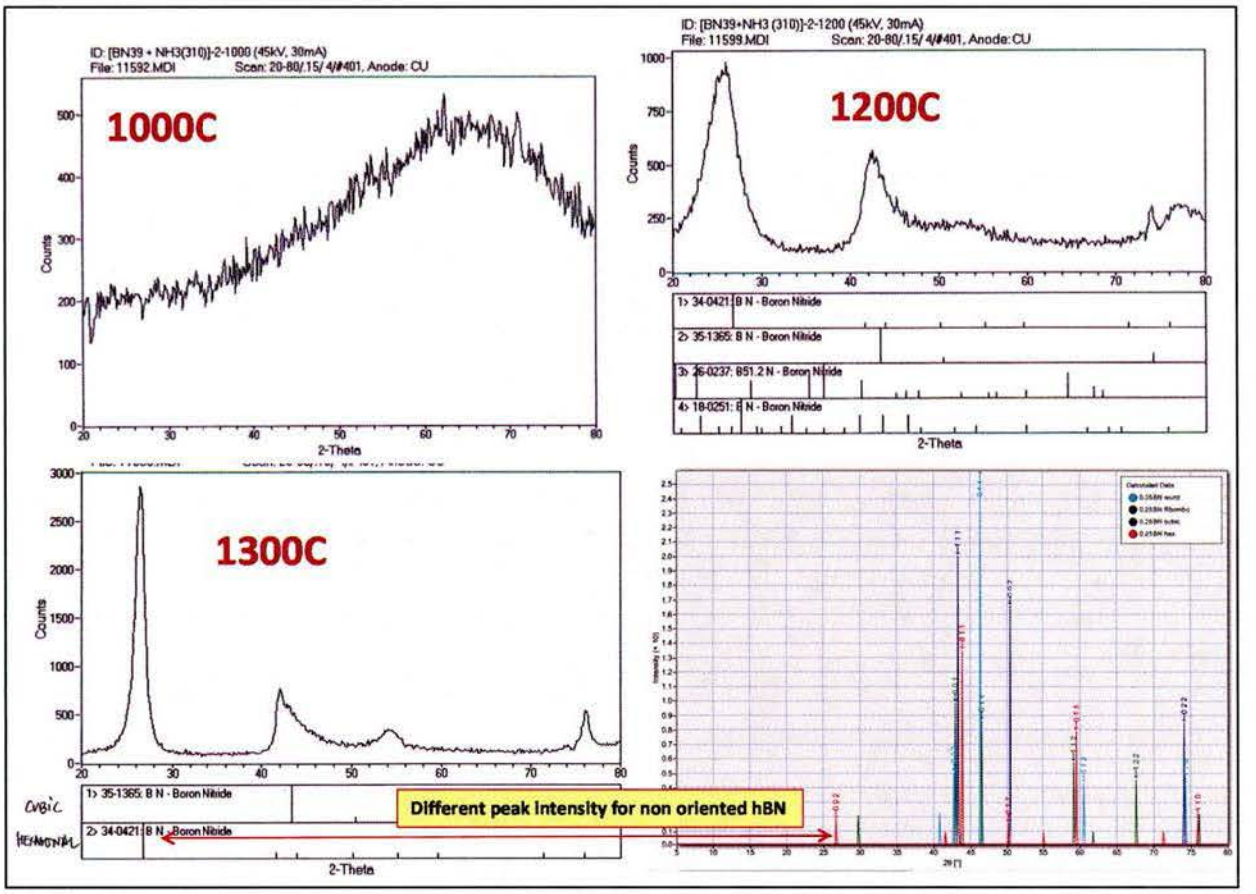

Figure 42. XRD pattern of PBAB pyrolyzed in nitrogen and further heated at various temperatures.

The FTIR analysis of polymer pyrolyzed in N_2 only versus NH_3/N_2 reveals some differences in-spite of the elimination of carbon in both cases. The IR of the product pyrolyzed in nitrogen indicates an additional absorption around 1100 wavelength that may represent sp^3 domains more than when the pyrolysis is carried out in ammonia. Also, The N-H absorption at 3500 cm^{-1} is distinctively sharper than in all other cases as shown in Figure 43.

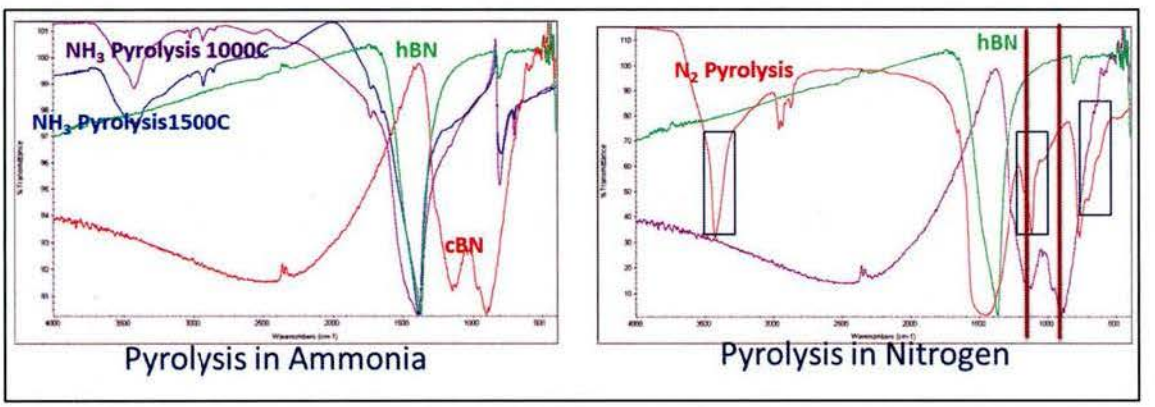

Figure 43. Comparison between PBAB pyrolyzed in N_2 versus NH_3/N_2

4.7.2 SiC/SiC Composite Fabrication

Materials. Silicon Carbide yarns were Hi-Nicalon, with 15 µm diameters and 500 fibers in the yarn (purchased through Goodfellow; catalog # SI675721). The SiC powder was 99+% pure, 7 µm particles (U.S. Research Nanomaterials; catalog #US1009M). The polycarbosilane used for making the matrix slurry was SMP10 purchased from Starfire Systems. Cyclohexane AR was used as the additional solvent for adjusting the viscosity of the matrix slurry.

Sample configuration and testing concept. The plan for making the SiC/SiC composites consisted of coatings fiber yarns of uncoated Hi-Nicalon short yarns with the two polyaminoborane candidates, adjust the coating thickness and then incorporate the short yarns into mini-composites made of Hi-Nicalon fabrics and SiC/polycarbosilane matrix. We had a small amount of such fabric, which was donated by AFRL to SRI during a previous collaboration. The SiC fabric was already coated with C and top BN layers. Our plan was to embed coated and uncoated short yarn of Hi-Nicalon fibers in between plies of coated fabric layers in the processed mini-composites. Such samples can be evaluated for the desired pullout effect of the coated SiC short yarns. The pullout effect is mandatory for achieving desired ceramic composite characteristics. Figure 44 illustrates the arrangement of such a mini-composite.

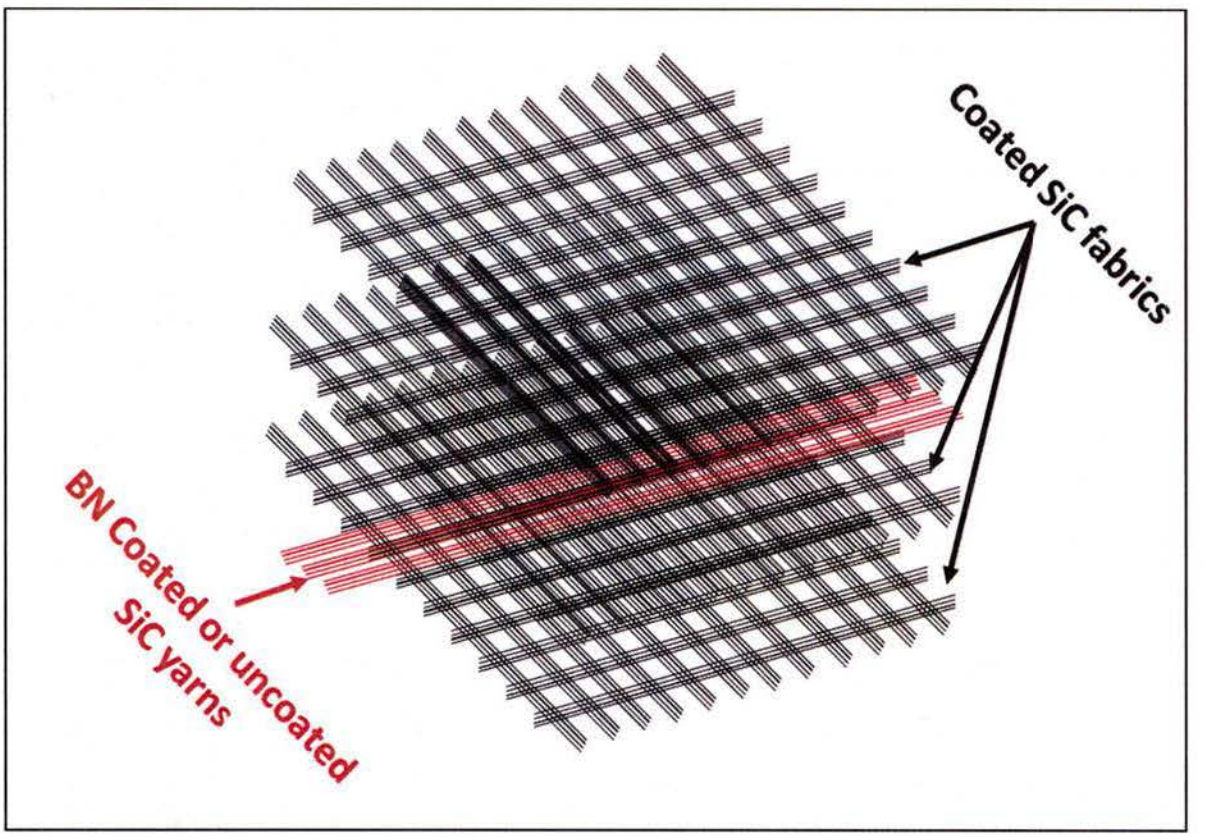

Figure 44. Arrangement of mini-composite for studying the pullout effect of coated yarns with polymer derived BN and BN/C

Yarn coating procedure. The final fiber yarn coating procedure, developed for this effort consisted of the following steps. The initial processing was performed inside a dry box.

a. Dip coat 5 pieces of 3" long SiC fiber in 5wt% polyaminoborane (PEDAB of PBAB in THF).

b. Hang the yarns to dry overnight inside the dry box.

c. Transfer the coated SiC yarn samples to 3 mm diameter quartz tubes and seal the tubes with a plastic cap. This arrangement does not allow the short yarn to bend.

d. Transfer the quartz tubes from a dry box to a furnace tube. Remove the caps and quickly seal the furnace tube with its cover. Start purging the tube with argon as quickly as possible.

e. Pyrolyze the coated yarn samples according to the following program:
   i. Heat at 5 °C/min to 300 °C, in a mixture of NH_3 & Argon, hold for 2 h at 300 °C,
   ii. Then, heat at 5 °C/min to 1000 °C, in argon (99.999%), and hold for 1 h at 1000 °C.

Coated yarns analysis. Fibers coated with 5wt% preceramic polymer solutions, remain separated as shown in Figure 45. At higher solution concentrations the coated fibers are significantly bonded to each other after pyrolysis at 1000 °C.

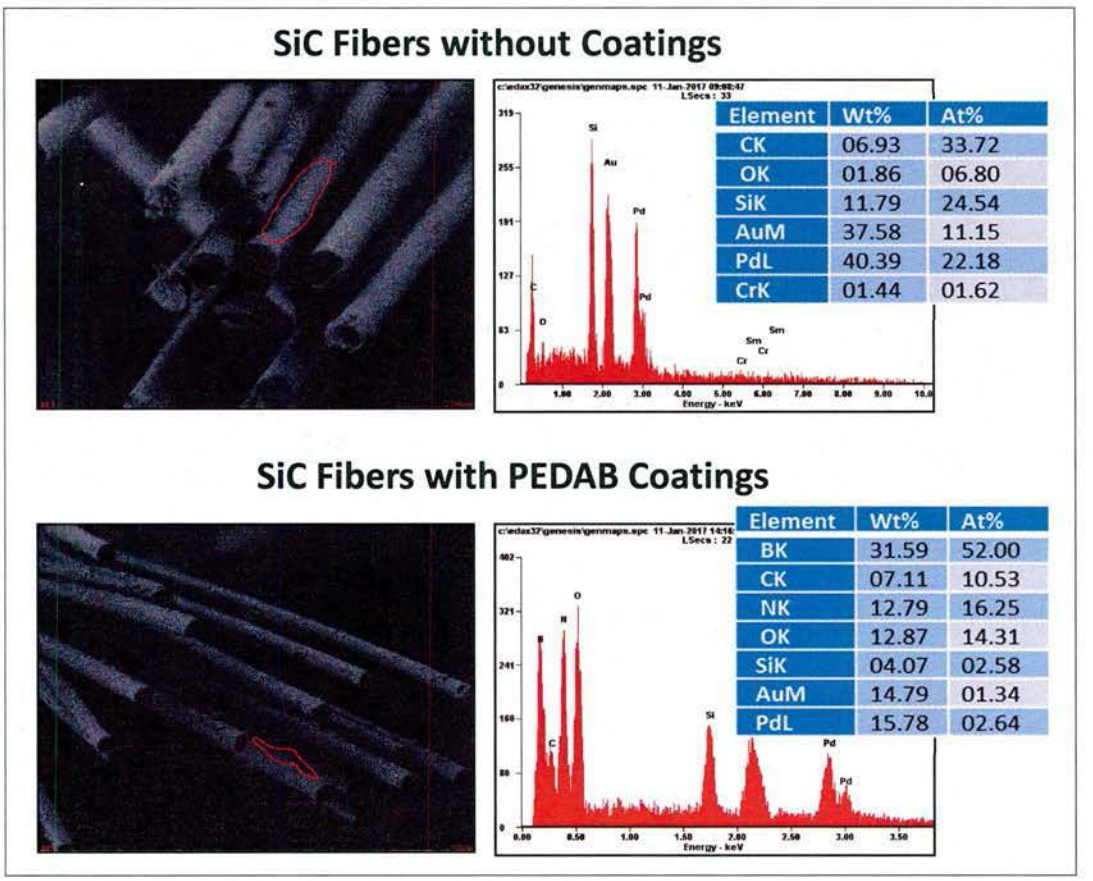

Figure 45. Uncoated SiC fibers and fibers coated with 5 wt% solutions of PEDAB and pyrolyzed in argon at 1000 °C.

The thickness of the coatings is in the range of 0.1 to 0.5 μm. The coatings have areas with some roughness, which is assumed to be a result of the fibers sticking to each other before the curing and pyrolysis. There is a strong indication to the presence of boron, carbon, and nitrogen in the pyrolyzed coatings according to the EDS analysis. However, a significant amount of oxygen is also incorporated during the coating processing and pyrolysis, in spite of the attempts to do most of the early processing in a dry box. However, during transferring the coated fibers to the curing or the pyrolysis chamber, the coatings are exposed to air for a short time, and the polymers are sensitive to hydrolytic reactions with moisture. Nevertheless, the oxygen incorporation seems to be a part of the entire BNC(O) amorphous structure and not the formation of a B_2O_3 phase, which would form a liquid phase during the pyrolysis. Also, the EDS analysis is qualitative, only regarding the light elements involved in the analysis; the high ratio of C to Si indicates the presence of high carbon levels in the coating layer.

Similar observations are found with 5 wt% coatings of PBAB deposited over the SiC yarns as shown in Figure 46. Again, oxygen is observed by EDS analysis in addition to boron, nitrogen, and carbon. In contrast to the EDS analysis of the PEDAB coatings, the analyses in this case indicate C to Si ratio in the range anticipated for SiC (the fiber composition). Hence, in this case, the carbon content in the coating layer must be low.

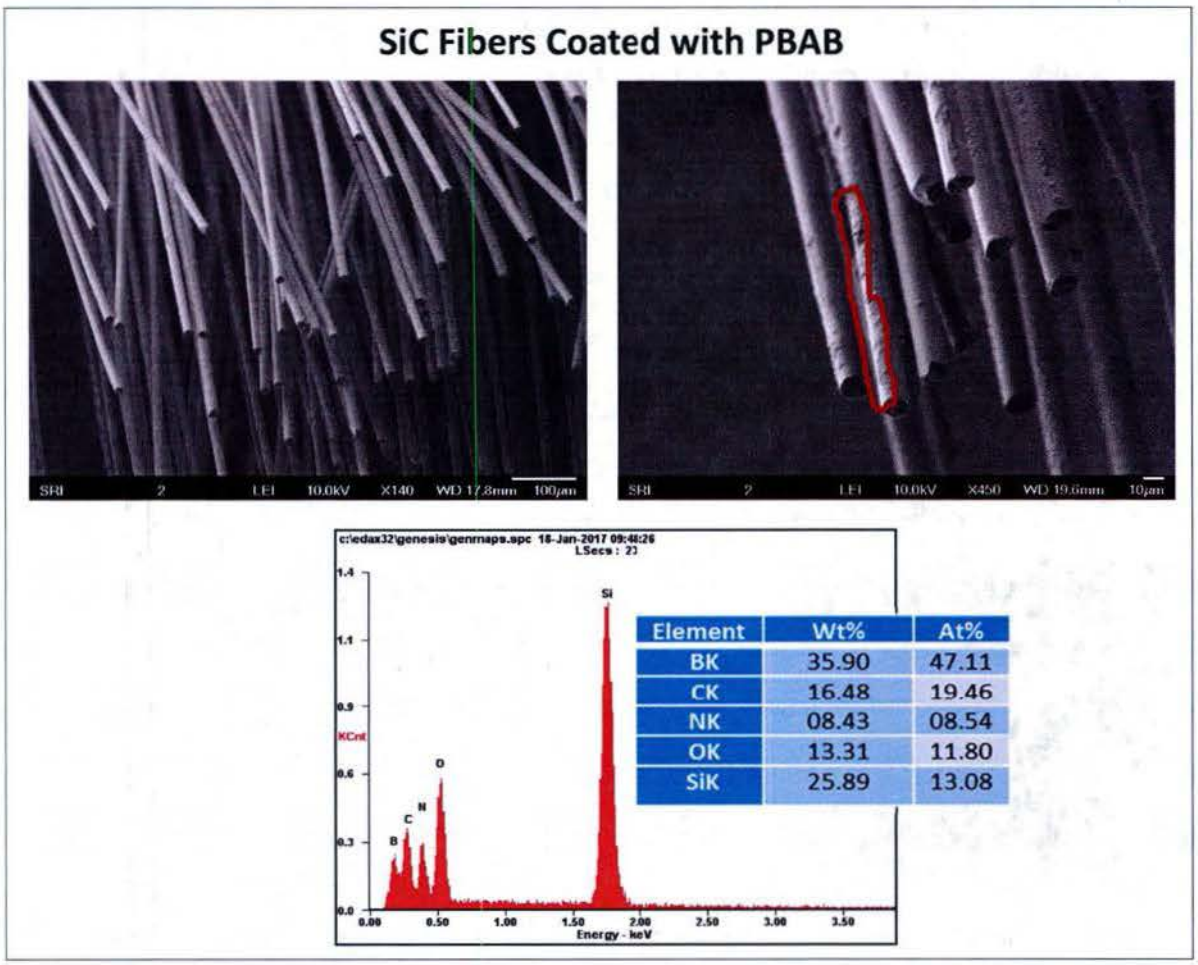

Figure 46. Fibers coated with 5 wt% PBAB, cured and pyrolyzed at 1000 °C.

Coated fibers embedded in matrix material. After the initial fibers were coated successfully, we have assessed the interaction between the planned matrix material and coated fibers. This effort was also used to assess the ratios of SiC powder to SMP10 polymer that would be used for making the slurries for the initial matrix infiltration. Based on the observations the ratio was set to 60 wt% SiC powder and 40 wt% polymer.

Coated yarns were immersed in slurries consisting the various SiC/SMP10 ratios and cyclohexane as a viscosity controlling solvent. The Solvent was then removed in a vacuum oven, while the slight weight is applied to press the slurry before it is cured. After solvent removal at RT, the oven was slowly heated to 180 °C to cure the polymer component in the slurry. The cures samples were further heat to 1000 °C at 5 °C/min and kept at 1000 °C for 1 h before cooling.

Figure 47 shows a sample made of fibers coated with PEDAB embedded in pyrolyzed matrix material. There is a strong evidence for weak interface as manifested by fiber pullout. Bot fiber brushes and tracks where fibers were pulled out, are observed. Also noticeable that in its free form the slurry is relatively dense after pyrolysis with no evidence for bubbles or microporosity. It is still assumed that nanoporosity due to the shrinkage of the polymer-derived ceramic exists in the evolved matrix composition.

Figure 47. SiC fibers coated with PEDAB embedded in pyrolyzed matrix material.

Some of the pulled out fibers still show remains of the polymer-derived coatings as shown in Figure 48 for fibers coated with PBAB.

Mini-composite fabrication procedure. The final procedure for making composite test specimens is as follows.

1) Prepare SiC powder/SMP-10 slurry in cyclohexane by mixing
   a) 7.5 g SiC powder (60 wt%)
   b) 2.5 g cyclohexane
   c) 5 g polycarbosilane (SMP-10) (40 wt%)

2) Infiltrate 3 to 5 pieces of 1.5"x3" SiC fiber cloth with SiC/SMP-10 slurry
3) Remove most cyclohexane by applying vacuum at RT.
4) Place uncoated or coated SiC short yarns on second layer of infiltrated SiC fiber cloth. The coated yarns are those coated with BN or BN/C fibers as described above.
5) Mount the composite samples (3 to 5 layers) on top of each other and pressurize them together using Teflon films on top and at bottom to squeeze out excess of slurry.
6) Place the composite on top of a metallic plate, insert it into in a vacuum bag, and apply vacuum at room temperature.
7) Place the vacuum bag on a press/heater. Apply pressure of in between 500 to 1000 psi. Slowly heat to 180 °C and hold for 5 h at 180 °C while maintaining the vacuum inside the bag.
8) Cool the press and release both pressure and vacuum and remove the cured composites from the vacuum bag.
9) Place the composite specimen in a tube furnace and pyrolyze the composite in Argon (99.999%) by ramping the temperature at 5° C/min to 1000 °C in argon, and hold for 1 h at 1000 °C.

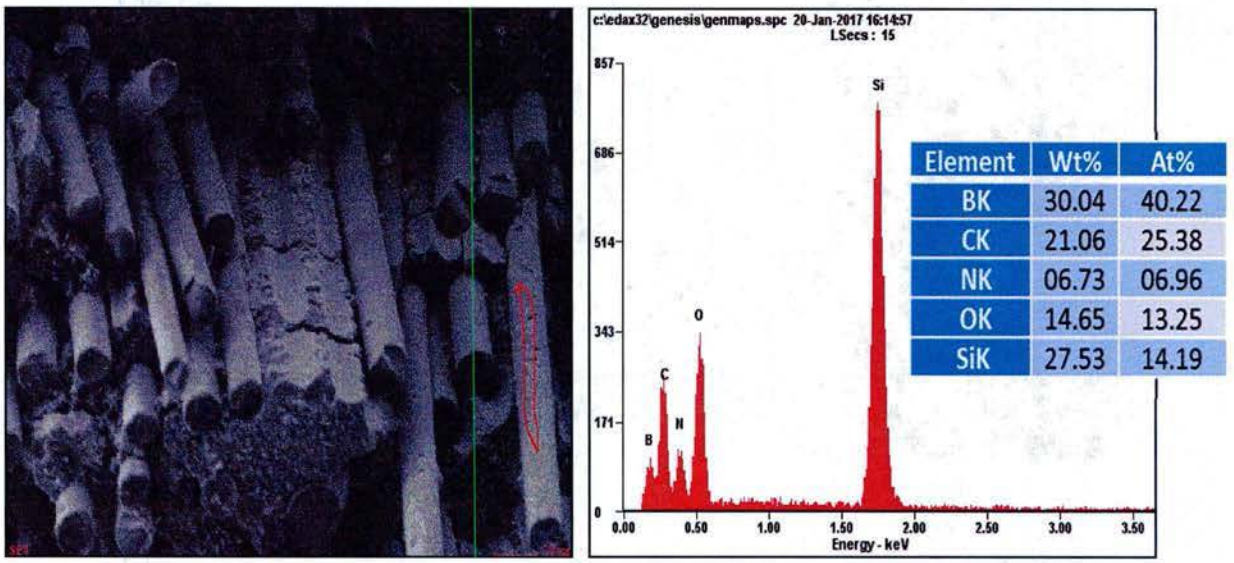

Figure 48. EDS of fibers coated with PBAB and pulled out of SiC matrix after pyrolysis of the matrix at 1000 °C.

Mini-composite analysis. The pictures in Figure 49 show mini-composites in which either coated or uncoated yarns of SiC were individually embedded. Figure 49a reveals strong bonding of the matrix to uncoated SiC yarns, while Figure 49b shows a weaker bonding of the matrix in the case of embedded fibers coated with PBAB. The pullout in the case of fibers coated with PEDAB is even more pronounced, as indicated in the cavity generated by the pullout in Figure 49c.

The matrix in these cases is still chalky in its nature, since the composite was not reinfiltrated.

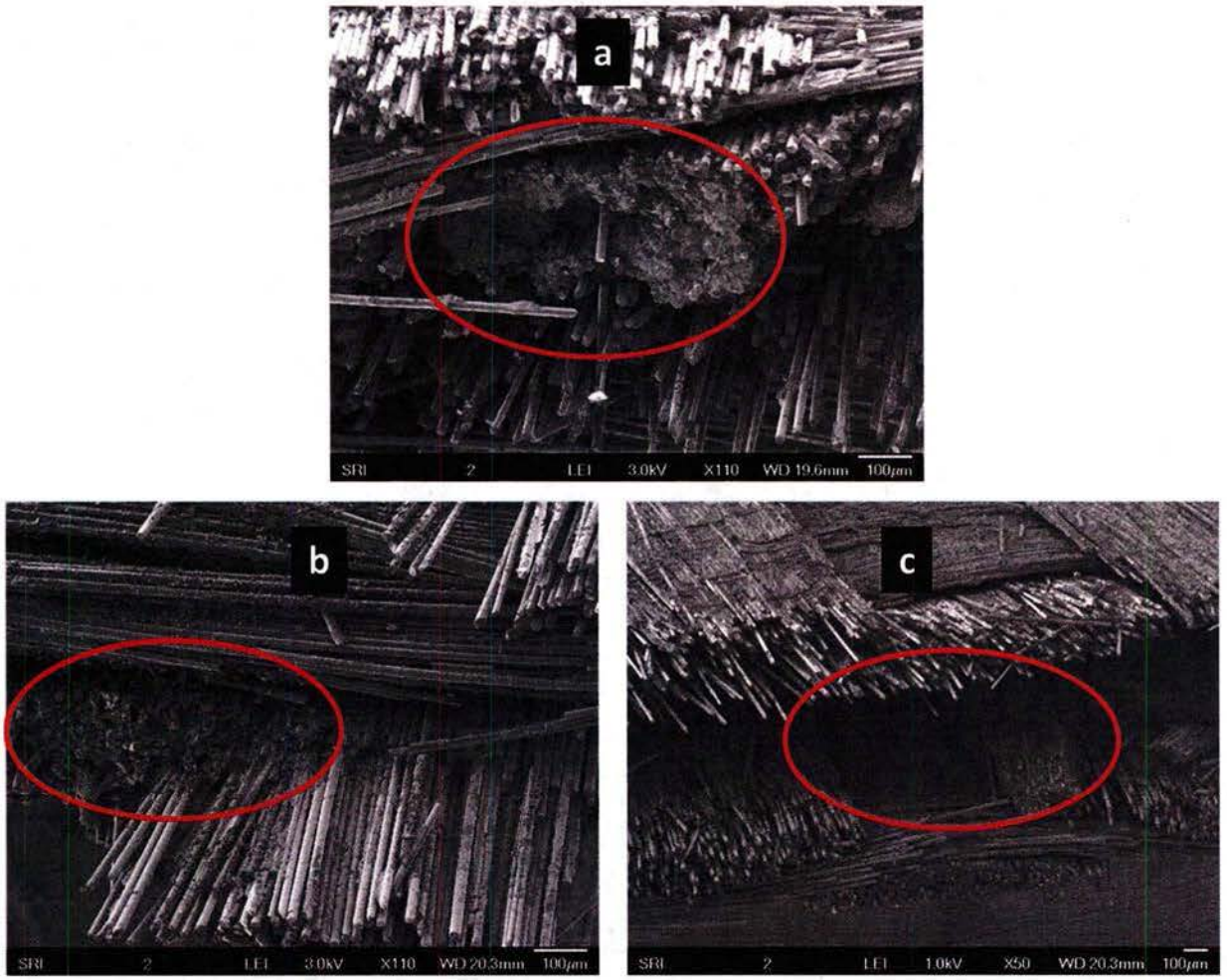

Figure 49. Uncoated and coated yarns, embedded in a mini-composite. (a) Uncoated fibers); (b) fiber coated with PBAB; (c) Fibers coated with PEDAP.

Reinfiltration of mini-composites. Mini-composites with embedded fibers were reinfiltrated twice with neat SMP10. The process starts, as detailed above, with slurry impregnation, followed by curing and pyrolysis to 1000 °C. After the first pyrolysis cycle, the specimen is placed in a large tube with a head connected to a vacuum line, in which neat but low-viscosity SMP10 is placed at the bottom of the wide tube. The placement is done when the tube is almost horizontal. One the vacuum top is placed on the reactor, the air is evacuated while the specimen is still above the liquid level. The tube is tilted upward to let the specimen slide into the neat SMP. The tube is then tilted again and the vacuum is released. Then, the infiltrated specimen is taken out and cured in a tube furnace at 180 °C in inert environment, as described above. Once the polymer is cured, excess polymer is wiped from the specimens and the specimens are heated to 1000 °C with a heating rate of 5 °C/min. The infiltration cycles were performed twice in this study.

Figure 50 compares between the differently treated yarns embedded in composites with two additional cycles of SMP10 infiltration-curing-pyrolysis. Figure 50a indicates that the uncoated fibers are broken in a brittle mode. Similarly, the fibers that were coated with PEDAB (Figure 50b). In contrast, fibers coated with PBAB show better pullout in Figure 50c. It should be noted that these are only early observation and there was no effort to adjust the BN or BN/C coating process, thickness composition, and pyrolysis temperature, as well as no attempt to further improve the composition (powder/polymer ratio) and processing of the composite fabrication.

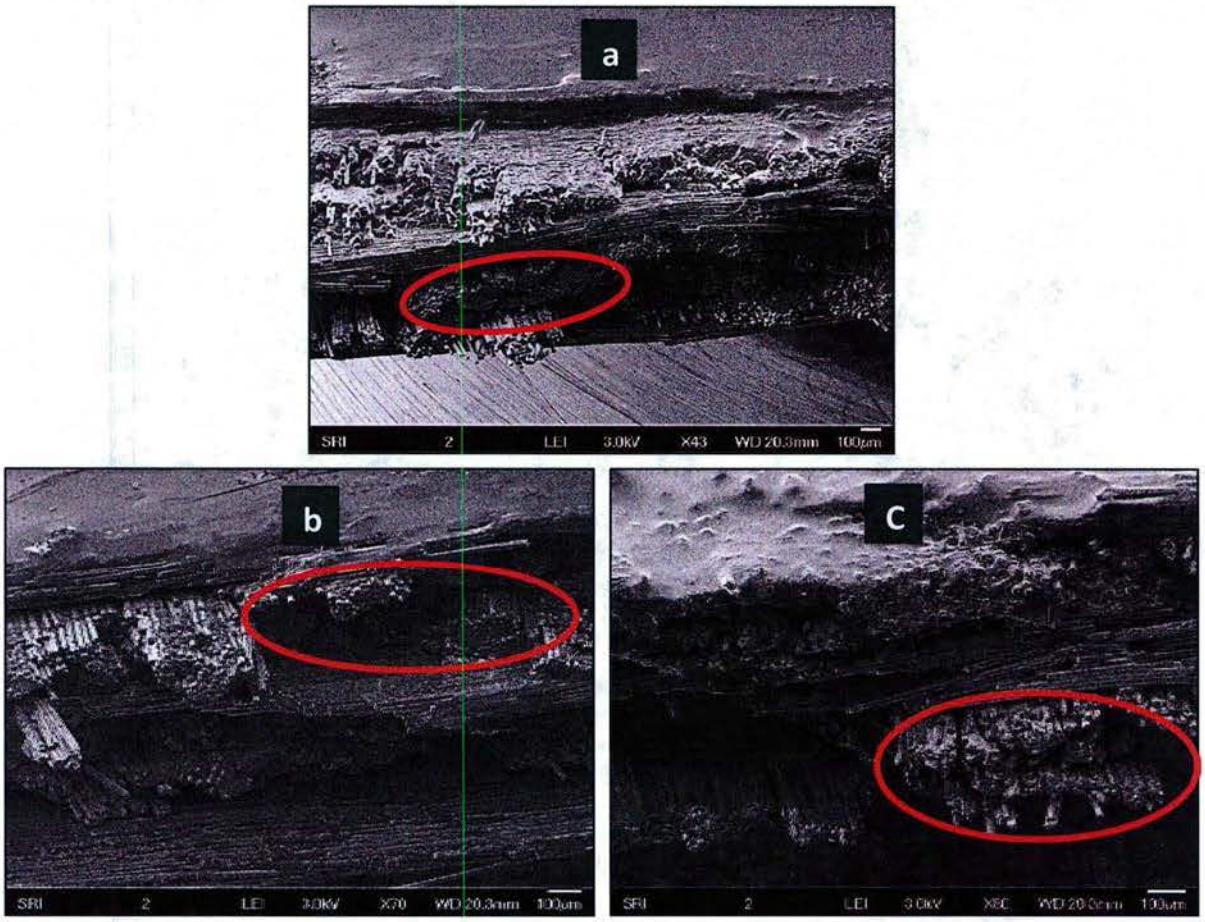

Figure 50. Composites with 2 additional infiltration cycles of SMP10 that contain embedded yarns: (a) with no interface coatings; (b) coated with PEDAB; (c) coated with PBAB.

The two additional infiltration cycles densify significantly the matrix and make it much less chalky than without the infiltration, even if the overall density and homogeneity of the matrix looks adequate before the additional infiltrations as shown in Figure 47 and Figure 48. In future activities, there will be a need to further adjust the original powder/polymer concentrations and the number of cycles to maximize the density of the matrix.

Tentative conclusions. The coating and mini-composite studies reveal the following aspects.

- Both polyaminoboranes can be coated over SiC fibers, with adequate adhesion to survive after pyrolysis at 1000 °C.

- The coatings can be deposited without causing significant bridging between the fibers, provided that the solution concentrations are at or below 5 wt%.
- It may be better if multiple thinner coatings are deposited and cured in between cycles. However, this aspect has not been explored yet.
- Both polymers require ammonia treatment for the curing stage. The ammonia serves as a crosslinking reagent and partial replacement of the organoamine that is making the original polymer.
- Coatings of fabric is also feasible, however the fabrics in our studies were already coated with carbon and boron nitride interface coatings.
- Slurries containing around 50 wt% SiC powders with particles smaller than 10 microns and preferably below 5 microns can be efficiently infiltrated in between fibers within the yarns of the fibers.
- The slurry requires an addition of about 30 wt% of solvent such as cyclohexane or another non-reactive solvent to reduce the viscosity and allow adequate infiltration of the SiC fiber plies.
- The infiltrated slurries are homogeneous and do not leave bubbles throughout the process.
- The pyrolyzed slurries do not show cracking due to polymer shrinkage, as observed in other matrix systems.
- When the composites are broken, the base slurries exhibit fragmentation associated with fine porosity of the base matrix material.
- The base pyrolyzed material, can be infiltrated with addition SMP10 polymer. Since the polymer viscosity is low, there is no need to add solvent to assist the reinfiltration cycles.
- Thus far, we performed 2 additional infiltration cycles. Additional cycles may further improve the density. However, each additional cycle is adding less material and there is an optimal number of infiltrations that make sense to apply.
- The presence of polymer derived coatings indicate improvement of fiber pullout relative to uncoated fibers. However, the results, thus far, are not decisive and require more parametric studies, to assess the various effects on achieving adequate coatings and matrix processing.
- It seems that BN derived material provides better (weaker) interface than the BN/C composition. However, this is a limited evidence and more can be done with both types of coatings.
- It should be noted that the evolved interface coatings, contain significant level of oxygen. Much of this oxygen is associated with inadequate processing steps, in which the coated fibers we expose to air between steps, especially before the pyrolysis of the interface coatings. Traces of oxygen and moisture can also severely attack the polymer coating during the curing and pyrolysis steps.
- Future studies will have to be done with fabrics that are not purchased with BN coatings. There is a need to analyze the mechanical strength as a function of various coating and slurry processing parameters.

5. IMPACT/APPLICATIONS

Lightweight materials that function at ultrahigh temperatures (above 1500 °C) are essential for enabling hypersonic vehicle performance for extended flying periods. Due to the extreme speeds of such vehicles at relatively low altitude, the friction with air and the presence of molecular or—even worse—single oxygen atoms causes severe heating of the vehicle surface. Under these conditions, typical aerospace materials, including carbon-based composites, degrade very rapidly or literally burn.

Non-oxide particulate composites and fiber-reinforced silicon carbide are the two main families of ceramic materials that are currently considered for the heated sections of hypersonic vehicles. Composites consisting of borides, carbides, and nitrides of early transition metals, combined with silica-forming phases such as silicon carbide and metal silicides, serve as the current advanced UHTC materials.

Such UHTC materials are the main candidates for leading edges and propulsion systems of future hypersonic vehicles. However, UHTC component consolidation is extremely difficult, requiring ultra-high temperatures under high pressure. Their machining is similarly difficult due to their remarkable hardness. UHTC nanoparticles are expected to provide advantageous sintering capabilities with consequently improved performance. Nevertheless, nanoparticle synthesis, handling, and processing impose a new set of technical hurdles and cost constraints.

Fiber-reinforced silicon-carbide matrix composites (SiC/SiC) are the lightweight materials considered to withstand the highest temperature in an oxidative environment out of all currently produced or studied high temperature composites. For achieving and maintaining their critical fracture toughness, fiber-reinforced composites require a weak interface between the fibers and the matrix, and this interface needs to be sustained at the operating conditions.

Current techniques for depositing weak interfaces in SiC/SiC systems are based on chemical vapor deposition (CVD) approaches for initially depositing a nanometric carbon layer and then boron nitride, which has higher stability in oxidative environment. This process is very expensive and limited in its deposition rate. Furthermore, once it is performed directly on a fabric of fibers, the deposition can easily lead to bridging between the fibers and formation of a rigid structure that is not easily infiltrated with the matrix material.

The preceramic polymer approach allows a very fast deposition of nanometric films over fiber yarns without excessive bridging. The deposition can likely be extended to fabrics, including 3D weaves, The processing of such fabrics is very similar to the processing techniques used to infiltrate the liquid polymeric precursor in between the fibers and yarns of the matrix. Hence, the same tools can be used for making both the coatings and the matrix, and, preferably, the coatings can be cured, reinfiltrated with the matrix formulations, and then the pyrolysis cycle can run on both at once.

All types of hypersonic vehicles and low trajectory missiles can benefit from these advanced high-temperature materials. Anti-ballistic missiles (ABM) that accelerate to extremely high speeds in seconds will also benefit.

6. RELATED PROJECTS

"Cubic Boron Nitride: A Model for Extended Solids Processing" was a related DARPA project that was performed prior to the scope of work change in the third year of this project. SRI was a subcontractor for Teledyne in an attempt to make cubic boron nitride at a pressure roughly ten times lower than that currently used to convert the conventional hexagonal phase to the cubic one. Linear and sterically hindered polymeric precursors to boron nitride were proposed as the source for generating the cubic phase, instead of the typical polymeric precursors to BN, which arebased on linking aromatic rings of borazine (B_3N_3). The synthesized precursors still converted to mostly hexagonal structures during the pyrolysis. These synthesized polymers serve as the interface coatings for this project.

The DARPA program was called Extended Solids, and information about the program can be found at http://www.darpa.mil/program/extended-solids.

7. REFERENCES

[1] Wuchina, E., E. Opila, M. Opeka, W. Fahrenholtz, and I. Talmy, UHTCs: Ultra-High Temperature Ceramic Materials for Extreme Environment Applications, Electrochem. Soc. Interface, 30 (Winter, 2007).

[2] Cotton, J., Ultra-High-Temperature Ceramics, Advanced Materials & Processes, 26-8 (June 2010).

[3] Zhu, S., W.G. Fahrenholtz, G.E. Hilmas, and S.C. Zhang, Pressureless Sintering of Zirconium Diboride Using Boron Carbide and Carbon Additions, J. Am. Ceram. Soc., 90(11) 3660-63 (2007).

[4] Licheri R., R. Orru', C. Musa, A.M. Locci and G. Cao, Spark Plasma Sintering of UHTC powders obtained by Self-Propagating High-Temperature Synthesis, J. Mater. Sci. 43, 6406-13 (2008).

[5] (a) G. Demazeau, J. Mater. Sci. 43, 2104 (2008); (b) B. Gersten, Chemfiles (Aldrich-Sigma) Vol. 5, Article 13.

[6] Demazeau, G., Solvothermal Reactions: an Original Route for the Synthesis of Novel Materials, J. Mater. Sci. 43, 2104-14 (2008).

[7] Suchanek, W.L. and R.E. Riman, Hydrothermal Synthesis of Advanced Ceramic Powders, Advances Sci. and Tech., 45, 184-93 (2006).

[8] Hayashi, H. and Y. Hakuta Hydrothermal Synthesis of Metal Oxide Nanoparticles in Supercritical Water Materials, 3, 3794-817 (2010).

[9] Kelly, J.P., R. Kanakala, and O.A. Graeve, A Solvothermal Approach for the Preparation of Nanostructured Carbide and Boride Ultra-High Temperature Ceramics, J. Am. Ceram. Soc., 93, 3035–8 (2010).

[10] Clark, B.M., J.P. Kelly, and O.A. Graeve, Exploring the Synthesis Parameters and Spark Plasma Sintering of Tantalum Carbide Powders Prepared by Solvothermal Synthesis, Mater. Res. Soc. Symp. Proc., 1373, 7 (2012).

[11] Purdy, A.P., S. Case and N. Muratore, Synthesis of GaN by High-Pressure Ammonolysis of Gallium Triiodide, J. Crystal. Growth, 252, 136–143 (2003)

[12] Gu, Y., Y. Qian, L. Chen and F. Zhou, A Mild Solvothermal Route to Nanocrystalline Titanium Diboride, J. Alloys & Comp. 352, 325-7 (2003).

[13] Chen, L., Y. Gu, Y. Qian, L. Shi, Z. Yang and J. Ma, A Facile One-Step Route to Nanocrystalline TiB2 Powders, Mater. Res. Bul. 39, 609-13 (2003).

[14] Dong, S., X. Hao, X. Xu, D. Cui and M. Jiang, The Effect of Reactants on the Benzene Thermal Synthesis of BN, Materials Letters 58 2791– 2794 (2004).

[15] Sardar, K. and C.N.R Rao, AlN Nanocrystals by New Chemical Routes, Solid State Sci., 7, 217–220 (2005).

[16] Solvothermal Approach Synthesis of Silicon Carbide and Other Nanomaterials, China Papers (online), posted 6/9/10.

[17] Zou, G., C. Dong, K. Xiong, H. Li, C. Jiang, and Y. Qian, Low-Temperature Solvothermal Route to 2H–SiC Nanoflakes, Appl. Phys. Lett. 88, 1913 (2006).

[18] Haensch, C., S. Hoeppener, and U.S. Schubert, Chemical Modification of Self-Assembled Silane Based Monolayers by Surface Reactions, Chem. Soc. Rev., 39, 2323-34 (2010).

[19] Wu, W., Q. He, and C. Jiang, Magnetic Iron Oxide Nanoparticles: Synthesis and Surface Functionalization Strategies, Nanoscale Res. Lett., 3, 397–415 (2008).

[20] Blum, Y.D., N Kambe, D.B. MacQueen, S. Kumar, S. Chiruvolu, and B. Chaloner-Gill. Nanocomposites by Covalent Bonding between Inorganic Nanoparticles and Polymers, MRS Proceedings, Vol. 676, edited by HW Hahn, R Tannenbaum, DL Feldheim, CP Kubiak, and RW Siegal, pp. Y1.8.1-Y1.8.6 (2002).

[21] Kambe, N., Y.D. Blum, B. Chaloner-Gill, S. Chiruvolu, S. Kumar, and D.B. MacQueen, Polymer-Inorganic Particle Composites. US Patent 6,599,631 (July 29, 2003).

[22] Blum, Y.D., D.B. MacQueen, D.K. Hui, and S. Liu. Method of Coating a Substrate Surface, and Coated Substrates Prepared Thereby. US Patent Application 20120107614 A (May 3, 2012).

[23] Hoebbel, D., T. Reinert, H. Schmidt, and E. Arpac, On the Hydrolytic Stability of Organic Ligands in Al-, Ti- And Zr-Alkoxide Complexes, J. Sol-Gel Sci. and Tech., 10, 115-26 (1997).

[24] Blum, Y.D., S Young, D Hui, and E Alvarez. Hafnium Reactivity below 1500°C in Search of Better Processing of HfB_2/SiC UHTC Composites, in Ceramic Engineering Science Proceedings, 27(2), R Tandon, A Wereszczak and E Lara-Curzio, eds, John Wiley and Sons, Inc. pp. 617-628 (2006).

[25] Blum, Y.D., J. Marschall, D. Hui, and S. Young. Thick Protective Coatings for SiC-Based Structures: Process Establishment. J Am Ceram Soc, 91, 1453-1460 (2008).

[26] Demazeau, G., V. Gonnet, V. Solozhenko, B. Tanguy, and H. Montigaud, C.R. Acad. Sci., 320 (IIb), 419 (1995).

[27] Hao, X., M. Yu, D. Cui, X. Xu, Q. Wang and M. Jiang, The Effect of Temperature on the Synthesis of BN nanocrystals, Journal of Crystal Growth, 241, 124–8 (2002).

[28] Jones, R.G. and S.J. Holder, High-Yield Controlled Syntheses of Polysilanes by the Wurtz-Type Reductive Coupling Reaction, 55, 711–8 (2006).

[29] Franzen, R.G., Utilization of Grignard Reagents in Solid-phase Synthesis: A Review of the Literature, Tetrahedron 56, 685–91 (2000).

[30] Bellosi, A. and F. Monteverde, Ultra High Temperature Ceramics: Microstructure Control and Properties Improvement Related to Materials Design and Processing Procedures, Thermal Protection Systems and Hot Structures, Proceedings of the 5th European Workshop held 17-19 May, 2006 at ESTEC, Noordwijk, The Netherlands. Edited by K. Fletcher.

[31] Sciti, D., A. Bellosi, S. Guicciardi, V. Medri and F. Monteverde, Ultra-High Temperature Ceramics (UHTC's) for Severe Environments, "Modern Ceramic Materials and Their Applications" Proceedings, Novosibirsk, 13-14 May 2010.

[32] Peters, D., Ammonothermal synthesis of aluminum nitride. *J Cryst Growth*, 104, 411-418 (1990).

[33] Hashimoto, T., and S. Nakamura, Chapter 8: A Pathway Toward Bulk Growth of GaN by the Ammonothermal Method. Technology of Gallium Nitride Crystal Growth. D. Ehrentrait, E. Mesissner, and M. Bockowski, eds., 133, 161-182 (2010).

[34] Demazeau, G., G. Goglio, and A. Largeteau, Contribution of solvothermal processes to the synthesis of novel nitrides and the development of shaping processes. *Mater Res Soc Symp Proc*, 1040 (2008).

[35] Ketchum, D.R. , and J.W. Kolis, Crystal growth of gallium nitride in supercritical ammonia. *J Cryst Growth*, 222, 431-434 (2001).

[36] Jacobs, H., D. Rechenbach, and U. Zachwieja, Structure determination of γ'-Fe_4N and ε-Fe_3N. *J Alloys Compd*, 227, 10-17 (1995).

[37] Hao, X.P., D.L. Cui, G.X. Shi, Y.Q. Yin, X.G. Xu, J.Y. Wang, M.H. Jiang, X.W. Xu, Y.P. Li, and B.Q. Sun, Synthesis of cubic boron nitride at low-temperature and low-pressure conditions. *Chem. Mater.,* 13, 2457-9 (2001).

[38] Dong, X., X. Xu, D. Cui, M. Jiang, The effect of reactants on the benzene thermal synthesis of BN. Shouyi Materials Letters, 58, 2791– 2794 (2004).

[39] Kai, L., J. HaiHui, L. Gang, W. QiLong, Z. Xian, C. DeLiang, and T. XuTang, Investigation on the key factors in the hydrothermal synthesis of BN: The way of introducing sodium azide. *Chin Sci Bull*, 52(13), 1785-1790 (2007).

[40] Meiyan, Y., S. Dong, K. Li, X. Hao, Z. Lai, Q. Wang, D. Cui, and M. Jiang, Synthesis of BN nanocrystals under hydrothermal conditions, *Journal of Crystal Growth* 270, 85–91(2004).

[41] Lian, G., X. Zhang, L. Zhu, M. Tan, D. Cui, and Q. Wang, New strategies for selectively synthesizing cubic boron nitride in hydrothermal solutions, *Cryst Eng Comm*, 12, 1159–1163 (2010).

[42] Ma, J., J. Li, G. Li, Y. Tian, J. Zhang, J. Wu, J. Zheng, H. Zhuang, T. Pan, One simple synthesis route to whisker-like nanocrystalline boron nitride by the reaction of $NaBH_4$ and NaN_3. *Materials Research Bulletin* 42, 982–988 (2007).

[43] Hao, X. P., D. L. Cui, X. Q. Yu, Z. G. Liu, X. G. Xu, and M. H. Jiang, The activation of benzene by BN nanocrystals. *Matter. Lett.* 57, 703-707 (2002).